CRITICAL CLOSING PRESSURES, VASCULAR WATERFALLS, AND THE CONTROL OF BLOOD FLOW TO THE HINDLIMB

BY

IAN SHRIER M.D.

Department of Physiology

McGill University, Montreal, Canada

April 1993

A thesis submitted to the Faculty of Graduate Studies and Research in partial fulfillment of the requirements for the degree of Doctor of Philosophy

Short Title:

VASCULAR WATERFALLS

AND THE CONTROL OF BLOOD FLOW

TO THE HINDLIMB

ABSTRACT

Pressure-flow relations in the hindlimb are best explained by a model which incorporates a vascular waterfall at the level of the arterioles. The mechanisms controlling the critical pressure at the waterfall (P_{crit}) and arterial resistance (R_a) were examined in the canine hindlimb. Lowering carotid sinus pressure (P_{car}) caused both P_{crit} and R_a to increase (neural response). Increases in local perfusion pressure (P_{per}) caused P_{crit} to increase (predominantly a myogenic response), but R_a to decrease (predominately a passive or flow-mediated response). When tone was increased by blocking the synthesis of endothelium-derived relaxing factor or through α_1-activation, the myogenic response of P_{crit} increased and the decrease in R_a with increasing P_{per} was abolished. The myogenic response of P_{crit} was not eliminated with a calcium-channel blocker, nor when reactive hyperemia was abolished with maximal vasodilation. However, maximal vasodilation lowered P_{crit} below the downstream pressure, thereby eliminating waterfall behaviour during normal flow. These findings suggest that P_{crit} and R_a are dependent on the interaction of several different control systems.

RÉSUMÉ

C'est le modèle intégrant une cascade de réactions vasculaires au niveau des artérioles qui peut le mieux rendre compte des relations entre la pression et le débit dans les membres antérieurs. Les méchanismes qui contrôlent la pression critique au point de cascade (P_{crit}) et la résistance artérielle (R_a) ont été étudiés dans les membres antérieurs de chiens. L'abaissement de la pression du sinus carotidien (P_{car}) a entraîné une augmentation de P_{crit} et de R_a (réponse neurale). L'augmentation de la pression locale a provoqué l'augmentation de P_{crit} (réponse avant tout myogénique), mais un abaissement de R_a (réponse avant tout passive ou à médiation par le débit). L'augmentation de tonus par blocage de la synthèse du facteur de relaxation dérivé de l'endothélium ou par activation α_1 a provoqué l'augmentation de la réaction myogénique de P_{crit} et l'abaissement de R_a, qui est fonction de l'augmentation de P_{per}, a été supprimé. L'administration d'un inhibiteur des voies du calcium n'a pas supprimé la réaction myogénique de P_{crit}, non plus que la vasodilatation maximale n'a fait disparaître l'hypérémie réactive. Toutefois, la vasodilatation maximale a abaissé P_{crit} sous la pression en aval, supprimant ainsi le phénomène de cascade pendant le débit normal. Ces résultats semblent indiquer que P_{crit} et R_a dépendent de l'interaction de plusieurs systèmes de contrôle distincts.

For Mom and Dad

ACKNOWLEDGMENTS

A good supervisor teaches a student how to ask proper questions, formulate a proper hypothesis, and carry out well-designed protocols. An excellent supervisor adds support when the frustration level became intolerable, encourages the student to fully develop their potential, and instills a sense of responsibility about the work being done. I am extremely fortunate to have met, worked, and learned with Dr. Magder. Perhaps the most important thing he has taught me is the Answer to the Universe: 42.

When I started my Ph.D., I had only a scarce background in research. I would like to especially thank Alain Deschamps for his time and energy in showing me the ropes of research, tolerating my telephone harassment, and teaching me that an "Index" is located at the back of most manuals.

No lab can function without support staff. I would like to thank Steve Nuara for his technical expertise, without whom I could not have completed my thesis. Thanks to Terry Kennedy, Joan Longo, and Roberta Carin for help in preparing abstracts and manuscripts. I would also like to thank Dr. Sabah Hussain for sharing his unique outlook on life. Finally, thanks to all the fellows whom I have had the pleasure of working with: Christy, Cathy, Giulio, Dimitri, Serafim, and Filippo. To Filippo, a special thanks for always making me smile (and Cathy too).

Positive self-esteem begins in early childhood. I wish to thank my mother for her unceasing compliments about everything. I wish to thank my father for always being there to listen, and helping me to crystallize my thoughts. Through long hours of discussion, and even longer hours by example, he has shown me how to live "happy".

In the end, enjoying life begins and ends with friends. Over the years, I have had many acquaintances and a select group of friends. There are several friends without whom my life would not have been the same. A very special thanks to Sonia,

who must be the nicest person that I have ever met. Perhaps an "Apple" really does keep the doctor away (from a computer). Thanks to Josh for support during my developing years and for those long talks, long walks, long drives, and special trips. To Alan, thanks for the balance you have added to my life. I don't think anyone else could have tolerated all those heated "discussions" on life, politics, economics, religion, nationalism, computers, television, apartments, cards, dice, etc. I will never forget my 30-31st birthday present. I had a dream...

TABLE OF CONTENTS

TABLE OF CONTENTS (con't)

PAGE

TABLE OF CONTENTS (con't)

PAGE

LIST OF FIGURES

LIST OF FIGURES (con't)

LIST OF FIGURES (con't)

LIST OF TABLES

PREFACE

This thesis is divided into eight chapters. The introduction in Chapter 1 provides a review of landmark studies about pressure-flow relations, and background information concerning the physics of flow and the factors affecting vessel tone and diameter. In chapters 2, 3, 4, 5, and 6, I have opted to include original papers on the mechanisms controlling the critical closing pressure and arterial resistance as per "The Guidelines Concerning Thesis Preparation" of McGill University. The study described in chapter 2 has been accepted for publication in the American Journal of Physiology. The studies in chapters 3-6 are under review at the American Journal of Physiology. Chapter 7 discusses the general conclusions of the thesis and is followed by Claims of Originality.

The experiments in chapter 2 were performed with the assistance of Dr. S.N.A. Hussain from the Royal Victoria Hospital and his name appears as co-author on the paper. My supervisor Dr. Magder is the senior author on all manuscripts published or under review.

I have used the American Physiological Society guidelines for the format of chapters 1-6 and in the units of measurements. The corresponding SI units are listed in Appendix I. Appendix II is a list of the abbreviations used in the thesis.

CHAPTER 1

INTRODUCTION

1.1. HISTORY OF PRESSURE-FLOW RELATIONS

The relationship between perfusion pressure (P_{per}) and circulatory flow has been studied for more than 50 years. Early studies measured steady-state flow during step-wise reductions in P_{per} (steady-state pressure-flow relation). Although the slope of the relationship is mathematically equivalent to 1/resistance (i.e. $\dot{Q}/\Delta P$ where $\dot{Q}$ is flow and ΔP is the pressure drop across the vascular bed), it actually represents a combination of baseline resistance and autoregulation (a change in resistance when P_{per} is changed in an attempt to maintain flow constant, figure 1.1) (42,127).

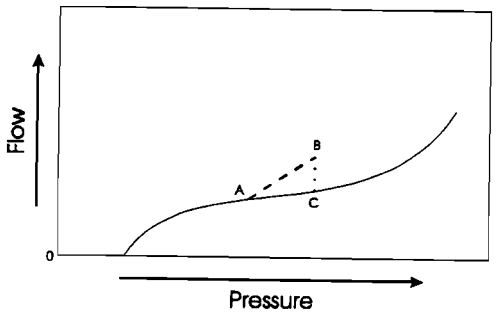

Figure 1.1: The solid line represents the steady-state pressure-flow relationship. If the perfusion pressure is increased from point A, the flow increases from A to B. The vasculature reacts to the increased pressure and/or flow by increasing resistance to flow, which decreases flow to C. The slope of AB is dependent on the baseline resistance and compliance. The change in resistance between point B and C is referred to as autoregulation.

More recently, investigators have measured the instantaneous changes in flow with changes in pressure in an attempt to eliminate reflex adjustments (dynamic pressure-flow relation, figure 1.2). The slope of the relationship is again equivalent to 1/resistance, but is also affected by vessel compliance. No matter which method is

used, i.e. steady-state or dynamic relations, the pressure-intercept at zero-flow (P_{zf}) is positive which indicates that a large arterial-venous pressure gradient exists at zero-flow. In addition, several authors have shown that raising venous pressure (P_v) does not affect inflow until a critical value is reached.

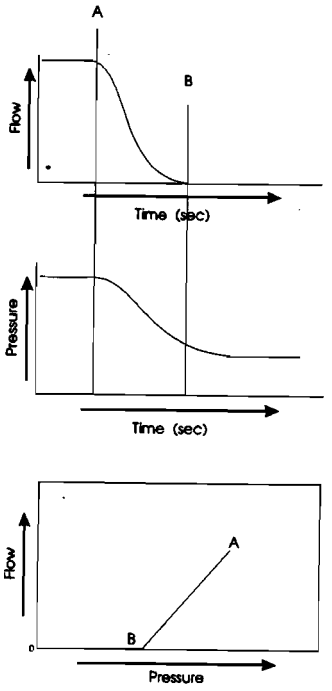

Figure 1.2: The top two figures represent analog signals for flow and perfusion pressure over time. Venous pressure is equal to zero. At point A, flow is decreased to zero over several seconds and the perfusion pressure falls. At point B, the flow is equal to zero, but a large arterial-venous pressure gradient remains. In the lower figure, the value of flow at any point in time is plotted against the perfusion pressure at that point in time, to yield the dynamic pressure-flow relation.

These findings are difficult to explain if the circulation is modelled as a series of rigid tubes. Instead, the weight of the evidence suggests that vessels behave like

collapsible tubes, and a Starling resistor-like mechanism may be operative at the arteriolar level. The goal of this thesis is to analyze the behaviour of the vasculature of the dog hindlimb in terms of this model. In Section 1.1, I will review the history of the steady-state pressure-flow relationship, the dynamic pressure-flow relationship, and the evidence supporting the existence of a Starling resistor-like mechanism in the circulation. In Section 1.2, I will discuss the physics of flow through rigid and collapsible tubes, and in Section 1.3, I will review the factors that might alter the Starling resistor-like mechanism or arterial resistance through a change in vessel tone.

1.1.a. Steady-State Pressure-Flow Relations

In 1933, Whittaker and Winton systematically studied pressure-flow relations in the canine hindlimb (134). They varied the hematocrit of blood and interpreted the changes in the steady-state pressure-flow relation as changes in the apparent blood viscosity. Pappenheimer and Maes later found that the steady-state pressure-flow relation was affected by vessel tone (106). Under control conditions, the pressure-flow relationship was linear down to low flows, but then became curvilinear (convex to the pressure axis). The curvilinearity of the relationship was increased when vascular tone was increased with epinephrine, and the curvilinearity was eliminated when smooth muscle tone was abolished with 0.1% chloral hydrate. They interpreted the results as an effect on the apparent blood viscosity rather than an affect on vessel diameter or resistance (106). Pappenheimer and Maes also noted that the extrapolation of the linear portion of the relationship to zero-flow gave a positive zero-flow pressure intercept (P_{zf}) which they attributed to a back pressure caused from edema compressing the vessel wall (106).

In 1951, Burton proposed a similar but slightly different explanation for the pressure gradient at zero-flow (23). Since arteriolar vessels are not rigid cylinders, Burton hypothesized that when the vessel wall is in an equilibrium state, the expanding

forces on the wall (intravascular pressure) must be balanced by the constricting forces on the wall (smooth muscle tension, elastic wall tension, interfacial tension).[1] If the intravascular pressure is decreased, the radius shortens until a new equilibrium is reached. However, if the intravascular pressure is reduced below the tension generated by the smooth muscle, the vessel is forced closed. Under these conditions, flow ceases even though a large arterial-venous pressure gradient remains. Burton called the arterial pressure at which the vessel collapses "the critical closing pressure". This explanation differs from Whittaker and Winton because 1) the critical closing pressure is due to the interaction of all compressive forces and not only interstitial pressure, and 2) the critical closing pressure does not act as a back pressure but instead, only affects flow when the vessel collapses.

Burton's concept was based on extrapolations of curvilinear pressure-flow relations. In order to measure the true zero-flow pressure intercept, Nichol et al. reduced pressure slowly but continuously over 10-30 minutes, and the fall in both pressure and arterial flow[2] were recorded until flow ceased (102). There was always a 15-20 mmHg pressure gradient across the vascular bed at zero-flow (i.e. P_{zf}). Furthermore, epinephrine increased P_{zf} and Ringers' solution decreased P_{zf} (but never eliminated it). Nichol et al. interpreted these findings to mean P_{zf} was tone-dependent, and the decrease in P_{zf} with Ringers' solution was due to the absence of circulating pressor agents. If vascular tone was eliminated with cyanide, a small gradient still existed. Since it could be abolished with wetting agents, this was attributed to interfacial tension as per Burton's analysis (23). Nichol et al. found that an arterial-

---

[1] This concept is covered in more detail in the section "Physics of Flow". Note that Burton did not include interstitial pressure since it is not important under normal circumstances.

[2] In this study, Nichol et al. measured arterial flow whereas previous authors measured venous outflow.

venous pressure gradient at zero-flow occurs in frog's legs, excised rabbit's ear, and in situ rabbit's leg.

Since Nichol et al. measured arterial inflow to the hindlimb instead of venous outflow, complete isolation was necessary for meaningful results (102). This is because collateral circulation will maintain microcirculatory flow even though pump flow through the flow-meter has stopped. The P_{zf} measured under these conditions will not represent a true "zero-flow pressure intercept", but will reflect the pressure drop across the collateral vessels, i.e. P_{zf} equals the pressure at the site where collateral vessels join with the artificially perfused arterial circulation (102). The excised rabbit ear was clearly isolated, and for the in situ hindlimb, the authors tied off any possible collateral vessels and clamped the tissues above the cannulation site.

Burton's analysis predicts closure of arteriolar vessels (23). Since venous vessels would remain open, Nichol et al. hypothesized venous outflow would continue after arterial inflow stopped. This hypothesis was confirmed (102).

According to Burton's analysis, the collapsible arteriolar vessels suddenly close when the expanding forces due to perfusion pressure decline below the constricting forces of the vessel wall. When the vessels are open, flow is determined by Poiseuille's Law. However, in 1963, Permutt and Riley noted that if the constricting forces surrounding a collapsible tube are greater than the downstream pressure but less than the upstream pressure, a Starling resistor-like mechanism is created (107). Under these conditions, the constricting forces that are responsible for the critical closing pressure act as a back pressure to flow.[3] Flow is therefore determined by the difference between perfusion pressure and the critical closing pressure, divided by the resistance between the two (as determined by Poiseuille's law). Changes in downstream

---

[3] This is actually the same explanation provided by Whittaker and Winton (134), only the force responsible for the back pressure is due to the sum of all constricting forces.

pressure or resistance have no effect on regional inflow, although they would affect capillary pressure, microcirculatory distribution, and venous return. Since this model is similar to a waterfall where the altitude or resistance in the river below the falls does not affect the amount of water flowing over the falls, the Starling resistor-like mechanism is sometimes called a vascular waterfall.[4]

Since the work of Nichol et al., many authors have decreased flow to zero and shown positive zero-flow pressure intercepts during steady-state perfusion. Regions studied include rabbit hindlimb (46), the human forearm, calf and finger (3), canine lung (111,126), canine liver (99), canine heart (31), the canine abdominal periphery (18), and the canine gastrocnemius muscle (127).

1.1.b. Dynamic Pressure-Flow Relations

In 1978, Bellamy studied dynamic coronary pressure-flow relations in conscious dogs (10). The purpose was to measure P_{zf} without the influence of autoregulation, anaesthesia, or surgical trauma. Bellamy examined recordings of pressure and flow in the aorta and circumflex artery during long diastoles, and plotted the instantaneous changes in flow against the instantaneous changes in P_{per} to obtain a dynamic pressure-flow relation. His approach was similar to that of Nichol et al. (102) except Nichol et al.'s apparatus decreased pressure so slowly that it required 10-30 minutes to reach zero-flow (102). These long periods meant that autoregulation could occur during the measurements (12,71), whereas in Bellamy's work, this was minimized since the measurements were completed within seconds.

Although the dynamic pressure-flow relation was linear in Bellamy's experiments, diastole was not long enough to allow flow to reach zero. Therefore, Bellamy also examined electrically paced dogs with complete heart block (10). In these

---

[4] This concept is covered in more detail in the section "Physics of Flow".

cases, the dynamic pressure-flow relation remained linear down to zero-flow and had a zero-flow pressure intercept of approximately 45 mmHg (compared to P_{zf} of 15-20 mmHg for the steady-state (102)). Bellamy also found that the P_{zf} and arterial resistance following a 15 second arterial occlusion were lower compared to control conditions. In 1980, Bellamy published another paper with Ehrlich and coworkers which showed a similar phenomenon in the canine hindlimb (34). These results strongly suggested that a tone-dependent critical closing pressure exists, and that it's value under control conditions is greater than previously hypothesized from steady-state pressure-flow relations. If true, arterial resistance, which is one of the most important measurements in vascular physiology, cannot simply be calculated as the $(P_{per}-P_v)/\dot{Q}$. Vascular beds in which dynamic pressure-flow relations indicate a zero-flow pressure intercept include monkey brain (33), canine hindlimb (34,92), and canine heart (10),

Bellamy's paper revived a dispute that continues today. In 1982, Eng, Jentzer, and Kirk recognized that a discharging arterial compliant region could theoretically cause the arterial pressure to remain above venous pressure, even though proximal flow decreased to zero (36). For instance, when arterial pressure is decreased to the value of the compliant region, flow between the two regions stops, whereas flow downstream from the compliant region continues. Therefore, a P_{zf} is present even though microcirculatory flow is still present. Eng et al. also noted that compliance effects are only important during dynamic changes, whereas they have no effect if pressure is maintained constant. Therefore, they developed an experimental setup in which coronary flow could be instantaneously switched to a reservoir source (constant pressure) at the same time that diastole was induced. The pressure of the reservoir could be varied, and flow was measured over a wide range of pressures. In order to avoid autoregulatory reflexes, measurements were taken as quickly as possible after switching perfusion sources. The authors compared the dynamic and static (constant

pressure) pressure-flow relations under both normal and maximally vasodilated conditions. Figure 1.3a is a schematic diagram of their observations taken from figure 4 of their paper. Eng et al. found the dynamic P_{zf} during control conditions was 27.1±6.6 mmHg, whereas the static P_{zf} was ≈11 mmHg. Furthermore, dynamic and static P_{zf} under vasodilated conditions were similar to the static P_{zf} under control conditions. Since the static P_{zf} under control conditions and the static P_{zf} under maximally-vasodilated conditions were approximately equal, the authors concluded that 1) 11 mmHg represents the true critical closing pressure (P_{crit}), 2) P_{zf} is affected by a discharging compliant region and 3) P_{zf} is not affected by vascular tone.[5]

The conclusions of Eng et al. were both supported and contradicted by Dole and Bishop (figure 1.3b (30)). Using similar methods, these authors also found the static P_{zf} was significantly less than the dynamic P_{zf} (at P_{per}=125 mmHg, 37.2±2.3 versus 48.4±1.8 mmHg), indicating that vascular compliance affects the dynamic P_{zf}. However, unlike Eng et al., these authors found that adenosine decreased the static P_{zf} (from 37.2±2.3 to 15.2±0.7 mmHg) in addition to decreasing the dynamic P_{zf} (from 48.4±1.8 to 23.7±1.5 mmHg). Therefore, these authors concurred with Eng et al. that P_{zf} is affected by compliance, but unlike Eng et al., their results suggested P_{zf} is tone-dependent.

---

[5] P_{zf} is dependent on both the true critical closing pressure (P_{crit}), and the vessel compliance.

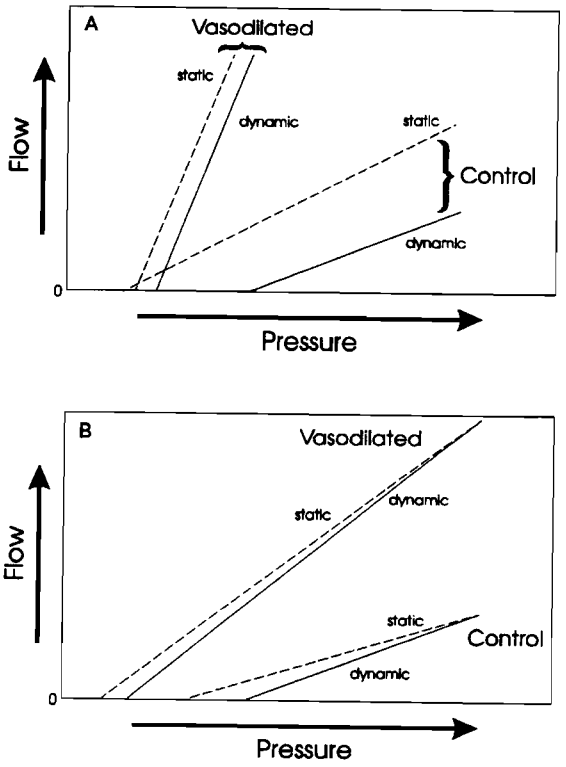

Figure 1.3: In A, schematic representations of the static (dashed lines) and dynamic (solid lines) pressure-flow relations under control and vasodilated conditions are shown as presented in the paper by Eng et al. (adapted from (36)). The static zero-flow pressure intercept (P_{zf}) under control conditions is much less than the dynamic P_{zf} under control conditions, but not different from the static or dynamic P_{zf} under vasodilated conditions. These results suggest P_{zf} is affected by compliance but is not tone-dependent. However, since the initial flow is higher during the static pressure-flow relation compared to the dynamic pressure flow relation despite the same initial perfusion pressure (for either condition), vasodilation must have occurred during the switch from normal perfusion to reservoir perfusion. In B, schematic representations of the static and dynamic pressure-flow relations under

control and vasodilated conditions are shown as presented in the paper by Dole and Bishop (adapted from 30). In these experiments, no vasodilation occurred during reservoir perfusion. Similar to the results of Eng et al., comparison of static and dynamic pressure-flow relations shows that compliance affects P_{zf}. However, unlike the results of Eng et al., comparison of vasodilated and control conditions suggests P_{zf} is tone-dependent.

The reason for the different results with vasodilation despite similar methods is unclear. Dole and Bishop suggested that the basal vasomotor tone during control conditions in the experiments by Eng et al. might have been very low, and therefore the static P_{zf} would be only minimally affected by vasodilation. However, since flow at normal perfusion pressures increased approximately three-fold with vasodilation, this is an unlikely explanation. Another possibility is that the preparation by Dole and Bishop was not completely isolated, and therefore collateral flow might have acted as a back pressure to flow. However, if this were the case, P_{zf} would be due to the collateral circulation and should not have been affected by local vasodilation through the perfused circumflex artery.

Although these papers have received considerable attention in the literature, there is an important observation that has not yet been noted. In figure 1.3a (figure 4 of Eng et al.), the static and dynamic pressure flow relations under control conditions are divergent and never intersect. This means that steady-state flow increased when perfusion was switched from natural perfusion to the reservoir source (for the static pressure-flow relation), even though P_{per} remained unchanged. In fact, according to the figure shown, flow more than doubled at P_{per}=80 mmHg. Therefore, resistance to flow (i.e. either arterial resistance, P_{zf}, or both) was considerably less during reservoir perfusion than during normal perfusion. In figure 1.3b, a schematic representation of

Dole and Bishop's results shows this was not the case in their preparation. It is not clear from Eng et al.'s paper why the reservoir apparatus would cause such an effect, but possibilities include infected tubing, temperature control, and red blood cell damage. Regardless of why it occurred, the effect makes comparison of the dynamic and static pressure-flow relations in Eng et al.'s paper questionable. The results from Dole and Bishop support Bellamy's conclusion that P_{zf} is tone-dependent.

In 1984, Aversano et al. used another method to eliminate the effect of compliance in the measurement of P_{zf} (4). Using the isolated, *maximally vasodilated*, paced canine heart, these authors recorded dynamic pressure-flow relations during a decrease in flow, and also during the subsequent increase in flow back to normal. The authors hypothesized that if the compliant region was discharging during diastole and causing measured flow to be artificially low at each pressure (pressure-flow relation shifted to the right), then flow during the up-ramp would be disproportionately large as the compliant region filled (pressure-flow relation shifted to the left). The compliance-free curve would be the line bisecting the two relationships. Aversano et al. found that the difference between the down and up curves narrowed as the rate of change in pressure was decreased, and at 3 $mmHg \cdot s^{-1}$, the pressure-flow relations for decreasing and increasing flow were identical (i.e. compliance-free curves). Finally, the P_{zf} obtained by these methods was similar to the P_{zf} obtained with steady-state methods (N.B.: autoregulation during steady-state measurements should have no effect because the vascular bed was maximally vasodilated). The authors concluded that dynamic pressure-flow relations with slow rates of decrease represent compliance-free curves.

The findings of Aversano et al. were interesting, but not conclusive. Most importantly, they studied the maximally vasodilated bed and it was not known whether their methods could be applied to a vascular bed with tone. In 1990, Magder published a study in which he isolated the effects of compliance on P_{zf} in a hindlimb with tone, and therefore measured the true P_{crit} (92). Magder realized that if a discharging

compliant region maintained proximal pressure high at "zero-flow" even though microcirculatory flow continued, then P_{zf} should decrease if the compliant region is allowed to empty. Therefore, P_{zf} should be dependent on the time taken to reach zero-flow (ramp time). With longer ramp times, the compliant region will partially discharge, and a lower P_{zf} will be recorded. On the other hand, if the P_{zf} was due to a Starling resistor-like mechanism creating a critical closing pressure, P_{zf} should be unaffected by the time taken to reach zero-flow. Magder used a pump-perfused canine hindlimb and recorded the dynamic pressure-flow relations as the ramp time was varied between 1-10 seconds. He then plotted the P_{zf} of each run against the ramp time for that run (figure 1.4). The results showed that P_{zf} decreased as the ramp time was increased from 1-4 seconds, confirming the effect of a discharging compliant region. However, the P_{zf} for ramp times between 5-10 seconds were similar. The author compared these observations with predictions from three different mathematical models of the circulation. The first model was based on one compliant region (venous) with resistances pre and post. The second model had two compliant regions in series (arterial and venous). The third model was identical to the second except a Starling resistor-like mechanism was added at the arteriolar level. Only the Starling resistor model could predict a constant P_{zf} with ramp times between 5-10 seconds (figure 1.4b). However, Magder also observed a decline in P_{zf} with ramp times between 1-4 seconds, indicating that compliance was an important variable and could not be ignored. Therefore, P_{zf} represents P_{crit} only if the ramp time is between 5-10 seconds. The ramp time required to allow the arterial compliant region to fully discharge is dependent on the system's time constant (τ), and is independent of the initial P_{per} or flow.

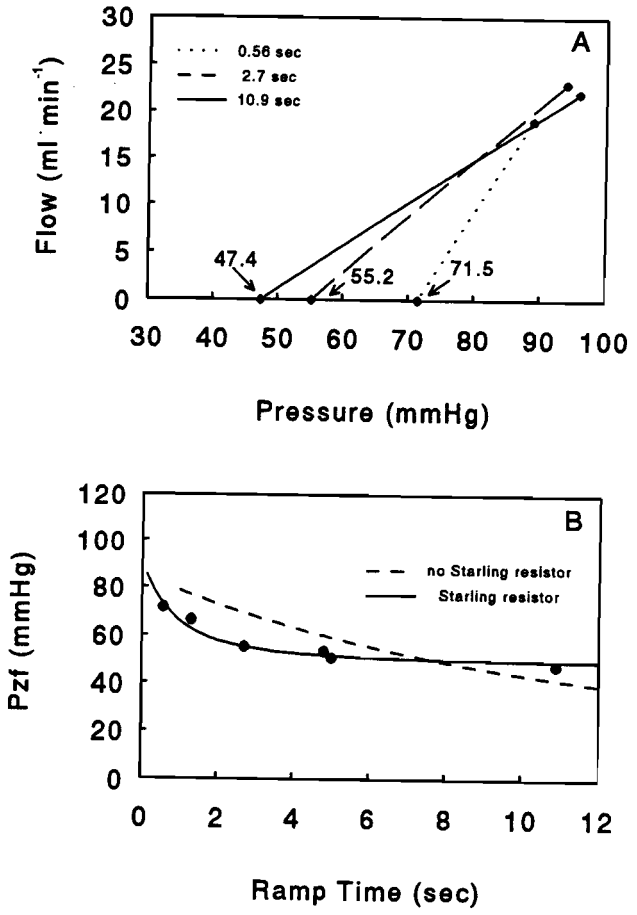

Figure 1.4: In A, three dynamic pressure-flow relations are shown using three different ramp times. When flow was decreased to zero over 0.56 seconds (dotted line), the zero-flow pressure intercept (P_{zf}) was 71.5 mmHg. When the ramp time was 2.7 seconds (dashed line), the P_{zf} was 55.2 mmHg, and when the ramp time was 10.9 seconds (solid line), the P_{zf} was 47.4 mmHg. In B, each P_{zf} in A is plotted against the ramp time for that run. The dotted line represents the best predicted data when no Starling resistor is present in the model of the circulation, whereas the solid line shows the predicted data when a Starling resistor is incorporated. P_{crit} is the P_{zf} with ramp times between 5-10 seconds.

During the dynamic pressure-flow relations, Magder noticed that P_{per} continued to decline after flow reached zero. However, if the vessels were closed as Burton predicted, then pressure should remain constant. In addition, during a sudden arterial occlusion, P_{per} rapidly falls below P_{crit} (within 2 seconds, i.e. before autoregulation), and stabilizes after 10-30 seconds at a much lower pressure. In the same paper, Magder showed that the Starling resistor model could still explain these observations if a small number of vessels did not exhibit a critical closing pressure (e.g. arterial-venous anastomoses) (92). In fact, the model exactly predicts the decline in pressure below P_{crit} if these channels accommodate only 1.5% of flow at normal perfusion pressures. These results are important because they indicate that compliance-free measurements of P_{zf} using the "static pressure-flow relation" as suggested by other authors (19,30,36) will underestimate P_{crit}, and hence overestimate arterial resistance. For instance, flow through these bypass channels allows perfusion pressure to decrease below P_{crit} during the sudden change in P_{per} that is used to obtain the static pressure-flow relations previously described by both Eng et al., and Dole and Bishop (i.e. static P_{zf}<dynamic P_{zf}, (30,36)). Finally, Magder also showed that P_{crit} is affected by reactive hyperemia, indicating tone-dependence of P_{crit}. However, he did not systematically study how vasodilation affects P_{crit}, arterial resistance, or arterial compliance (92).

The predictions for the P_{zf} versus ramp time relationship shown in figure 1.4b were based on models in which resistance and compliance remained constant throughout the pressure-flow relation. Although a Starling resistor-like mechanism is the simplest explanation, one could also explain the data with a two-compartment model (no Starling resistor) in which both compliance and resistance varied during the pressure-flow relation. However, experiments by Judd and Mates suggest that impedance to flow (dependent on resistance and compliance) is unchanged during the

dynamic pressure-flow relation (74)[6]. If resistance and compliance are constant during the dynamic pressure-flow relation, then a Starling resistor-like mechanism becomes the only explanation for Magder's observations. Since Judd and Mates studied heart rates between 60 and 150 beats·min^{-1}, it is still possible that resistance and compliance vary during longer diastolic periods.

The actual force responsible for creating P_{crit} is controversial. Some authors believe it is the interstitial pressure (106). However, this would not explain the tone-dependent behaviour of P_{crit} (19,81,92). In fact, vasodilation should cause an increase in interstitial pressure (and hence an increase in P_{crit}) through an increase in capillary hydrostatic forces, whereas experimentally, vasodilation causes a decrease in P_{crit} (19,81,92). Returning to Burton's analysis, P_{crit} is most likely created by the addition of all compressive forces, i.e. interstitial pressure, passive elastic recoil, smooth muscle tone, and interfacial tension. The relative importance of each depends on the conditions of the experiment.

1.1.c. Waterfall Behaviour

If the arteriolar vessels are behaving as collapsible tubes, then waterfall behaviour should be observed in addition to vessel closure (107)[7]. Waterfall behaviour means that flow is unaffected by changes in downstream resistance or pressure until the downstream pressure becomes greater than the pressure at the waterfall (32,60). Magder showed that a vascular waterfall does indeed exist in the isolated canine hindlimb (92). When P_v was increased during constant pressure conditions there was no effect on flow until a critical value was reached, and when P_v was raised during

---

[6] These authors actually showed that coronary impedance to flow is unchanged throughout the cardiac cycle (systole and diastole).

[7] This concept is covered in detail in the section "Physics of Flow".

constant flow conditions, there was no effect on P_{per} until a critical value was reached. Similar observations have also been made in the heart (38), liver (99), and lung (126). Other studies that have not shown this effect increased venous pressure in large steps and the waterfall was probably overcome with the first increase in venous pressure (29,34). These results strongly suggest the presence of waterfall behaviour, although one could still theoretically explain the results with a model in which increasing venous pressure results in decreasing resistance through passive effects. However, this is an unlikely explanation because the decrease in resistance would have to exactly offset the decrease in driving pressure.

Another explanation for waterfall behaviour was suggested by Dole et al. in 1984 (29). These authors hypothesized that the microcirculation behaved like a variable resistor and exhibited a critical closing pressure similar to Burton's analysis, except the model incorporated compliant arterial and venous regions. Unlike the Starling resistor model in which waterfall behaviour was due to a true dissociation between arterial and venous pressure, the variable resistor model explained the same effect through a combination of changing resistance, compliance, and P_{zf}. According to their model, changes in venous pressure **always** affect the pressure-flow relation (i.e. P_{zf} and R_a), although the overall effect on regional inflow may be negligible. This hypothesis was recently refuted by Braakman et al. who showed that the compliance-free measurement of P_{zf} under control conditions in *in vitro* skeletal muscle is **not** affected by venous pressure elevation until P_v is increased by 28.5 ± 9.5 mmHg (19). Therefore, the most likely explanation for pressure-flow relations and waterfall behaviour is that a Starling resistor-like mechanism is operative at the arteriolar level.

1.1.d. In Vivo Microscopy

The phenomenological observations noted above support the concept of a critical closing pressure and waterfall behaviour. If P_{crit} is due to vessel closure, then

this should be observable using *in vivo* microscopy techniques. Before discussing the results of microscopic studies, several points should be noted.

The waterfall model hypothesizes that the back pressure to flow is created by an external force that dissociates the hydraulic gradient from the energy gradient (32). Vessels are not closed during conditions of flow but only when pressure is decreased below P_{crit}. It should therefore be stressed that when pressure is reduced in steps, the decreased myogenic stimulus and increased metabolic stimulus cause the vessel smooth muscle tone to decrease (12,71). Whereas this causes a decrease in P_{crit}, the change in vessel diameter will depend on the interaction between passive and active factors. Therefore, one may see vasodilation during step-wise reductions in pressure. Actual vessel closure would occur only if pressure was reduced fast enough so that autoregulation could not occur, i.e. less than 10 seconds (12,71). All studies to date have used step-wise reductions in pressure.

On the other hand, even during step-wise reductions in pressure, a large arterial-venous pressure gradient remains at zero-flow, and vessel closure should be observed at this time. Direct visualization of blood vessels *in vivo* has led to conflicting reports about vessel closure during step-wise reductions in pressure. From 1962 through 1977, Baez and colleagues published a series of articles showing that metarterioles and precapillary vessels close when pressure is decreased below a critical value (6-8,89). They measured external and internal wall diameter simultaneously, and have also shown that increasing sympathetic tone will cause previously open metarterioles and precapillary sphincters to close (8). This work has been supported by the findings of some authors (16,132) but not others (71,78,122-124). In fact, some studies show vasodilation with reductions in pressure as per the myogenic response, even if flow is decreased to zero. The reason for the conflicting results is not clear at the present time.

1.1.e. Clinical Relevance

The presence of a vascular waterfall in the circulation means that systemic arterial pressure or local flow can be controlled through changes in either P_{crit} or arterial resistance (R_a). The advantages of this system are discussed below using the example of hemorrhagic blood loss (decrease in cardiac output) and hypotension.

If no waterfall is present, arterial pressure after hemorrhage can only be increased by increasing total resistance (R_{tot}). Since the blood vessels to a region (e.g. hindlimb) can be modelled as several resistances in series (i.e. arterial, capillary, and venous), R_{tot} can be increased by increasing any of the individual resistances, presumably through an increase in sympathetic activity. However, the sympathetic nervous system would require an extremely sensitive feedback system to accurately return blood pressure to normal. This is because the proportional change in resistance (R_2/R_1) is equal to r_1^4/r_2^4 where R_1 is the original resistance, R_2 is the new resistance, r_1 is the original radius, and r_2 is the new radius. Therefore, a small change in radius would have a large effect on blood pressure. This type of control system is appropriate for coarse changes, but is not appropriate for a system requiring fine control. Furthermore, the important radius determining resistance is the internal radius. As will be shown in the next section, the lumen of a thick-walled vessel such as an arteriole (lumen to wall ratio of 0.5) is obliterated if the external smooth muscle layer shortens by only 13.5%. Therefore, the ability of the body to fine-tune resistance in thick-walled arterioles is even more limited when the anatomical features of the blood vessel wall are considered.

A waterfall model allows the pressure to be controlled through changes in either P_{crit} or R_a. In this model, changes in R_a represent the coarse control for pressure, and changes in P_{crit} represent the fine control. This is because P_{crit} is determined by the force generated by the smooth muscle, and not by the diameter of the vessel. For instance, if the sympathetic activity is increased and augments smooth muscle tension

by the equivalent of 5 mmHg, arterial pressure will increase by 5 mmHg, . The actual change in vessel diameter is not important because the increased tone is acting as a back pressure to flow, and not as a change in resistance.

There are other advantages to the presence of a waterfall. First, variations in venous pressure such as those that occur with respiration, do not affect regional flows because they occur downstream from the waterfall. Second, capillary pressure can be maintained constant through changes in venous resistance without affecting flow into the region. Third, in contrast to the no waterfall condition, local changes in capillary resistance will redistribute flow without causing changes in total flow to the region. Finally, a sudden decrease in cardiac output will not cause as rapid a fall in arterial pressure when a waterfall is present. This is because the decay in pressure follows a monoexponential curve (104,128) which is dependent on both the time constant of the system and the final pressure that is reached. Therefore, the rate at which arterial pressure falls is dependent on the magnitude of the total decrease in pressure. For the same time constant, the pressure drop during sudden decreases in cardiac output in a circulation without a waterfall has to be greater than one in which a back pressure is present because the pressure drop [(P_{per}-P_v) versus (P_{per}-P_{crit})] is greater. Thus, a vascular waterfall may help prevent syncope during sudden decreases in cardiac output that occur upon changing position, or sudden cessation of exercise.

1.1.f. Summary

Recent experimental evidence strongly supports the Starling resistor hypothesis. First, compliance-free dynamic pressure-flow relations have a positive zero-flow pressure intercept (4,92). Second, resistance and compliance are constant during dynamic pressure-flow relations (74). Third, raising P_v has no effect on flow until a critical value is reached (38,92). Finally, although some investigators did not observe

critical closure of vessels using *in vivo* microscopic techniques (78,122), others claim to see it often (7,16,132).

Clinically, the presence of a Starling resistor means 1) a more precise control of regional inflow and blood pressure, 2) variations in P_v that occur with respiration will not affect regional blood flow, 3) capillary pressure can be independently controlled from inflow, 4) redistribution of blood flow can easily occur downstream from the Starling resistor without affecting total inflow, and 5) a sudden drop in cardiac output will not produce as large a fall in arterial pressure.

Despite the phenomenological evidence presented in this section, controversy over the Starling resistor hypothesis remains. One major objection was raised by Azuma and Oka in 1971. These authors challenged Burton's analysis and showed that critical closure of vessels was theoretically impossible (5). Although this article has been cited in several major reviews (28,58), there is an undiscovered flaw in their analysis. Once corrected for, the methods described by Azuma and Oka show that critical closure of arteriolar vessels as originally described by Burton, and modified by Permutt and Riley, can occur under certain conditions. The following section first describes Burton's analysis in detail, then Azuma and Oka's analysis, and finally, my revision of Azuma and Oka's analysis after correcting their error.

1.2. THE PHYSICS OF FLOW

1.2.a. Poiseuille's Law

In 1840, Poiseuille developed the following equation which relates pressure and flow through a rigid cylinder:

$$\Delta P = 128 \frac{\mu L}{\pi d^4} \dot{Q} \qquad \text{.....(1.1)}$$

where ΔP is the pressure drop across the cylinder, μ is the viscosity of the fluid, L is the length of the cylinder, $\dot{Q}$ is flow, and d is diameter (24). This equation can be simplified to resemble Ohm's Law for an electrical circuit

$$\Delta P = \dot{Q} * R \quad \text{.....(1.2)}$$

where R is resistance and is equal to

$$R = 128 \frac{\mu L}{\pi d^4} \quad \text{.....(1.3)}$$

Vascular physiologists often rearrange the equation to describe the determinants of flow through a vascular bed:

$$\dot{Q} = \frac{P_{per} - P_v}{R_{tot}} \quad \text{.....(1.4)}$$

where P_{per} is the perfusion pressure, P_v is the venous pressure, and R_{tot} is the total resistance of the vessels between the two. If one assumes a constant vessel length (89) and constant blood viscosity, then resistance changes are indicative of changes in vessel diameter. Furthermore, if intravascular pressures are measured at various sites along the arteries and veins, the total resistance of the vascular bed can be divided into an arterial resistance, microcirculatory resistance, and venous resistance (12-14).

Although Poiseuille's Law is routinely used by vascular physiologists, there are several assumptions that are not valid for the circulation. These include constant viscosity, laminar flow, and modelling the vessels as straight, rigid cylinders.

Assumption 1: Viscosity

There are several factors in the circulation that affect blood viscosity. First, because blood contains large particles (i.e. cells), it is not a Newtonian fluid. Unlike a Newtonian fluid in which viscosity is independent of shear rate, there is a decrease in the apparent viscosity of blood with increases in shear rate because of 1) the deformation and rotation of individual red cells, and 2) the breakup of rouleaux formations (24). The relationship is asymptotic, with rapid declines in viscosity as

shear rate is increased from 0.1 to 10 s^{-1}. At shear rates between 10 and 1000 s^{-1} (e.g. femoral artery $\approx$170 s^{-1}), the viscosity decreases only slightly with increases in shear rate, and viscosity is constant at shear rates above 1000 s^{-1} (arterioles and capillaries) (24).

Second, the apparent blood viscosity increases with increasing hematocrit (134). Since the cells do not deform as easily as the plasma in which they are suspended, there must be an increased deformation of the plasma at any given flow as the concentration of cells is increased (24). This translates into an increased energy dissipation (i.e. greater pressure drop) for higher hematocrits. Based on Poiseuille's Law, an increased pressure drop must be due to an increase in viscosity if the length and diameter are kept constant. Furthermore, in blood, a second fluid-solid interface exists between the red blood cell wall and the plasma in addition to the fluid-solid interface at the vessel wall (24). Therefore, there is an additional shearing rate which increases the energy dissipation, and thus increases the apparent viscosity. The effect of hematocrit on apparent blood viscosity means that whenever resistance is calculated *in vivo*, hematocrit should be maintained constant through saline infusion (to replace fluid losses) or blood infusion (to replace hemorrhagic losses).

A third factor affecting blood viscosity is plasma skimming (24). When blood flows through large vessels, the red blood cells migrate toward the center and leave a plasma-rich area near the vessel wall. Since the blood supply to a small vessel branching off the larger vessel comes from the region near the wall, the hematocrit in the small vessel will be less than the large vessel, and consequently the viscosity will be less.

Finally, the Fårhaeus-Lindqvist effect says that apparent blood viscosity decreases as the tube diameter decreases below 1 mm (39). This is because the cell-free plasma layer adjacent to the vessel wall occupies a greater percentage of the vessel lumen as the vessels become smaller.

The apparent blood viscosity in the large arteries is therefore affected by changes in flow that accompany changes in perfusion pressure. This effect is not observed in the microcirculation (arterioles, capillaries, and venules) because apparent blood viscosity is constant at the high shear rate present in these vessels. Apparent blood viscosity may be different in different vessels due to plasma skimming and the Fårhaeus-Lindqvist effect.

Assumption 2: Laminar Flow

Poiseuille's Law accounts for the energy loss due to viscous forces that occur during laminar flow, but not for the energy loss due to inertial forces that occur during turbulent flow. Turbulent flow occurs when the Reynolds number is greater than 2500 (24). The Reynolds number is a dimensionless term that represents the ratio of inertial to viscous forces and is given by the equation

$$Re = \frac{inertial\ forces}{viscous\ forces} = \frac{\rho U d}{\mu} \qquad \text{.....(1.5)}$$

where Re is the Reynolds number, ρ is the density of the fluid, U is the mean fluid velocity, d is the diameter of the tube, and μ is the viscosity of the fluid. Inertial energy loss is relatively minimal in the microcirculation since the Reynolds number is only 0.09 in the arterioles, and decreases even further in the capillaries (24). However, the peak Reynolds number for the descending aorta is 3400 and turbulence should occur. Therefore, resistance calculations of the aorta based on Poiseuille's Law may lead to erroneous conclusions about changes in vessel diameter. The peak Reynolds number in the femoral artery is normally around 1000 during resting flow (24), but may increase above 2500 when flow increases during exercise.

Since flow at the entrance of a tube is never Poiseuille Flow (e.g. any bifurcation), and the arterial tree repeatedly divides, there are numerous regions of non-Poiseuille Flow in the circulation. The length of the tube downstream from the bifurcation before Poiseuille Flow returns is known as the entrance region. When the

Reynolds number is less than 1, the entrance region extends for only one diameter of the tube. This means resistance calculations in the microcirculation (e.g. arterioles and capillaries) should represent a good approximation of the true resistance to flow (24). In the larger vessels, the entrance length can be predicted by the formula

$$X=0.03d\ (Re) \quad \text{.....(1.6)}$$

where X is the entrance length before laminar flow exists, d is the diameter of the tube, and Re is the Reynolds number. Thus, the entrance length for the femoral artery with a Reynolds number of 1000 and an internal diameter of 0.4 cm, is 12 cm (24). Therefore, resistance calculations of this region must take into account non-Poiseuille Flow and should not be calculated with Poiseuille's Law.

Assumption 3: Vessel Shape and Rigidity

The circulation is not a single tube and a certain percentage of blood vessels are closed during normal perfusion (8). Decreasing vasomotor tone may result in recruitment of previously closed vessels, and an overestimation of changes in vessel diameter as predicted by Poiseuille's Law. Furthermore, Poiseuille's Law is only true for straight cylinders, whereas the large vessels are often curved (e.g. aortic arch). As the blood is forced around the curve, energy is lost. Therefore, the pressure drop across these vessels is greater than predicted by Poiseuille's Law (24).

Finally, the arterioles sometimes exhibit vasomotion which means their diameter oscillates about a mean value (121). Under these conditions, the effective resistance is less than the resistance calculated using the mean radius (121). For example, if a vessel has a constant radius of 1 unit (i.e. resistance=1 unit), and the pressure gradient across the vessel is 100, then flow is equal to 100. To illustrate the effect of vasomotion, let us say that the vessel radius oscillates in a square-wave manner between 2 units (resistance=1/16 units) and 0 units (resistance=infinity), and spends 50% of its time in each state (i.e. mean radius equals 1). Under these conditions, when

the radius=2, flow=1600, and when the radius=0, flow=0. Since the vessel spends equal time in each state, the average flow is 800. Thus, for the same mean radius, flow is much greater when vasomotion occurs (i.e. the effective resistance is less). This effect is dependent on the amplitude of the oscillations, and also on the pattern of oscillations (i.e. sinusoidal-wave, square-wave, etc). Therefore, when vasomotion occurs, calculations of changes in vessel diameter based on resistance changes (and vice versa if the mean radius is used) will lead to inaccurate conclusions.

In summary, the application of Poiseuille's Law in the large arterial vessels is not appropriate because viscosity is dependent on flow rate, turbulent flow exists, the entrance length is large, and the vessels are curved. However, in the microcirculation, viscosity is independent of flow rate, the entrance length is minimal, and flow will be laminar except at large curves of the vessels. Therefore, one might suggest the application of Poiseuille's Law in the microcirculation creates only a small error. However, Poiseuille's Law actually creates a large error because it applies to flow through rigid cylinders. Blood vessels, which can be compressed by external forces, could also be modelled as collapsible tubes which close when the extraluminal pressure is greater than the intraluminal pressure (107). Flow under these conditions is therefore partially dependent on the forces compressing the vessel. Since the extraluminal pressure is not incorporated into Poiseuille's Law, some modifications to equation 1.1 are required to accurately describe the physical determinants of flow through collapsible tubes. Before discussing these modifications, I will first review the theoretical analyses which discuss the possibility of arteriolar vessel closure.

1.2.b. Do Arterioles Collapse?

Some authors have hypothesized that arteriolar vessels will be forced close if the pressure generated by the arteriolar smooth muscle tone is greater than the intraluminal pressure (23,107). There has been much disagreement in the literature about whether

or not arteriolar vessels collapse. Based on theoretical analyses, there are those who believe they do and quote Burton (23), and those who believe they do not and quote Azuma and Oka (5). This section discusses each of their assumptions, points out the fallacies in both, and shows that vessels can collapse under certain conditions.

Burton's Analysis

In 1951, Burton and colleagues showed that arterial pressure remains well above venous pressure at zero flow (102). To explain these findings, Burton hypothesized that arteriolar vessels act as collapsible tubes and close when the intravascular pressure declines below a critical value which they called the critical closing pressure (P_{crit}). A brief description of his theoretical analysis is provided below (23).

Based on the Law of Laplace for a cylinder, Burton noted that wall tension of a blood vessel is equal to

$$T_w = P_{tm} * r \quad \text{.....(1.7)}$$

where T_W is wall tension, P_{tm} is transmural pressure, and r is the radius of the cylinder. He pointed out that T_W has three components, elastic tension (T_E) generated by tissue elastance if the wall is stretched, active tension generated by the smooth muscle (T_A), and interfacial tension due to the interaction between the intravascular fluid and the surface wall. In addition, since the external pressure of a blood vessel is usually assumed to be atmospheric and was used as the reference point, P_{tm} was simplified to be the intravascular pressure, P_{in}.

In his analysis, Burton superimposed the graph for T_W versus radius based on Laplace's Law (a straight line through the origin with a slope equal to the intraluminal pressure (P_{in}) from equation 1.7), with a graph of T_E versus radius for the relaxed vessel (i.e. $T_A=0$, figure 1.5a). At equilibrium, the expanding forces are balanced by the passive stretch of the relaxed wall, and the radius is r_1 (point A). If the smooth muscle develops tone, the vessel contracts to a new radius r_2 at point B. The total wall

tension is the sum of the passive elastic tension (T_E) and the smooth muscle active tension (T_A).[8] Burton pointed out that if the radius exceeds r_1 without a change in active tension, the elastic wall tension will exceed the wall tension produced by the intravascular pressure and the vessel will return to the equilibrium state at r_1.

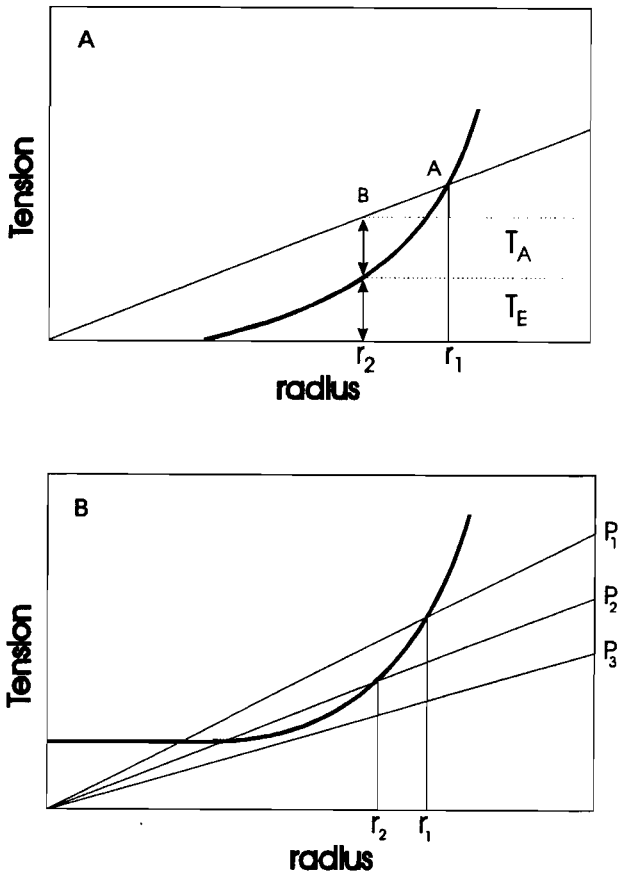

Figure 1.5: A plot of wall tension versus radius. In A, the straight line through the origin (with a slope equal to the intravascular pressure) gives the intravascular tension at any given radius as calculated by the Law of Laplace. The dark curved line represents the passive elastic tension of the wall at any given radius. If the vessel has no tone, then the vessel

[8] Interfacial tension is small and was not included in this part of Burton's analysis.

radius is r_1, since this is where the intravascular tension and wall tension are in equilibrium (point A). If the vessel develops tone and the lumen decreases to r_2 (point B), then the total wall tension is given by the sum of the passive elastic tension (T_E) and the active tension (T_A). In B, the wall tensions for several different intravascular pressures are given ($P_1 > P_2 > P_3$). The dark solid line represents the same vessel as Panel A, but T_A is kept constant (i.e. the graph of Tension versus radius is shifted upwards by T_A). If the intravascular pressure declines from P_1 to P_2, the equilibrium point changes and the vessel shortens from r_1 to r_2. However, if the pressure declines further to P_3, the wall tension is always greater than the intravascular tension and therefore the vessel is forced closed (adapted from Burton, (23)).

Figure 1.5b is also a plot of tension versus radius. The dark solid line now represents the theoretically possible **total wall tension** when T_A is kept constant at some positive value, i.e. the T_E versus radius graph in figure 1.5a is shifted upwards by a constant value equal to T_A. Note that once the radius is shorter than the "unstretched radius" in figure 1.5a (i.e. $T_E=0$), T_W is constant and is equal to T_A. If P_{in} is P_1, the equilibrium tension would occur at a radius equal to r_1, and if it is P_2, the equilibrium tension would occur at a radius equal to r_2. However, if the pressure is P_3, T_W is always greater than the tension generated by the intravascular pressure, i.e. the forces tending to close the vessel are greater than the forces keeping it open and the vessel collapses. Burton called the intraluminal pressure below which the vessels closed, the "critical closing pressure" (P_{crit}).

There are two major problems in Burton's analysis. The first is that arterioles are thick-walled vessels whereas his analysis used the Law of Laplace which is only suitable for thin-walled vessels. Burton argued that one could model the wall as if it

were made of several different layers of tissue, and the mean of the tensions across all the layers represents the average tension across the wall. This assumption was later shown to be incorrect by Azuma and Oka (see below) (103). The second problem was that the rigidity of thick walled vessels might prevent complete closure. However, he pointed out that this is only a theoretical problem since thick walled vessels are often observed to close when their wall is traumatized.

In summary, Burton hypothesized that arteriolar vessels will close when the intravascular pressure declines below a critical value. In Burton's analysis, the vessel would have a sizeable lumen just above the critical closing pressure, and suddenly close when the pressure was decreased below P_{crit}. In addition, his analysis predicts that flow through the open vessel is governed by Poiseuille's Law, and that flow into a region is immediately affected by changes in venous pressure or resistance.

Azuma and Oka's Analysis

Burton's analysis assumed that Laplace's Law can be applied to thick-walled vessels. However, Azuma and Oka (5,103) argued that Laplace's Law cannot be used for a thick cylindrical wall that is homogenous, isotropic, and has Hookean elasticity. Instead, they developed a general formula for wall tension that could be applied to any cylinder regardless of its homogeneity, isotropicity, or length-tension characteristics. Their equation was:

$$T_w = P_i r_i - P_e r_e \quad \text{.....(1.8)}$$

where P_i and P_e represent the internal and external pressures respectively (in mmHg), and r_i and r_e represent the internal and external radii respectively (103). Azuma and Oka suggested that critical closure of blood vessels as discussed by Burton (23) is theoretically impossible (5). In their analysis, arteriolar closure could occur, but it depends only on smooth muscle tone, and is independent of the intravascular pressure. If true, this means that if T_A is high enough to cause the vessel to collapse, no amount

of intravascular pressure can open the vessel. Thus, their theory did not contradict the observation that vessels close when the lumen is traumatized. However, it did contradict Burton's theory that vessels collapse when the intravascular pressure is lowered below a critical value (23).

An important point in Azuma and Oka's analysis was that Burton's use of atmospheric pressure as zero was arbitrary. Instead, they argued that the absolute pressure in mmHg should be used to calculate wall tension. Since r_e is always greater than r_i, equation 1.8 means that unless $P_i=P_e=0$, wall tension must be negative at zero transmural pressure. In a thick walled arteriole with $r_i=10$ um, $r_e=20$ um, and $P_e=760$ mmHg, the wall tension is negative until the internal pressure reaches 1520 mmHg. Azuma and Oka therefore concluded that under physiological conditions, the vessel wall is always being compressed (negative wall tension).

If $P_i>P_e$, how can wall tension be negative? According to Newton's Second Law, a stationary object experiences no net force. At an atmospheric pressure of 760 mmHg, the external force tending to collapse a vessel segment is the outside pressure multiplied by the surface area i.e. $760*2\pi r_e l$ where l is the length of the vessel segment. The internal force tending to expand the vessel is $760*2\pi r_i l$. Since $r_e>r_i$, the compressive force is greater than the expansive force. If the wall is in equilibrium, there must be a force resisting the compression, i.e. the mean wall tension is negative.

Azuma and Oka based their analysis on several principles that must be reviewed. First, the Law for Conservation of Mass means that the volume of a thick-walled vessel cannot change when the vessel constricts. If the arterial tree is tethered at either end thereby fixing length, then cross-sectional area of the wall must be constant. This has been studied *in vivo*, and no significant difference in cross-sectional area was noted with changes in perfusion pressure (89). Therefore:

$$r_e^2-r_i^2=\frac{K}{\pi}=k^2 \qquad \text{.....(1.9)}$$

where K and k are constants. Solving this equation for r_e and substituting into equation 1.8 gives:

$$T_w = P_i r_i - P_e\sqrt{(k^2 + r_i^2)} \quad \text{.....(1.10)}$$

When the vessel is collapsed, $r_i = 0$ and the wall tension equals

$$T_w = -P_e * k \quad \text{.....(1.11)}$$

In figure 1.6, T_W is plotted against internal radius for a vessel with a cross-sectional area of 942 um (e.g. $r_i = 10$ um and $r_e = 20$ um). These dimensions were chosen because vessels with internal diameters of 10-20 um have been shown to close when sympathetic activity is increased (8).

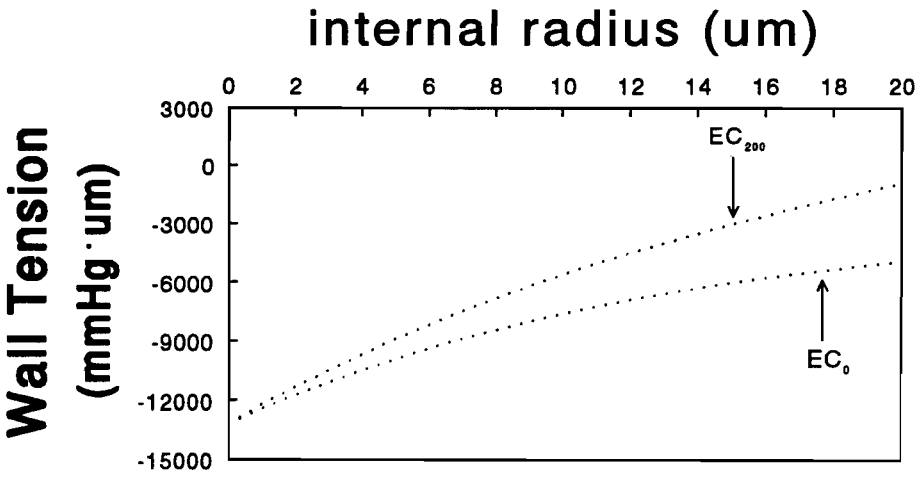

Figure 1.6: Wall tension is plotted against the internal radius (um) of a hypothetical vessel with a cross-sectional wall area of 942 um (e.g. $r_i = 10$ um and $r_e = 20$ um). The dotted line EC_0 represents the equilibrium tension curve for the vessel when the internal and external pressure both equal 760 mmHg (transmural pressure, $P_{tm} = 0$ mmHg). The dotted line EC_{200} represents the equilibrium tension curve for the same vessel when the external pressure=760 mmHg, and the internal pressure=960 mmHg. These equilibrium curves represent all the

possible wall tensions and internal radii that can exist for this vessel under the specified pressure conditions, and are analogous to the straight lines through the origin illustrated in figure 1.5b. The actual radius or wall tension will depend on the smooth muscle tone (see figure 1.8).

Line EC_0 is called the equilibrium curve and represents all the possible wall tensions for the vessel when $P_e=P_i=760$ mmHg ($P_{tm}=0$). In Burton's analysis, the equilibrium curve was the straight line through the origin with a slope equal to the intravascular pressure. Similar to Burton's analysis, the actual value of T_W requires information about the elastic tension curve of the vessel, and T_w cannot be discerned simply from the equilibrium curves (see below). If P_i is increased to 960 mmHg (line EC_{200}), the equilibrium curve rotates counter-clockwise (equivalent to a change in slope in Burton's analysis), and the wall tension is increased (i.e. less negative) at the same radius because P_i is increased. The y-intercept however, is unchanged because it is only dependent on P_e (equation 1.11).

The elastic tension curve of a vessel is dependent on its resistance to stretch and is derived from the pressure-volume curve of the vessel (this assumes no reflex adjustments in vessel diameter). Figure 1.7 (solid line) shows a hypothetical pressure-volume curve for a short vessel segment when $P_e=760$ mmHg. Note that the y-axis is plotted as transmural pressure. Under the specified hypothetical conditions, this vessel has an "unstressed volume" of 100 units (1 unit=volume of vessel when $r_i=1$ um), and internal pressure only begins to rise when the volume is increased above this level. In order to decrease r_i below 10 microns, transmural pressure must become negative. Azuma and Oka extrapolated the elastic tension curve by increasing external pressure, and calculated the theoretical wall tension. The dotted line represents the extrapolation and I have kept the shape sigmoidal in order to be consistent with Azuma and Oka's analysis.

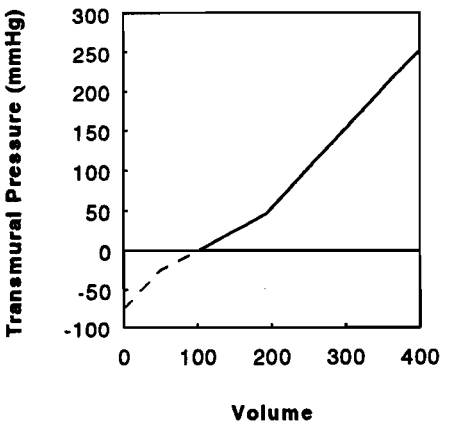

Figure 1.7: A hypothetical pressure-volume curve for a vessel with the same wall cross-sectional area as figure 1.6. P_{tm} is measured in mmHg. For volume, 1 unit represents the volume of a vessel with an internal radius of 1 um and a fixed length. The solid line represents P_{tm} obtained by increasing intravascular pressure above 760 mmHg. The dashed line represents an extrapolation of P_{tm} below 0 mmHg by increasing external pressure above 760 mmHg, or by decreasing internal pressure through the application of negative pressure. The shape of the curve is sigmoidal in order to be consistent with the analysis of Azuma and Oka (5).

Azuma and Oka converted the pressure-volume curve to a tension-radius graph, and superimposed it over the equilibrium curves just as Burton had done (figure 1.8a). The actual radius of the vessel wall at a given P_i is derived from the intersection of the elastic tension curve and the equilibrium curve.

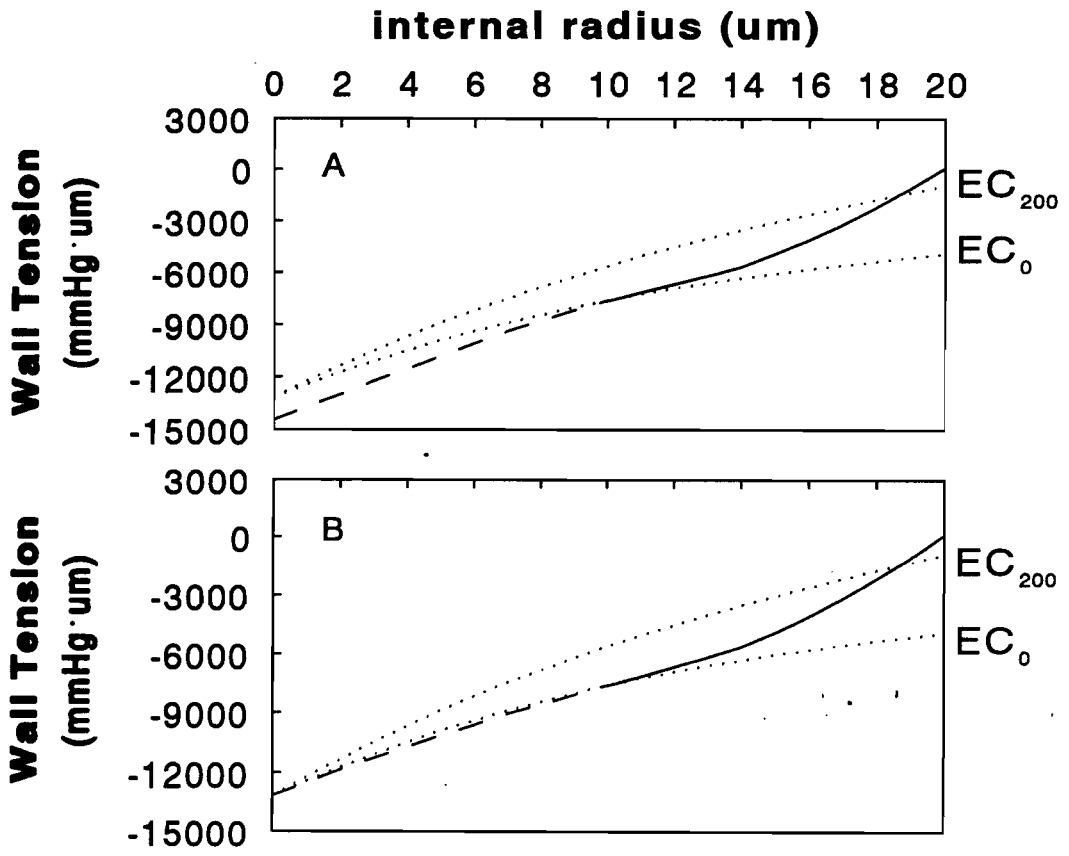

Figure 1.8: In A, the elastic tension curve calculated from the pressure-volume relationship in figure 1.7 is superimposed on the equilibrium curves in figure 1.6. The solid line represents the elastic tension curve for $P_{tm} > 0$ mmHg obtained by increasing internal pressure. The dashed line represents the extrapolation of the elastic tension curve that would be obtained if P_{tm} is decreased below 0 mmHg through an increase in external pressure. The vessel radius at a given internal pressure is given by the intersection of the equilibrium curve for that pressure, and the elastic tension curve. In B, the dashed line now represents the elastic tension curve obtained when P_{tm} is decreased below 0 mmHg through a further decrease in internal pressure. The shape of the elastic tension

curves are different, even though they were obtained from the same pressure-volume curve.

In figure 1.8a, r_i=10 at a P_{tm}=0. At a P_{tm}=200, r_i≈19.5 um. If smooth muscle tone is increased, Azuma and Oka said the elastic curve would shift upwards thereby affecting the y-intercept. When smooth muscle tone increased enough to cause closure at P_{tm}=0 (line EC_0), the vessel would also be closed for P_{tm}=200 (line EC_{200}). Therefore critical closure of the vessel wall would be dependent only on smooth muscle tone, and would be independent of internal pressure.

Azuma and Oka's Analysis Revisited

In their analysis, Azuma and Oka superimposed equilibrium tension curves for a vessel of a given cross-sectional area, with a hypothetical elastic tension curve for the vessel. Both the equilibrium curves and the elastic tension curves at positive P_{tm} were calculated with a constant external pressure. However, Azuma and Oka then calculated the elastic tension curves at negative transmural pressures by continuously increasing the external pressure. This shift in the reference point means the equilibrium curves are no longer valid because they refer to a vessel with a constant external pressure. The authors should have obtained the elastic wall tension curves for negative P_{tm} by decreasing internal pressure below 760 mmHg instead of increasing the external pressure. This is important because $r_i \neq r_e$ and therefore the calculated total wall tension will be different depending on whether P_i or P_e is changed (equation 1.8). Figure 1.8b shows the change in wall tension when P_{tm} is decreased by lowering P_i instead of raising P_e. The y-intercept of the elastic tension curve is the same as the equilibrium curves if P_e is unchanged because the wall tension must equal $-P_e*k$ at r_i=0. When smooth muscle tone is increased, an external force is applied and the elastic tension curve will change shape. However, the y-intercept of the tension versus radius graph

still remains constant because it must be equal to P_e*k at r_i=0. Correcting this small error in Azuma and Oka's analysis results in very different conclusions.

In order to examine the effects of increasing smooth muscle tone on the shape of the elastic tension curve, one must first study the effects on the pressure-volume curve. Figure 1.9 shows that when vessel tone is increased, the pressure-volume relationship may theoretically be shifted upwards (a change in capacitance, dashed line), rotated to the left (a change in compliance, broken line), or a combination of both (not shown). I will first examine what happens if the curve is shifted upwards.

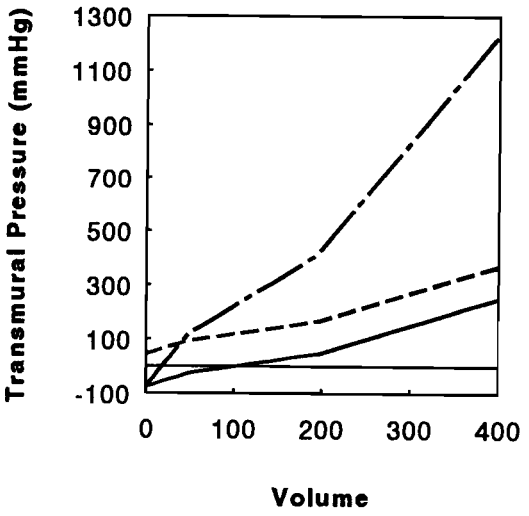

Figure 1.9: Theoretical changes in the pressure-volume curve of figure 1.7 (solid line) that might occur if smooth muscle tone is increased. An increase in tone may cause a parallel upward shift in the curve (dashed line, y-intercept=45.5 mmHg), a change in the slope (broken line), or a combination of both (not shown).

According to the pressure-volume curve, the vessel lumen is closed until the internal pressure exceeds the external pressure by a critical value (45.5 mmHg). After the lumen opens, pressure increases as volume is injected.

The new pressure-volume curve can now be converted into an elastic tension curve. The change in the shape of the elastic tension curve is not the same as the pressure-volume curve because Tension $\propto r_i$ but volume $\propto r_i^2$. This actually represents a second fault in Azuma and Oka's analysis. They extrapolated the tension-radius graph to yield a sigmoidal shape, since the aorta pressure-volume curve was sigmoidal. However, the slope of the graph in their paper at small and large radii are almost identical, implying a pressure-volume curve with a very steep initial slope and only a gradual slope at higher volumes. In fact, the pressure-volume curve of a vessel is very steep at high volumes, presumably due to the low compliance of the outer fibrous layer (70).

Figure 1.10 shows equilibrium curves for EC_0, EC_{20}, EC_{40}, EC_{100}, EC_{200}, and the shift in the elastic tension curve when vessel tone is increased.

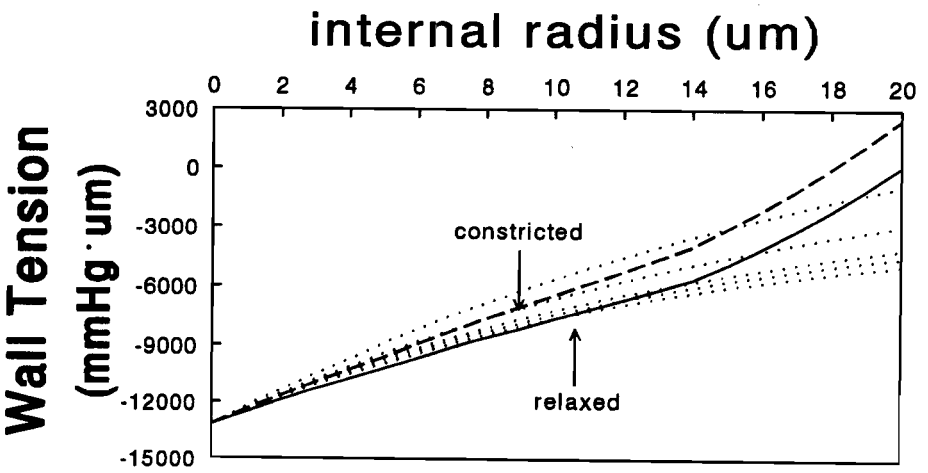

Figure 1.10: This graph of wall tension versus radius shows five different equilibrium curves (dotted lines) for the hypothetical vessel in figure 1.7 with external pressure always equal to 760 mmHg. The five curves represent P_{tm} of (from inferior to superior) 0 mmHg, 20 mmHg, 40 mmHg, 100 mmHg, and 200 mmHg. The solid line represents the elastic tension curve in figure 1.8b, whereas the dashed line represents

the elastic tension curve if smooth muscle activation causes a parallel upward shift in the pressure-volume curve of the vessel (figure 1.9 - dashed line). Although all the lines appear to converge below a radius of 2 um, it can be shown that the elastic tension curve with increased smooth muscle tone never intersects the EC_{40} curve (see figure 1.11).

First, in contrast to Azuma and Oka's analysis, increasing smooth muscle tone does not affect the y-intercept because their equation predicts that T_W at zero radius is constant if P_e and wall cross-sectional area are kept constant (equation 1.11). Under conditions of increased smooth muscle tone, the elastic tension curve rotates to the left, and intersects EC_{200} at a smaller radius.

The analysis can also be used to predict the critical closing pressure. In figure 1.10, there is a clear intersection of the elastic tension curve with both EC_{200} and EC_{100}. If critical closure is to occur at 45.5 mmHg as the pressure-volume curve predicts (dashed line in figure 1.9), there should be no intersection between the elastic tension curve and the equilibrium curves EC_{40} or EC_0 (EC_{40} was chosen instead of $EC_{45.5}$ for clarity). However, all the lines in the figure appear to converge below r_i=3. Figure 1.11 is therefore an enlargement of figure 1.10 at r_i=1 um. Since the elastic tension of the constricted vessel wall is greater than the equilibrium tension of EC_{40}, the vessel will continue to close. It can be shown that this occurs until r_i=0 for any equilibrium curve of 45.5 mmHg or less, and the vessel therefore exhibits critical closure at a P_{tm}=45.5 mmHg.

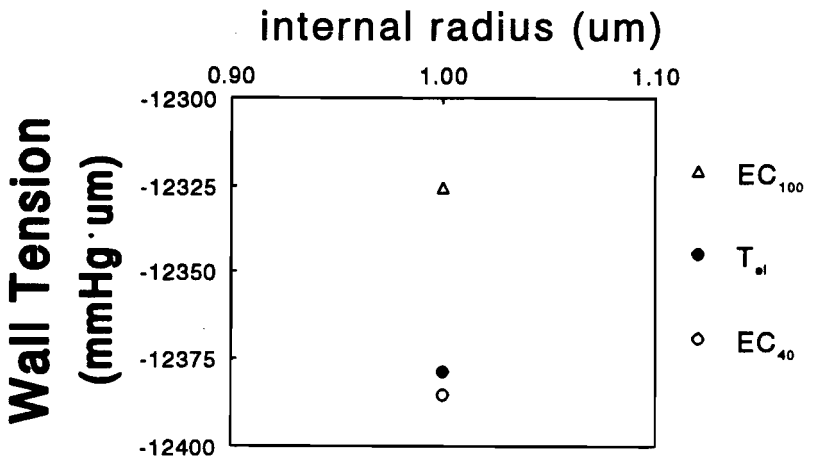

Figure 1.11: An enlargement of figure 1.10 at an internal radius of 1 um. The elastic tension of the vessel with increased tone (T_{el}) is still greater than the EC_{40} curve. The vessel wall will therefore continue to constrict if intravascular pressure is only 40 mmHg.

The preceding analysis assumed that an increase in smooth muscle tone caused a parallel upward shift of the pressure-volume curve. However, it is also possible that the curve rotates instead of shifting, i.e. a change in compliance rather than a change in capacitance (figure 1.9, broken line). If this occurred, the elastic diagram would still rotate to the left (figure 1.12). The elastic tension curve would continue to intersect every equilibrium curve it had previously intersected, but the radius at the intersection points would be decreased. In figure 1.12, r_i would change from 10 um to 4.5 um if smooth muscle tone increased and P_{tm} was kept constant at zero. Critical closure would effectively exist when the red blood cells could no longer squeeze through the lumen (≈2-3 um).

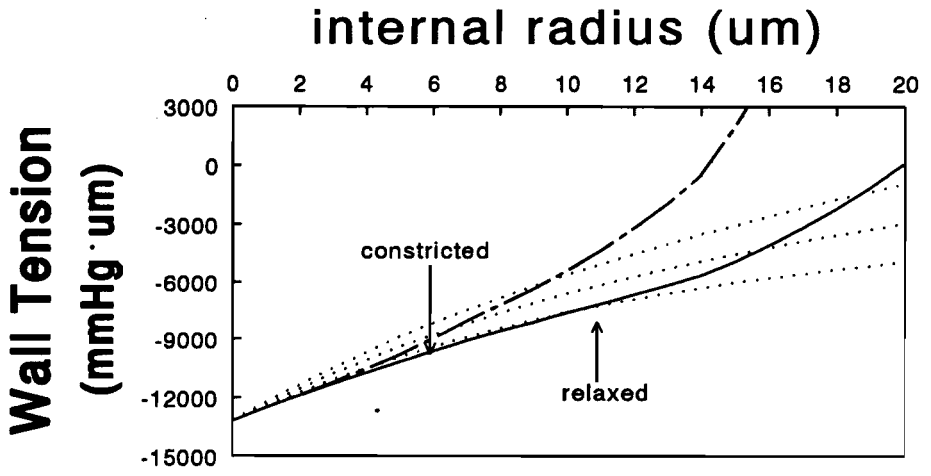

Figure 1.12: Equilibrium curves for P_{tm}=0, 100, and 200 mmHg (external pressure=760 mmHg), and the shift in the elastic tension curve that would occur if the slope of the pressure-volume curve is affected by smooth muscle activation (figure 1.9 - broken line). In this example, smooth muscle activation (keeping P_{tm}=0) decreases the internal radius from 10 um to 4.5 um, and decreases the total wall tension (more negative).

Discussion of the Models

Using the same formula for wall tension as Azuma and Oka (5,103), I have shown that critical closure can theoretically exist in the arterial vasculature if the pressure-volume curve for a short segment of the arterial tree corresponds to the dashed line in figure 1.9. The dynamic pressure-volume curve of the microvascular tree is unknown. Experimentally, Baez et al. used *in vivo* microscopy and observed critical closure of metarterioles and precapillary sphincters during steady-state measurements following intravascular pressure reductions in an isolated intestine preparation (6,7).

Thus, correcting the false assumption in Azuma and Oka's analysis reconciles the theoretical analysis with experimentally obtained results.

A few salient points of my analysis should be discussed. Some authors have commented on the folding of the endothelium and internal elastic lamina that occurs with blood vessel constriction (47). My analysis, and that of Azuma and Oka's, assumes the lumen to be circular. This simplification only means that closure would exist at a higher pressure than the analysis predicts. For example, a relaxed vessel that is distended by intravascular pressure will have a circular internal and external circumference. If the vessel wall contracts, the new external r_e can be measured. One can then calculate the total lumen area by subtracting the total wall cross-sectional area (which is unaffected by vessel contraction) (89). r_i represents the maximal radius possible for this calculated total lumen area. If folds exist, the area actually available for blood flow is the calculated total lumen area minus the area between the folds. Therefore, the effective lumen area is smaller than the calculated total lumen area, and blood flow will cease even when the calculated r_i is well above zero (i.e. P_{crit} is higher than predicted).

In order for the vessel to close, smooth muscle shortening must occur. *In vitro* and *in vivo*, smooth muscle shortens only 30-40% (109). Therefore, Alexander suggested that the smooth muscle must be helical and have a pitch of 30-45 degrees in order for the lumen to close (1). However, the amount of shortening required to obliterate the lumen of a thick-walled vessel is affected by the ratio of r_i to r_e. For example, using the vessel described in my analysis (r_e=20 um, r_i=0.5r_e at full relaxation and zero transmural pressure), the external smooth muscle layer only has to shorten 13.5% to obliterate the lumen (i.e. r_e=17.3 um). If r_i=0.7r_e, then 28.6% shortening must occur before closure results. Therefore, vessel closure does not require helical arrangement of smooth muscle cells in the arterioles, although such an

arrangement would decrease the magnitude of the smooth muscle tension necessary to cause vessel closure.

Finally, several control systems interact to determine the new vessel diameter following an increase in perfusion pressure. These are discussed in the section on vessel tone and include central factors, the myogenic response, endothelial-derived factors (EDRF, prostaglandins), metabolic stimulus, and passive mechanics of the vessel wall. Thus far, my analysis dealt only with the equilibrium states that are present during stable conditions. If perfusion pressure is increased, myogenic reflexes and metabolic control would tend to increase smooth muscle tone, whereas EDRF would decrease tone. Observations in cat skeletal muscle arterioles show an immediate dilation of the vessels when the pressure is increased, followed by a constriction to a radius below the previous level (17). Figure 1.13 shows how these vessel diameter changes might occur as predicted by the model. First, an increase in pressure from 100 mmHg to 200 mmHg results in an increase in radius from point A to point B along the elastic tension curve. This is followed by an increase in smooth muscle tone shifting the elastic tension curve to the left, and a decrease in radius to point C. The radius is now less than the original point A, and the total wall tension is greater (less negative). The model also illustrates that P_{crit} is dependent on tone and not diameter. For instance, if the increase in smooth muscle tone following the pressure rise was not as great as shown in figure 1.13, curve C would have intersected EC_{200} at a radius which was still greater than control conditions. Although the vessel would be dilated compared to control, P_{crit} would still be increased.

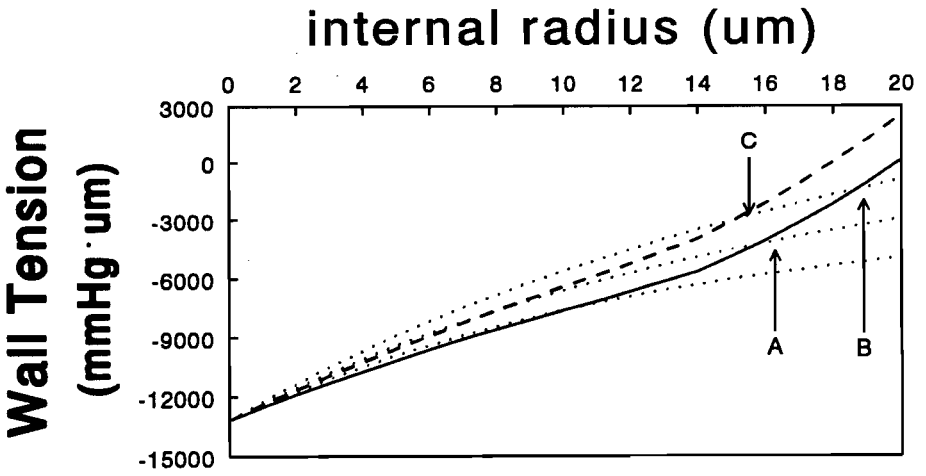

Figure 1.13: This figure illustrates how the model would predict wall tension and radius changes if myogenic reflexes were present. Equilibrium curves EC_0, EC_{100}, EC_{200}, and the elastic tension curves in figure 1.10 are superimposed. Point A refers to the starting point at P_{tm}=100 mmHg. An increase in intravascular pressure to 200 mmHg causes movement along the elastic tension curve to Point B, and therefore an increase in radius. When the myogenic reflex increases vascular tone in response to the increased perfusion pressure, the elastic tension curve is rotated to the left, and now intersects EC_{200} at Point C. This represents a radius smaller than that at P_{tm} of 100 mmHg. The final internal radius will be dependent on the strength of the myogenic response, and might be less than or greater than the original radius. The critical closing pressure however, will always be increased with increases in smooth muscle tone.

In summary, I have shown that Azuma and Oka's conclusion that critical closure cannot exist is based on a false assumption. Once corrected, the model shows that arterioles can theoretically exhibit a critical closing pressure. The critical closing

pressure is dependent on the tone of the smooth muscle and not the absolute vessel diameter. Furthermore, this analysis suggests that the vessels gradually close as intraluminal pressure is reduced, whereas Burton's analysis suggested a sudden collapse of the vessels. Since Poiseuille's Law assumed a rigid tube, it cannot be applied to a model incorporating a collapsible segment. I will now discuss the effects of a collapsible segment on the physical determinants of flow, and how the incorporation of a collapsible segment at the arteriolar level can explain both the zero-flow pressure intercept and waterfall behaviour noted in the section "History of Pressure-Flow Relations".

1.2.c. Effects of a Collapsible Segment on Flow

Once one accepts that closure of vessels is theoretically possible, the next step is to discuss the mechanism behind waterfall behaviour and the zero-flow pressure intercept.

Starling's Variable Resistor

In 1912, Knowlton and Starling diverted aortic blood flow through a collapsible rubber tube placed within a pressurized chamber in an attempt to control arterial pressure (82). They found that if the chamber pressure was greater than the downstream pressure, the tube collapsed and the pressure in the aorta was equal to the pressure surrounding the collapsible tube over a wide range of flows. The authors suggested that this occurred because the collapsed segment of the rubber tube began to open as the flow rate was increased, and therefore resistance declined with increasing flow. Arterial pressure was maintained constant because the tendency towards an increased pressure with increases in flow was balanced by the tendency towards a decreased pressure with decreases in resistance. In honor of the principle investigator in the study, a collapsible tube placed inside a pressurized chamber has become known as the Starling resistor.

Although Starling used collapsible tubes as a method to control arterial pressure, it was Holt who showed that blood vessels sometimes act as Starling resistors *in vivo* (60). Holt studied the large veins as they entered the thorax, and found that decreases in right atrial pressure are only transmitted to the femoral vein if the right atrial pressure is above zero. Once right atrial pressure becomes negative, the great veins collapse near their entry into the thorax where the extraluminal pressure (outside the thorax) is greater than the pressure inside the vein. When veins collapse, femoral venous pressure is unaffected by further decreases in right atrial pressure. Holt concluded that veins are collapsible tubes and can act as variable resistors.

Waterfall Behaviour

The study of flow through collapsible veins was elaborated upon by Duomarco and Rimini (32). These authors brought attention to the importance of Bernoulli's Theorem and energy gradients in determining flow through collapsible tubes, rather than the previously stressed hydraulic (pressure) gradients used for rigid tubes. When the pressure surrounding a collapsible tube is greater than the intraluminal pressure, the cross-sectional area of the lumen decreases. The tube is no longer in the shape of a cylinder and Poiseuille's Law cannot be used. For example, the velocity of flow increases as tube diameter decreases. This results in the conversion of potential energy (pressure) into kinetic energy and is measured as a fall in pressure. If the tube diameter increases downstream, pressure rises as kinetic energy is converted back into potential energy. Therefore, in a non-cylindrical tube, flow can occur against a pressure gradient and it is the energy gradient that should be used to describe flow through the tube. Duomarco and Rimini used several examples to show that energy and hydraulic gradients are often dissociated in nature. One example is a river interrupted by a waterfall. In this situation, the altitude (pressure) of the river below the falls can be increased or decreased, without affecting the flow over the falls, unless the downstream river becomes higher than the falls themselves. This is analogous to

the effect observed by Holt previously noted, in which changes in right atrial pressure below atmospheric pressure were not transmitted to the femoral vein (60). The dissociation between downstream pressure/resistance and flow has therefore been called "waterfall behaviour" or "vascular waterfall" (107).

Permutt and Riley's Analysis

In 1963, Permutt and Riley used the waterfall concept to reinterpret Burton's results concerning the critical closing pressure in the arterial circulation. These authors hypothesized that if the arterioles act as collapsible tubes, then flow through the vascular bed should be governed by the physics of flow through collapsible tubes. In contrast to previous authors who hypothesized venous waterfalls, Permutt and Riley suggested that waterfall behaviour is present at the level of the arterioles. Furthermore, they hypothesized that if the outflow pressure (P_{out}) is less than the pressure surrounding the tube (P_{crit}), then flow is determined by the difference between the inflow pressure (P_{in}) and P_{crit}, divided by the resistance between the two (i.e. arterial resistance up to the site of vessel collapse). As in Duomarco and Rimini's waterfall model (32), downstream resistance (venous resistance) has no effect on flow through the collapsed vessel unless the waterfall is overcome. As I have shown in the section on "History of Pressure-Flow Relations", waterfall behaviour has been shown in the heart (38), liver (99), lung (126), and skeletal muscle (92). Finally, Permutt and Riley also hypothesized that flow is zero when P_{in} is less than P_{crit} (i.e. the altitude of the upstream river was lower than the falls).

Wave-Speed Hypothesis

Following Permutt and Riley's analysis, many authors began investigating flow through collapsible tubes using a penrose drain in a pressurized chamber. In contrast to Permutt and Riley's hypothesis, Conrad showed that flow occurred as soon as $P_{in} > P_{out}$, even when $P_{in} < P_{crit}$ (figure 1.14 (26)). Although the tube was collapsed, its shape was similar to a dumbbell and flow occurred through two side channels that

always remained open. As P_{in} was increased, flow increased linearly until $P_{in}=P_{crit}$. At this point, further increases in flow caused the length of the collapsed segment to become shorter as the tube began to open, and inflow pressure remained essentially constant. This was due to the decrease in resistance of the penrose drain (i.e. decrease in length of the collapsed segment) with increases in flow, as previously explained by Starling (82). Eventually, the tube opens completely and under these conditions, P_{in} increases as per Poiseuille's Law.

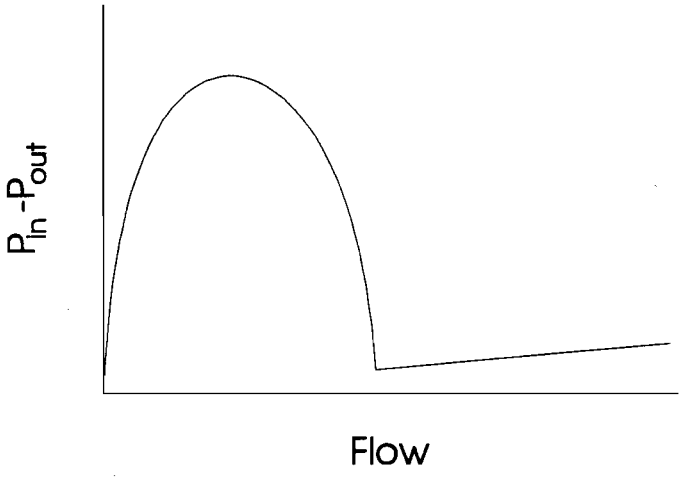

Figure 1.14: Inflow pressure (P_{in}) minus outflow pressure (P_{out}) is plotted against flow (adapted from Conrad (26)). Once P_{in} is greater than P_{out}, flow occurs through side channels and the slope of the line is approximately equal to the resistance of the collapsed tubing. As flow increases, P_{in} increases and when it exceeds P_{crit}, the tube begins to open. Further increases in flow cause the collapsed segment to open and P_{in} remains essentially constant. However, the increase in flow causes an increase in P_{out} because there is a fixed resistance downstream from where P_{out} is measured. Therefore, P_{in} minus P_{out} decreases with increases in flow. With any further increases in flow, the

continuous rise in P_{out} means P_{out} will eventually exceed P_{crit} and the collapsible tube will be fully open. The relationship between P_{in} and P_{out} then becomes linear with a slope equal to the resistance of the open collapsible tube.

The occurrence of flow when $P_{in} < P_{crit}$ is incompatible with the waterfall model as described by Permutt and Riley. Although one might suggest this is an artifact due to the low compliance of penrose tubing, no one has yet shown that higher pressures, or more compliant tubing, will eliminate the effect. Furthermore, Permutt and Riley's "critical closing pressure-waterfall hypothesis" does not explain the constant P_{in} with increasing flow that occurred in both Starling's and Conrad's experiments. Since the critical closing pressure-waterfall hypothesis did not correlate with the observed data using penrose drains, other hypotheses were proposed to explain the waterfall phenomenon of the Starling resistor.

In 1969 and 1971, Griffiths published a series of articles describing flow through collapsible tubing and used the term "flow-limitation" to describe "waterfall behaviour" (48-51). The term flow-limitation is appropriate because for a constant P_{in}, flow increases as P_{out} is decreased but reaches a maximum when $P_{out}=P_{crit}$. There is no further increase in flow as P_{out} is decreased below P_{crit}. Griffiths showed that flow-limitation could be due to transitions in "supersonic flow" to "subsonic flow" and a resultant hydraulic jump associated with energy dissipation through turbulence. This is analogous to the wave-speed limitation theory which suggests that decreasing downstream pressure results in the velocity of flowing fluid becoming greater than the wave-speed through the tube. Therefore, the increased fluid velocity cannot be transmitted upstream and flow-limitation occurs (77,119). In Griffiths analysis, flow limitation will occur if there is a sudden constriction in the vessel, and does not require that the vessels close when $P_{in} < P_{crit}$. Therefore, this analysis explains waterfall

behaviour, and does not contradict Conrad's experiments. On the other hand, Griffiths analysis does not explain the arterial-venous pressure gradient measured at zero-flow as observed in the previously mentioned section on the "History of Pressure-Flow Relations". The combination of Griffiths analysis and Azuma and Oka's analysis has been used to suggest that waterfall behaviour is not due to a critical closing pressure, and that the zero-flow pressure intercept is due to an as yet unexplained phenomenon. However, more recent experiments by Lyon et al. on the effects of the Reynolds number allow for a unifying hypothesis of all the observed data.

Reynolds Number and the Starling Resistor

In 1980, Lyon et al. examined the effect of the Reynolds number on flow through a Starling resistor (91). When they used a low viscosity fluid with a maximum Reynolds number of 2000 (water; 0.01 stoke), they obtained similar results to Conrad (26) in that flow occurred through side channels and increased linearly as soon as $P_{in} > P_{out}$, even though $P_{in} < P_{crit}$. Furthermore, at high flows, P_{in} remained essentially constant, and flow was associated with marked flutter of the tubing. In contrast to Conrad's experiments, Lyon et al. did not incorporate a resistance downstream from where P_{out} was measured, but instead kept P_{out} constant. Therefore, P_{in}-P_{out} did not decrease with increasing flow. When Lyon et al. increased the viscosity so that the maximum Reynolds number was only 40 (Dow Corning series 200 silicone fluid; 0.5 stoke), the observations were similar except that the rise in pressure with increasing flow for the initial phase was greater. However, when the viscosity of the fluid was increased further so that the maximum Reynolds number was 2 (Dow Corning serries 200 silicone fluid; 10 stokes), flow no longer occurred through the side channels of the collapsed tubing, and a true zero-flow pressure intercept was obtained. The value of the intercept was equal to the pressure surrounding the tube, i.e. P_{crit}. Furthermore, when flow did occur at the higher pressures, the relationship between flow and pressure was linear and the slope was only slightly higher than the calculated resistance from

Poiseuille's Law for the fully open tube. Finally, the authors noted that the tube never fluttered, even at the highest flow rates. These results indicate that the physical determinants of flow through collapsible tubes is dependent on the Reynolds number, and that "critical closing pressures" can only be observed when the viscous forces approach the magnitude of the inertial forces (Reynolds number of 1 by definition). Since the Reynolds number in the arterioles is 0.09 (24), a Starling resistor at this level (as hypothesized by Permutt and Riley) would reveal both a critical closing pressure and waterfall behaviour, but not a constant P_{in} with increasing flow, i.e. exactly what has been observed experimentally (92).

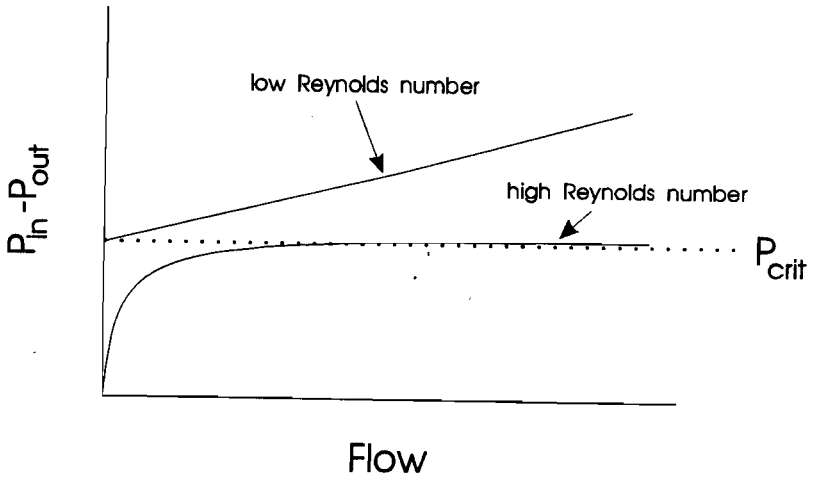

Figure 1.15: Inflow pressure (P_{in}) minus outflow pressure (P_{out}) is plotted against flow at high Reynolds numbers (solid line) and low Reynolds numbers (dashed line) (adapted from Lyon et al. (91)). At high Reynolds numbers, flow occurs as soon as $P_{in} > P_{out}$ through open side channels in the collapsed tube, even though $P_{in} < P_{crit}$. As flow increases, the collapsible tube begins to open, and the slope of the apparent plateau in the relationship reflects the resistance of the completely open collapsible tube. This is barely distinguishable from the

x-axis. At low Reynolds numbers, no flow occurs until $P_{in} > P_{crit}$ and a true zero-flow pressure intercept is obtained.

Although Lyon et al.'s experiments were done using large penrose drains and highly viscous fluids, the results have been supported by experiments using blood and 240 um diameter penrose tubing (120). Sipkema and Westerhof observed a shift in the pressure-flow relation when the Reynolds number was only 18 that was similar to Lyon's observations at Reynolds number of 40. Although they did not obtain a true zero-flow pressure intercept, it is very likely that smaller diameter tubes (lower Reynolds number) would have exhibited a "critical closing pressure" just as Lyon et al. showed at a Reynolds number of 2.

The experiments by Lyon et al. (91) and Sipkema and Westerhof (120) now allow for the unifying concept of the Starling resistor. First, if waterfall behaviour is defined as the dissociation of energy and hydraulic gradients [i.e. increases in P_{out} do not affect flow (under constant pressure conditions), or pressure (under constant flow conditions), until a critical value is reached (figure 1.16)], then waterfall behaviour is always observed in a Starling resistor model regardless of the Reynolds number. This effect is adequately explained by both the wave-speed hypothesis, and the critical closure hypothesis. If the analogy to a waterfall includes the fact that the upstream pressure (altitude of river) must be greater than the waterfall pressure (altitude of waterfall) in order for flow to occur, then a Starling resistor only exhibits waterfall behaviour when the Reynolds number is low, i.e. when a critical closing pressure exists (figure 1.15). When the Reynolds number is high, the Starling resistor results in an almost constant inflow pressure despite large increases in flow. Since this does not occur with flow over a waterfall, the waterfall analogy is not valid for high Reynolds numbers. Therefore, figures 1.15 and 1.16 show that both the wave-speed hypothesis and the critical closure hypothesis can explain the relationship between flow and venous

pressure, but only the critical closure hypothesis can explain the relationship between flow and perfusion pressure.

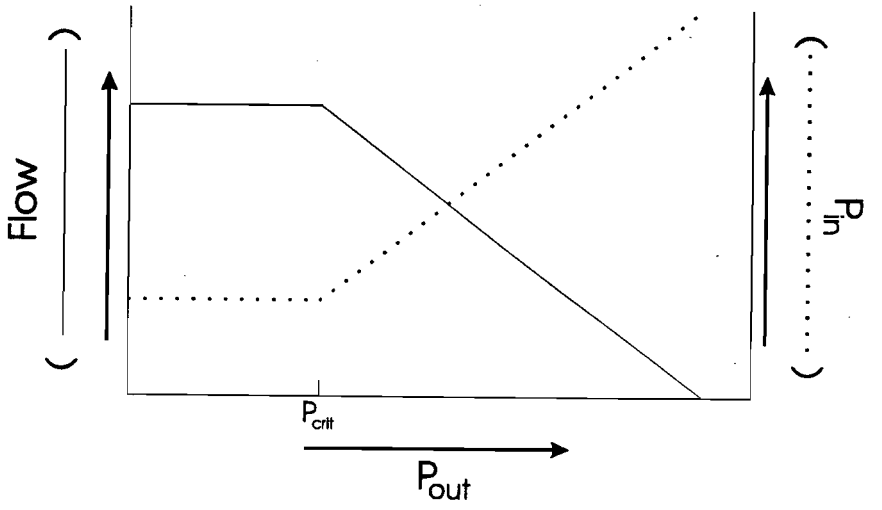

Figure 1.16: The solid line (left y-axis) illustrates the concept of flow limitation that occurs with a Starling resistor. If inflow pressure (P_{in}) is kept constant and outflow pressure (P_{out}) is decreased, flow increases until P_{out} becomes less than the pressure surrounding the tube (P_{crit}). Further decreases in P_{out} do not increase flow, i.e. maximum flow is limited. The dotted line (right y-axis) shows the relationship between P_{in} and P_{out} when flow is kept constant and P_{in} is allowed to change. As P_{out} is increased, there is no effect on P_{in} until the $P_{out} > P_{crit}$. These relationships are true at low and high Reynolds numbers.

Finally, it is important to note the differences between the penrose drain models and blood vessels. When the pressure surrounding the penrose drain is increased, the tubing becomes dumbbell shaped (26). However, the pressure generated by smooth muscle constriction produces a different effect because the smooth muscle actually shortens which creates a physical limitation to the shape of the vessel lumen. Indeed,

the endothelium and internal elastic lamina of the vessel become folded and do not take on the dumbbell shape (47). This means blood cells will occlude the vessel lumen at a higher intraluminal pressure than would occur if the dumbbell shape occurred.

1.2.d. Summary

Poiseuille's Law is valid for laminar flow of a Newtonian fluid through a rigid cylinder. Whereas many of these assumptions are not met in the circulation, the most important difference is that arteriolar vessels can be modelled as collapsible tubes surrounded by an external pressure that is generated by the smooth muscle tone. This model is similar to the variable resistor described by Knowlton and Starling in 1912 (82) that is now known as the Starling resistor. Recent evidence suggests that flow through a Starling resistor is partially dependent on the Reynolds number. Flow-limitation occurs at both low and high Reynolds numbers. However, a critical closing pressure will only occur at low Reynolds number, whereas flow at high Reynolds numbers results in a constant inflow pressure over a wide range of flows. The analogy to a waterfall is completely applicable for flow at low Reynolds numbers, but only partially applicable for flow at high Reynolds numbers.

When a vascular waterfall is present, flow is determined by the difference between inflow pressure and P_{crit}[9], divided by the arterial resistance between the two. Since both P_{crit} and arterial resistance can be affected by changes in smooth muscle activation, I will now discuss some of the factors that alter vessel tone and diameter.

---

[9] Critical closing pressure, critical pressure, and waterfall pressure are all synonymous with P_{crit}.

1.3. FACTORS AFFECTING TONE AND DIAMETER

Vessel tone is affected by central and local factors. Central factors include the sympathetic nervous system, parasympathetic nervous system, and hormones (e.g. epinephrine, norepinephrine, angiotensin II, atrial natriuretic hormone). Activation of the sympathetic system generally results in vasoconstriction (15). Activation of the parasympathetic system results in vasodilation but the mechanism may be indirect through the release of local endothelial-derived factors (22). Some hormones cause vasoconstriction (e.g. angiotensin II, (95)) whereas others cause vasodilation (e.g. atrial natriuretic peptide, (115)). Platelets and inflammatory cells can also affect vessel tone through inflammatory mediators such as histamine, bradykinin, etc. (76).

Whereas central factors are well characterized, many questions remain about local regulation of blood flow. The following sections discuss the role of pressure, flow, ischemic metabolites, and passive mechanics of the vessel wall in the local control of vessel tone. The role of the endothelium in coordinating the vasodilator responses of the micro- and macro-circulations are also discussed.

1.3.a. Myogenic Factors

In 1902, Bayliss suggested that vessel resistance was affected by the local perfusion pressure (9). In his experiments, he measured changes in hindlimb blood volume and inferred changes in vessel tone. When Bayliss increased systemic blood pressure by stimulating the peripheral ends of the splanchnic nerves, the hindlimb blood volume increased. Bayliss suggested this effect was due to vessel distention secondary to the higher pressures. When he then reduced arterial pressure back to normal, hindlimb volume decreased substantially below control which suggested that the blood vessels held less volume compared to the control condition, i.e. vasoconstriction had

occurred during the increased arterial pressure. Bayliss also observed the opposite effect if he initially reduced arterial pressure by partially clamping the abdominal aorta. The volume changes occurred in both the innervated and denervated hindlimb which suggested that the responses were due to local effects and were not sympathetically mediated.

In Bayliss' experiments, the increase in arterial pressure was associated with an increase in flow. To rule out flow-mediated changes, he studied carotid arteries under no flow conditions *in vitro* (9). When he increased intraluminal pressure, he visually observed an initial dilation of the arterial segment, but this was followed by an active constriction which reduced the diameter towards control. When Bayliss reduced the pressure back to normal, the opposite effect was noted. Since the response occurred in excised tissue, Bayliss suggested the constriction was due to a change in vessel wall tension, and called it a "myogenic response". These *in vitro* results suggest the *in vivo* "Bayliss response" was due to the same myogenic mechanism.

In 1912 Anrep suggested that the *in vivo* Bayliss response was due to changes in circulating epinephrine from the adrenal glands (2). Bayliss had increased arterial pressure with splanchnic nerve stimulation and asphyxia, both of which might cause adrenal release of norepinephrine and epinephrine. Anrep showed that the Bayliss response was eliminated in the adrenalectimized animal. However, in these experiments, Anrep increased the blood pressure over 20 seconds, and the subsequent decrease in blood pressure took up to 90 seconds. These long periods of time mean that autoregulatory mechanisms may have occurred during the lowering of blood pressure and therefore might have masked the myogenic response. In another series of experiments, Anrep rapidly changed perfusion pressure to the *forelimb* by occluding the abdominal aorta and observed similar results (2). However, in this protocol, the elevated blood pressure was maintained for only 10 seconds which may not have been long enough to observe the myogenic response. More recent studies using *in vivo*

microscopy suggests that the myogenic response in mesenteric arterioles has a lag time which averages 13 seconds and a time constant of 36.9 seconds (71). Upon careful examination of published tracings, the same conclusion can be made for rat cremasteric arterioles (100) and porcine coronary arterioles (86). In fact, the decreases in volume that Bayliss observed also only began to occur after approximately 20 seconds (9).

Anrep also found that arterial pressure occasionally remained constant during asphyxia (i.e. centrally-induced vasoconstriction did not occur). In these experiments, vasodilation occurred instead of vasoconstriction. He therefore hypothesized that the vasodilation Bayliss observed during a decrease in systemic arterial pressure was actually due to local tissue release of vasoactive metabolites (acids and carbon dioxide) secondary to ischemia. To test this hypothesis, he clamped the inflow and outflow of the rabbit ear for 30 seconds. Following the occlusion, the volume of the ear increased, i.e. vasodilation occurred, and Anrep again concluded the Bayliss response was not pressure-mediated. However, Anrep did not comment on the fall in arterial pressure during the time of occlusion. Therefore, changes in myogenic and metabolic factors occurred, both of which would cause vasodilation. Therefore, it is not possible to separate myogenic and metabolic causes of vasodilation in these experiments. Finally, with regards to Bayliss' *in vitro* experiments, Anrep was unable to reproduce the findings. The reason for this is unclear since observations from more recent experiments support Bayliss' observations (37,85).

In 1949, Folkow showed convincing evidence that Bayliss' original hypothesis was correct (41). Unlike Bayliss and Anrep who only measured regional volumes, Folkow measured venous outflow directly and calculated changes in resistance. First, he examined the role of vasoactive metabolites during reactive hyperemia following partial aortic occlusions in the cat hindlimb. After measuring reactive hyperemia during control conditions, Folkow denervated the hindlimb and found that resting flow doubled. He then decreased flow in the denervated limb by partially occluding the

aorta, but still maintained it higher than pre-denervation levels. When the partial occlusion was released, reactive hyperemic flow still occurred. Folkow suggested it was unlikely that vasoactive metabolites were being produced during the partial occlusion because flow under these conditions was greater than flow during control conditions.

Folkow also studied the effect of hypoxemia and hypercapnia on regional flow. He showed that reducing the oxygen concentrations down to 50%, or increasing carbon dioxide concentrations up to 5%, had only minimal effects. Since these concentrations are more extreme that those reached during short periods of arterial occlusion which also cause vasodilation, these results further support the hypothesis that metabolites play a minimal role in the regulation of blood flow to the *resting* hindlimb.

Finally, Folkow showed a myogenic response must exist by comparing changes in reactive hyperemic flow due to 1) arterial occlusion and 2) venous occlusion. Whereas decreasing arterial pressure results in both a myogenic and metabolic vasodilator stimulus, venous occlusion results in a metabolic vasodilator stimulus, but a myogenic vasoconstrictor stimulus. Therefore, the two methods should have identical effects on flow if the myogenic response did not exist, but different effects if it did. Folkow found that immediately after a 15 second **arterial occlusion**, there was a decrease in blood pressure and an increase in flow (due to distal vasodilation). However, a 50 second **venous occlusion** produced no change in blood pressure, and only a slight increase in venous outflow.[10] These results strongly suggest that vasodilation from a 15 second arterial occlusion is not due to vasodilator metabolites, and most likely reflects a myogenic response. The lack of vasoconstriction during the

---

[10] The increased venous outflow was most likely due to engorgement of the capillary and venous systems during venous occlusion, and does not necessarily reflect an increase of inflow to the hindlimb.

50 second occlusion in which arteriolar pressure was significantly increased probably reflects the balance between an increased myogenic stimulus which produces vasoconstriction, and a vasodilator stimulus due to accumulation of metabolites over 50 seconds of ischemia.

Considered together, these results strongly suggest that the myogenic response is the major factor responsible for reactive hyperemia following short occlusions in the resting hindlimb. Interestingly, Folkow also noted an increase in venous outflow following arterial occlusions as short as 3 seconds. According to the *in vivo* microscopic studies previously mentioned which showed more than a 10 second time lag before the myogenic response occurs (71,86,100), this could not have been due the myogenic response. Furthermore, it could not have been due to refilling of a compliant region because Folkow measured venous outflow and not arterial inflow. These discrepancies have not yet been addressed in the literature and the mechanism for reactive hyperemia of short occlusions remains unknown. One possibility is that during the short occlusions, vessel diameter does not change because the decrease in forces compressing the vessel (myogenic tone) is balanced by the decrease in forces distending the vessel (intravascular pressure). When the occlusion is released, the intravascular pressure suddenly increases, distends the vessel, and flow increases secondary to the decrease in resistance. With longer occlusions, the decreased myogenic tone may become more important than the decreased pressure, and microscopic studies will measure an increase in diameter. This hypothesis underscores the need for careful interpretation of studies using microscopy, and the importance of understanding that the relationship between tone and diameter is *indirect* and dependent on changes in transmural pressure.

The Mechanism of the Myogenic Response

Since Folkow's article in 1949, various studies have shown that the myogenic response occurs in arteries (113), arterioles (37,85), and veins (133). The response is

eliminated if a calcium-free medium is used, or if calcium is chelated with EDTA (130). Some studies have shown dihydropyridine calcium channel blockers eliminate the myogenic response (84), whereas others show either no effect on the myogenic response or only a partial inhibition depending on which calcium channel blocker is used (55,64).

Originally, it was believed that pressure-induced vasoconstriction was a property of smooth muscle (130), perhaps resulting from stretch-induced depolarization (72). However in the late 1980's, some studies suggested that the myogenic response of vascular smooth muscle was dependent on the presence of endothelium (52,79,113). For example, Rubanyi used a bioassay technique to study the response in canine carotid arteries (113). Briefly, he perfused a donor vessel segment and allowed the effluent to superfuse another vessel segment (the bioassay ring) which was connected to a tension transducer. Therefore, if a stimulus applied to the donor segment caused an increase in the bioassay ring tension, then a transferable vasoconstrictor substance must have been released into the effluent. When Rubanyi increased perfusion pressure in the donor vessel from 0 mmHg to 33.5 mmHg by increasing outflow resistance at constant flow, both the donor vessel and bioassay ring constricted. However, if the endothelium of the donor segment was removed with mechanical rubbing, the donor segment passively dilated and there was no effect on the bioassay ring.

Although the work by Rubanyi and others was convincing, more recent work has shown the myogenic response is not always dependent on endothelium (37,85). Kuo, Chilian, and Davis dissected out 40-70 um vessels from the coronary circulation and cannulated both ends with glass pipettes (85). The pipettes were then connected to reservoirs hung from the ceiling. The authors varied the intraluminal pressure of the vessel between 20-140 cmH_2O by adjusting the height of the reservoirs and showed that mechanical removal of the endothelium in these vessels had no effect on the observed

myogenic response. Similar results were obtained with 135-200 um cremasteric skeletal muscle arterioles (37).

The differing results with respect to endothelial-dependence were explained by Falcone et al. who noted that all studies indicating an endothelial dependence of the myogenic response were done on large vessels and/or cerebral arteries (37). Endothelium-independent myogenic responses were shown in lung, heart, ear, and skeletal muscle arteries and arterioles (37). It is therefore likely that cerebral and large artery smooth muscle behave differently from the peripheral microcirculation.

Finally, there is some evidence suggesting that *in vitro* responses may be different from *in vivo* responses. Meininger et al. showed that an increase in P_{per} caused first order cremasteric arterioles to dilate *in vivo* (94), but constrict *in vitro* (37). The different results in the two studies may be due to different pressure ranges, an intact neural supply, anaesthesia, etc. Therefore, extrapolation of *in vitro* results to *in vivo* conditions should be done cautiously.

1.3.b. Metabolic Factors

Even though Folkow's experiments suggested that metabolic factors do not contribute to vascular tone in resting skeletal muscle, they may play a role during reactive hyperemia and exercise. For instance, although the normal oxygen supply to skeletal muscle is sufficient to support muscle metabolism for short periods of ischemia, longer periods would certainly decrease O_2 concentration below 50% and therefore cause vasodilation (41). In addition, several vasodilator substances including CO_2, lactic acid, and adenosine are released during ischemia (101) and during muscle contractions (114). Recently, Björnberg et al. showed that myogenic mechanisms alone could not fully explain reactive hyperemia for occlusions longer than 10 seconds (12). Which of the proposed metabolites is the major factor remains unknown.

Finally, one should not make conclusions on the role of vasoactive metabolites in exercise based on studies using reactive hyperemia because the effects of decreasing oxygen supply (reactive hyperemia) and increasing oxygen demand (exercise) are not necessarily the same. When Harrison et al. reduced the oxygen supply to skeletal muscle with hypoxia, there was an initial **decrease** in capillary flow but an **increase** in femoral arterial flow (54). If instead they increased the oxygen demand of the muscle with low level muscle stimulation, they observed an initial **increase** in capillary flow with **no change** in femoral arterial flow (53). These results show that decreasing oxygen supply does not necessarily produce the same results as increasing oxygen demand, and therefore, changes observed during reactive hyperemia may not necessarily apply to exercise-induced vasodilation.

1.3.c. Passive Factors

Since the vessel wall is a visco-elastic tissue, passive factors also affect vessel diameter. An increase in intraluminal pressure should cause a passive increase in diameter. Since the elastance of the vessel wall is curvilinear and the wall becomes stiffer at higher pressures, the change in diameter for a given change in pressure is dependent on the initial pressure (70). In addition, when a load is applied to a visco-elastic tissue and maintained, the initial change in length is followed by a slow, passive increase in tissue length due to "creep" (24).[11] *In vivo* however, arterioles actively constrict in response to an increased pressure (94). Therefore, creep is not a major factor in determining arteriolar vessel diameter although it may attenuate the vasoconstrictor responses observed. In contrast to the behaviour of arterioles, venous

---

[11] Creep is similar to Stress Relaxation. Creep occurs when a constant load is applied to a visco-elastic tissue, whereas stress relaxation refers to the decline in tension after a constant length change is applied.

resistance decreases with increases in pressure (73,97) and passive factors may play a larger role in these vessels.

1.3.d. The Role of the Endothelium

During exercise, local microcirculatory vasodilation is most likely due to the release of metabolites from working muscles. However, the large proximal arteries also dilate even though they are not exposed to vasoactive metabolites (56). This proximal vasodilation is crucial if the increased demands for oxygen during exercise are to be met (117). For instance, the pressure in the mid-size cremasteric muscle arterioles (70-110 um) or mid-size spinotrapezius arterioles (130-186 um) is only 65-75% of the femoral artery pressure in an intact muscle preparation (27). Therefore, if the pressure drop across the bed is from 100 mmHg in the femoral artery to approximately 0 mmHg in the femoral vein, then the pressure in the arterioles is approximately 70 mmHg. Assuming a resting flow of 5 $ml \cdot min^{-1} \cdot 100g^{-1}$ and no Starling resistor-like mechanism, total resistance (R_{tot}) is 20 units, with proximal resistance being 6 units (R_1) and distal resistance (R_2) being 14 units. If blood pressure remains constant and distal resistance approaches zero, then flow would increase only 3-fold to 16.7 $ml \cdot min^{-1} \cdot 100g^{-1}$. However, flow can increase 4-5 fold during exercise (21,90,129). Therefore, proximal vessels must receive a signal to relax. A model incorporating a Starling resistor-like mechanism at the arteriolar level would require even more proximal vasodilation because decreases in resistance downstream from the vascular waterfall would not affect regional inflow. The myogenic response may be partly responsible through the following mechanism. The decrease in downstream resistance and increase in flow means that the pressure drop across the proximal vessels not exposed to vasodilator metabolites must increase ($\Delta P = \dot{Q} * R_a$, where ΔP is the pressure drop across the arterial vessels and R_a is constant because the vessels have not

yet changed diameter). If inflow pressure is constant (i.e. arterial pressure), then intraluminal pressure must decrease along the entire length of the vessel (117). Thus, the myogenic stimulus is decreased and relaxation might occur. However, the endothelium may also mediate the response through flow-mediated vasodilation or intercellular communication.

The Endothelium and Flow-mediated Vasodilation

In 1980, Furchgott and Zawadzki showed that the endothelium is not simply a passive barrier, but also releases vasoactive substances into the local environment (45). Previous to 1980, it was known that acetylcholine infusion *in vivo* consistently caused vasodilation whereas acetylcholine infusion *in vitro* caused vasoconstriction. Furchgott and Zawadzki found that if the endothelium was carefully protected during the *in vitro* setup, acetylcholine caused vasodilation similar to the *in vivo* results (45). They hypothesized that the endothelium released a substance into the abluminal space (endothelial-derived relaxing factor (EDRF)) which was responsible for the smooth muscle relaxation. This substance was not a prostenoid because vasodilation occurred in the presence of cyclooxygenase inhibitors. Other substances which stimulate the release of EDRF include bradykinin, thrombin, and calcium ionophore A23187 (44).

Besides its role in mediating pharmacologically-induced vasodilation, the endothelium is also responsible for mediating flow-induced vasodilation (61,108,125). For instance, Pohl et al. isolated a segment of the canine femoral artery *in vivo*, and measured both flow and diameter (108). When the authors infused acetylcholine distal to the segment under study, flow increased and the proximal arterial segment dilated. This was not a myogenic vasodilation secondary to the flow-induced decrease in intraluminal pressure because arterial pressure reduction by other means caused a passive vasoconstriction. After endothelial removal by either intimal damage or hydrogen peroxide infusion, flow-mediated increases in diameter were abolished. The absence of vasodilation after endothelium removal was not due to smooth muscle

damage because reactivity to nitroglycerin and norepinephrine were unchanged. The stimulus for EDRF release is now believed to be an increase in shear stress (87).

The vasodilator substance released by endothelium in response to different chemical (e.g. acetylcholine, or bradykinin, or thrombin) and mechanical stimuli (shear stress) is 1) species dependent (43), 2) region dependent (112), and 3) stimulus dependent (76). The different substances hypothesized include nitric oxide (EDRF[12]), endothelial-derived hyperpolarizing factor (EDHF, (40,96)), and prostaglandins (76,83). Some of these substances also play a larger role in homeostasis. For instance, EDRF is also a neurotransmitter (20) and inhibits platelet aggregation (59). The role of these substances in the control of vascular tone will now be discussed individually.

Endothelial-derived Relaxing Factor

Many authors have confirmed the findings of Furchgott and Zawadzki's since 1980. Acetylcholine-mediated EDRF is not a prostaglandin because Furchgott and Zawadzki showed that acetylcholine-induced vasodilation is not affected by cyclooxygenase inhibitors (45). Studies which showed that the half-life is prolonged by free-radical scavengers led to the hypothesis that EDRF is a free radical (66,93). In addition, the action of EDRF is associated with an increase in smooth muscle [cGMP], similar to the nitrovasodilators already commonly in use (68,93). Finally, EDRF is inactivated *in vivo* by hemoglobin which results in a very short half-life (66,80). These results have led to the current hypothesis that the original EDRF described by Furchgott and Zawadzki is nitric oxide (NO) (63,66,67) or an S-nitrosothiol (65). The enzymes responsible for EDRF synthesis have been characterized (20,65), and L-arginine may be an essential substrate (105). This has led to the development of

---

[12] The original EDRF described by Furchgott and Zawadzki is now believed to be nitric oxide. Some authors now abbreviate this substance as EDNO.

pharmacological agents designed to block EDRF synthesis. The most commonly used drugs are L-nitro-monomethyl-arginine (L-NMMA) (131), L-nitro-arginine (L-NNA) (11,69), and L-nitro-arginine-methyl-ester (L-NAME) (22,62).

Endothelial-derived Hyperpolarizing Factor

During the 1980's, it became apparent that other substances may also contribute to acetylcholine-induced vasodilation. Feletou and Vanhoutte demonstrated that acetylcholine releases a substance that hyperpolarizes the smooth muscle membrane (endothelial-derived hyperpolarizing factor, EDHF), which should theoretically cause relaxation through a decrease in calcium release (40). Removal of the endothelium eliminated both hyperpolarization and relaxation. However, ouabain blocked only the hyperpolarization and had no effect on relaxation (40). In a subsequent study using large canine coronary arteries, Hoeffner et al. (57) showed that ouabain (a blocker of EDHF) reduces acetylcholine-induced relaxation, but not bradykinin-induced relaxation. These results suggest acetylcholine causes the release of a second substance besides EDRF, and this substance is associated with smooth muscle hyperpolarization.

Despite the report by Hoeffner et al., EDHF remains a controversial topic. Some authors have suggested that nitric oxide (EDRF) also causes hyperpolarization, but this response is not necessary for relaxation. For instance, Rand and Garland measured both tension and membrane potential simultaneously in the rabbit basilar artery (110). They showed that repeated exposure to acetylcholine eliminated the hyperpolarization, but did not affect relaxation. In addition, L-arginine analogues known to block EDRF synthesis abolished the hyperpolarizing effect. Therefore, they concluded that both effects are due to NO. Alternatively, it is possible the L-arginine analogues blocked the formation of the still unknown EDHF.

Prostaglandins

Prostaglandins represent a family of compounds derived from arachidonic acid. Some have vasoconstrictor properties and others have vasodilator properties. Although

Furchgott and Zawadzki originally showed that cyclooxygenase inhibitors do not affect acetylcholine-induced relaxation, Koller and Kaley found that indomethacin abolishes flow-induced vasodilation in a rat cremasteric muscle preparation (83). Later studies showed that cyclooxygenase inhibitors also affect bradykinin-induced endothelium-dependent vasodilation (75) and hypoxia-induced endothelium-dependent vasodilation (98) in rat cremasteric muscle. Finally, prostaglandins are also involved in acetylcholine-induced vasodilation in rabbit heart (88).

The Endothelium and Intercellular Communication

Although flow-mediated and myogenic factors may be involved in coordinating micro- and macrocirculatory vasodilation, other mechanisms may also play a role. As early as 1959, Hilton showed that cat femoral artery dilates with muscle contraction, or with infusion of 1) acetylcholine, 2) histamine, 3) bradykinin, and 4) nicotine, even when the infusion is distal to the site of measurement (56). The dilation occurred in the denervated limb and therefore was not due to spinal or central reflexes. However, it was abolished by eliminating intercellular communication with transection of the femoral artery, or by abluminal application of cocaine (56).

Recently, Segal and Duling have confirmed that intercellular communication can coordinate dilation of large and small vessels (116,118). This cross-talk occurs via the endothelial cells and not via smooth muscle or neural reflexes. Using the hamster cheek pouch, Segal and Duling applied pulses of acetylcholine or adenosine to arterioles. After a delay of 1-3 seconds, they observed vessel diameter changes more than 800 um upstream (116,118). Vasodilation was not due to local diffusion of acetylcholine because an identical stimulus applied in the interstitial space 215 um away from any vessel had no effect. In addition, they found that the amount of dilation decayed with the distance from the applied pulse, and had a length constant of approximately 2.1 mm (116). The ascending vasodilation was not flow-mediated because it also occurred in vessels that were occluded proximally with external

pressure. It was not due to nerve involvement because the response was unaffected by tetrodotoxin (116). Further investigations showed that intercellular dye transfer occurred only between endothelial cells, but not between smooth muscle fibers, or between endothelial cells and smooth muscle fibers (117). These results strongly suggest that endothelial intercellular communication may play a role in micro/macrocirculatory coordination.

1.3.e. Interactions Between Different Factors

Vessel tone and diameter are affected by central (autonomic nervous system and hormones) and local (myogenic response, vasoactive metabolites, vessel wall mechanics, and endothelium-dependent factors) factors. In order to show that each variable is important, one must attempt to control all other variables so that it is clear which factor is responsible for the effects observed. However, changes in one variable may affect the response of other variables, and so keeping all other variables constant cannot give a complete picture of vascular physiology. For example, Kuo et al. showed that there is an interaction between myogenic activity and flow-induced vasodilation (86). Similar to their paper previously discussed in the section on "Myogenic Factors" (85), the authors used two reservoirs connected to an isolated arteriole *in vitro*, and raised the height of the reservoirs to increase the myogenic stimulus. To study the effects of flow-mediated vasodilation, they raised one reservoir and lowered the other by exactly the same amount. Therefore, the pressure in the middle of the arteriole was unaffected and the authors could manipulate pressure (mean height of the reservoirs above the vessel) and flow (difference in height between the reservoirs) independently. The authors showed that flow-mediated vasodilation was attenuated when intraluminal pressure was increased, and similarly, the myogenic response was attenuated when flow was increased (85). Other studies have also shown an interaction between EDRF and the vasoconstrictor effects of angiotensin II,

norepinephrine, phenylephrine, and vasopressin (25). These results suggest there is a complex interaction between the different variables responsible for vasomotor tone.

1.3.f. Summary

Vessel diameter and tone are affected by many different variables which include myogenic, metabolic, endothelium-dependent, passive and central factors. The effect of changing any individual factor may be different in different experiments due to anaesthesia, surgical preparation, or basal levels of the other factors known to affect tone.

The goal of this thesis is to examine the mechanisms controlling the critical closing pressure and arterial resistance in the hindlimb. In "History of Pressure-Flow Relations", I discussed the phenomenological evidence supporting the critical closing pressure and waterfall hypothesis. In "Physics of Flow", I discussed the assumptions behind Poiseuille's Law, the conflicting theoretical evidence concerning the critical closing pressure hypothesis, and the effect of the Reynolds number on flow through collapsible tubes. The preceeding section discussed those factors that could theoretically change the critical closing pressure or arterial resistance through a change in vascular tone. The final section of the introduction will discuss the rationale for the experiments discussed in chapters 2-6.

1.4. RATIONALE FOR THESIS EXPERIMENTS

Since the original hypothesis of a tone-dependent vascular waterfall was proposed (107), there has been very little work on reflex and metabolic control of P_{crit} and R_a. The studies described in Chapters 2-4 were designed to test the neural, mechanical, and flow-mediated control of P_{crit} and R_a. In the studies in Chapters 5 and 6, the effects of vasodilators on P_{crit} and $R_a$were analyzed.

1.4.a. Neural Control of P_{crit} and R_a

The carotid sinus baroreflex is responsible for maintaining arterial pressure relatively constant despite wide fluctuations in cardiac output that occur with positional changes, exercise, or hemorrhage. Sympathetic activation releases norepinephrine from nerve terminals along the vascular tree, and also hormonal vasoconstrictors from the adrenal medulla. In Chapter 2 of this thesis, I tested the hypothesis that altering sympathetic tone through the carotid sinus baroreflex would affect P_{crit} in addition to affecting R_a. We measured these variables in the canine hindlimb during both an increase and decrease in carotid sinus pressure. The carotid sinuses were isolated and perfused with a pump. The animals were vagotomized to remove the effects of other baroreceptors.

1.4.b. Mechanical Control of P_{crit} and R_a

Arterial and arteriolar vessels exhibit a myogenic response *in vitro* (37,113). *In vivo*, Meininger et al. have shown that an increase in P_{per} results in vasoconstriction of 3rd and 4th order cremasteric arteriolar vessels, but vasodilation of 1st and 2nd order vessels (94). Chapter 3 of the thesis therefore investigates what the mechanical effects of increased P_{per} are on the variables P_{crit} and R_a. In the study, we measured P_{crit} and R_a in the canine hindlimb over perfusion pressures ranging from 75 to 175 mmHg. In addition, we also lowered carotid sinus pressure and repeated the measurements over the same range of perfusion pressures to investigate the interaction between neural and mechanical stimuli.

1.4.c. Flow-mediated Control of P_{crit} and R_a

In 1980, Furchgott and Zawadzki showed that acetylcholine causes the endothelium to release a non-prostenoid powerful vasodilator (45). This substance was later termed endothelial-derived relaxing factor (EDRF), and is released by the

endothelium in response to increases in shear stress (87). EDRF is believed to be important in mediating the large vessel vasodilation that is necessary to allow appropriate flow increases to muscle during exercise (117). Therefore, Chapter 4 investigates the role of EDRF in the control of P_{crit}, R_a, and R_v. Since *in vitro* experiments suggest a reciprocal inhibition between EDRF and the myogenic response (86), we also investigated the interaction between EDRF and the effects of increasing P_{per}.

1.4.d. The Effect of Vasodilators on P_{crit} and R_a

The back pressure at the site of the waterfall is believed to be created by arteriolar smooth muscle tone (92,107). In order for waterfall behaviour to be observed, the downstream pressure must be less than the pressure generated by the constricting vascular smooth muscle. It is therefore possible that decreasing smooth muscle tone will abolish waterfall behaviour, but P_{crit} could still be observed if the perfusion pressure declined below a critical value. Chapter 5 describes a series of experimental protocols designed to investigate the effects of vasodilation with a solution of nitroprusside and adenosine on waterfall behaviour. The drugs were infused at a rate that eliminated reactive hyperemia. Three protocols were used. First, we measured P_{zf} during dynamic pressure-flow relations with ramp times varying between 1-10 seconds before and after vasodilation. The relationship of P_{zf} versus ramp time was plotted and the results compared with different models of the circulation (presence or absence of vascular waterfall). Second, we raised venous pressure during constant flow conditions and measured changes in perfusion pressure. Third, we measured the changes in P_{crit} and R_a with changes in P_{per}.

1.4.e. Effects of a Calcium Channel Blocker on P_{crit} and R_a

In chapters 3-5, I found that P_{crit} increases when P_{per} is increased, i.e. there was a myogenic response. The effect was accentuated when vascular tone was increased with both EDRF blockade and phenylephrine, and was reduced when vascular tone was decreased with a nitroprusside/adenosine solution.

As previously discussed, the myogenic response *in vitro* requires calcium (130). Therefore, in chapter 6, I tested the hypothesis that nifedipine (a calcium channel blocker) eliminates the myogenic response of P_{crit}.

1.5. REFERENCES

1. Alexander, R.S. Critical closure reexamined. *Circ. Res.* 40: 531-535, 1977.

2. Anrep, G. On local vascular reactions and their interpretation. *J. Physiol. (Lond)* 45: 318-327, 1912.

3. Ashton, H. Critical closing pressure in human peripheral vascular beds. *Clin. Sci.* 22: 79-87, 1962.

4. Aversano, T., F.J. Klocke, R.E. Mates, and J.M. Canty,Jr.. Preload-induced alterations in capacitance-free diastolic pressure-flow relationships. *Am. J. Physiol.* 246: H410-H417, 1984.

5. Azuma, T. and S. Oka. Mechanical equilibrium of blood vessel walls. *Am. J. Physiol.* 221: 1310-1318, 1971.

6. Baez, S. Response characteristics of perfused microvessels to pressure and vasoactive stimuli. *Angiology* 12: 452-461, 1961.

7. Baez, S. Bayliss response in the microcirculation. *Fed. Proc.* 27: 1410-1415, 1968.

8. Baez, S., S.M. Feldman, and P.M. Gootman. Central neural influence on precapillary microvessels and sphincter. *Am. J. Physiol.* 233: H141-H147, 1977.

9. Bayliss, W.M. On the local reactions of the arterial wall to changes of internal pressure. *J. Physiol. (Lond)* 28: 220-231, 1902.

10. Bellamy, R.F. Diastolic coronary artery pressure-flow relations in the dog. *Circ. Res.* 43(1): 92-101, 1978.

11. Bellan, J.A., R.K. Minkes, D.B. McNamara, and P.J. Kadowitz. N-nitro-L-arginine selectively inhibits vasodilator responses to acetylcholine and bradykinin in cats. *Am. J. Physiol.* 260: H1025-H1029, 1991.

12. Björnberg, J., U. Albert, and S. Mellander. Resistance responses in proximal arterial vessels, arterioles and veins during reactive hyperaemia in skeletal muscle and their underlying regulatory mechanisms. *Acta Physiol. Scand.* 139: 535-550, 1990.

13. Björnberg, J., P.-O. Grände, M. Maspers, and S. Mellander. Site of autoregulatory reactions in the vascular bed of cat skeletal muscle as determined with a new technique for segmental vascular resistance recordings. *Acta Physiol. Scand.* 133: 199-210, 1988.

14. Björnberg, J., M. Maspers, and S. Mellander. Metabolic control of large-bore arterial resistance vessels, arterioles, and veins in cat skeletal muscle during exercise. *Acta Physiol. Scand.* 135: 83-94, 1989.

15. Boegehold, M.A. and P.C. Johnson. Response of arteriolar network of skeletal muscle to sympathetic nerve stimulation. *Am. J. Physiol.* 254: H919-H928, 1988.

16. Bohlen, H.G. Arteriolar closure mediated by hyperresponsiveness to norepinephrine in hypertensive rats. *Am. J. Physiol.* 5: H157-H164, 1979.

17. Borgström, P., P.-O. Grände, and L. Lindbom. Responses of single arterioles *in vivo* in cat skeletal muscle to change in arterial pressure applied at different rates. *Acta Physiol. Scand.* 113: 207-212, 1981.

18. Braakman, R., P. Sipkema, and N. Westerhof. Steady-state and instantaneous pressure-flow relationships: characterisation of the canine abdominal periphery. *Cardiovasc. Res.* 17: 577-588, 1983.

19. Braakman, R., P. Sipkema, and N. Westerhof. Two zero-flow pressure intercepts exist in autoregulating isolated skeletal muscle. *Am. J. Physiol.* 258: H1806-H1814, 1990.

20. Bredt, D.S., P.M. Hwang, and S.H. Snyder. Localization of nitric oxide synthase indicating a neural role of nitric oxide. *Nature* 347: 768-770, 1990.

21. Britton, S.L., P.J. Metting, T.F. Ronau, J.R. Strader, and D.L. Weldy. Autoregulation of hind-limb blood flow in conscious dogs. *J. Physiol. (Lond)* 368: 409-422, 1985.

22. Broten, T.P., J.K. Miyashiro, S. Moncada, and E.O. Feigl. Role of endothelium-derived relaxaing factor in parasympathetic coronary vasodilation. *Am. J. Physiol.* 262: H1579-H1584, 1992.

23. Burton, A.C. On the physical equilibrium of small blood vessels. *Am. J. Physiol.* 164: 319-329, 1951.

24. Caro, C.G., T.J. Pedley, R.C. Schroter and W.A. Seed. *The mechanics of the circulation*, New York:Oxford University Press, 1978,

25. Conrad, K.P. and S.L. Whittemore. N-monomethyl-L-arginine and nitroarginine potentiate pressor responsiveness of vasoconstrictors in conscious rats. *Am. J. Physiol.* 262: R1137-R1144, 1992.

26. Conrad, W.A. Pressure-flow relationships in collapsible tubes. *IEEE Trans. Biomed. Eng.* 16: 284-295, 1969.

27. DeLano, F.A., G.W. Schmid-Schönbein, T.C. Skalak, and B.W. Zweifach. Penetration of the systemic blood pressure into the microvasculature of rat skeletal muscle. *Microvasc. Res.* 41: 92-110, 1991.

28. Dobrin, P.B. Vascular mechanics. In: *Handbook of Physiology. Section 2: The Cardiovascular System. Volume III. Peripheral Circulation and Organ Blood Flow, Part 1*, edited by J.T. Shepherd, F.M. Abboud and S.R. Geiger. Bethesda, Md.: American Physiological Society, 1983, p. 65-102.

29. Dole, W.P., G.M. Alexander, A.B. Campbell, E.L. Hixson, and V.S. Bishop. Interpretation and physiological significance of diastolic coronary artery pressure-flow relationships in the canine coronary bed. *Circ. Res.* 55: 215-226, 1984.

30. Dole, W.P. and V.S. Bishop. Influence of autoregulation and capacitance on diastolic coronary artery pressure-flow relationships in the dog. *Circ. Res.* 51: 261-270, 1982.

31. Downey, J.M. and E.S. Kirk. Inhibition of coronary blood flow by a vascular waterfall mechanism. *Circ. Res.* 36: 753-760, 1975.

32. Duomarco, J.L. and R. Rimini. Energy and hydraulic gradients along systemic veins. *Am. J. Physiol.* 178: 215-219, 1954.

33. Early, C.B., R.C. Dewey, H.P. Pieper, and W.E. Hunt. Dynamic pressure-flow relationships of brain blood flow in the monkey. *J. Neurosurg.* 41: 590-596, 1974.

34. Ehrlich, W., R.W. Baer, R.F. Bellamy, and R. Randazzo. Instantaneous femoral artery pressure-flow relations in supine anesthetized dogs and the effect of unilateral elevation of femoral venous pressure. *Circ. Res.* 47: 88-98, 1980.

35. Ekelund, U. and S. Mellander. Role of endothelium-derived nitric oxide in the regulation of tonus in large-bore arterial resistance vessels, arterioles and veins in cat skeletal muscle. *Acta Physiol. Scand.* 140: 301-309, 1990.

36. Eng, C., J.H. Jentzer, and E.S. Kirk. The effects of the coronary capacitance on the interpretation of diastolic pressure-flow relationships. *Circ. Res.* 50: 334-341, 1982.

37. Falcone, J.C., M.J. Davis, and G.A. Meininger. Endothelial independence of myogenic response in isolated skeletal muscle arterioles. *Am. J. Physiol.* 260: H130-H135, 1991.

38. Farhi, E.R., F.J. Klocke, R.E. Mates, K. Kumar, R.M. Judd, J.M. Canty,Jr., S. Satoh, and B. Sekovski. Tone-dependent waterfall behaviour during venous pressure elevation in isolated canine hearts. *Circ. Res.* 68: 392-401, 1991.

39. Fåhræus, R. and T. Lindqvist. The viscosity of the blood in narrow capillary tubes. *Am. J. Physiol.* 96: 562-568, 1931.

40. Feletou, M. and P.M. Vanhoutte. Endothelium-dependant hyperpolarization of canine coronary smooth muscle. *Br. J. Pharmacol.* 93: 515-524, 1988.

41. Folkow, B. Intravascular pressure as a factor regulating the tone of the small vessels. *Acta Physiol. Scand.* 17: 289-310, 1949.

42. Folkow, B. and B. Öberg. Autoregulation and basal tone in consecutive vascular sections of the skeletal muscles in reserpine-treated cats. *Acta Physiol. Scand.* 53: 105-113, 1961.

43. Förstermann, U., G. Trogisch, and R. Busse. Species-dependant differences in the nature of endothelium-derived vascular relaxing factor. *European J. Pharmacol.* 106: 639-643, 1984.

44. Furchgott, R.F. The role of endothelium in the responses of vascular smooth muscle to drugs. *Annu. Rev. Pharmacol. Toxicol.* 24: 175-197, 1984.

45. Furchgott, R.F. and J.V. Zawadzki. The obligatory role of endothelial cells in the relaxation of arterial smooth muscle by acetylcholine. *Nature* 288: 373-376, 1980.

46. Girling, F. Critical closing pressure and venous pressure. *Am. J. Physiol.* 171: 204-207, 1952.

47. Greensmith, J.E. and B.R. Duling. Morphology of the constricted arteriolar wall: physiological implications. *Am. J. Physiol.* 247: H687-H698, 1984.

48. Griffiths, D.J. Urethral elasticity and micturition hydrodynamics in females. *Med. Biol. Engng.* 7: 201-215, 1969.

49. Griffiths, D.J. Hydrodynamics of male micturition - I. Theory of steady flow through elastic-walled tubes. *Med. Biol. Engng.* 9: 581-588, 1971.

50. Griffiths, D.J. Steady fluid flow through veins and collapsible tubes. *Med. Biol. Engng.* 9: 597-602, 1971.

51. Griffiths, D.J. Hydrodynamics of male micturition - II. Measurements of stream parameters and urethral elasticity. *Med. Biol. Engng.* 9: 589-596, 1971.

52. Harder, D.R. Pressure-induced myogenic activation of cat cerebral arteries is dependent on intact endothelium. *Circ. Res.* 60: 102-107, 1987.

53. Harrison, D.K., S. Birkenhake, S.K. Knauf, and M. Kessler. Local oxygen supply and blood flow regulation in contracting muscle in dogs and rabbits. *J. Physiol. (Lond)* 422: 227-243, 1990.

54. Harrison, D.K., M. Kessler, and S.K. Knauf. Regulation of capillary blood flow and oxygen supply in skeletal muscle in dogs during hypoxemia. *J. Physiol. (Lond)* 420: 431-446, 1990.

55. Haws, C.W. and D.D. Heistad. Effects of nimodipine on cerebral vasoconstrictor responses. *Am. J. Physiol.* 247: H170-H176, 1984.

56. Hilton, S.M. A peripheral arterial conducting mechanism underlying dilatation of the femoral artery and concerned in functional vasodilatation in skeletal muscle. *J. Physiol. (Lond)* 149: 93-111, 1959.

57. Hoeffner, U., M. Feletou, N.A. Flavahan, and P.M. Vanhoutte. Canine arteries release two different endothelium-derived relaxing factors. *Am. J. Physiol.* 257: H330-H333, 1989.

58. Hoffman, J.I.E. and J.A.E. Spaan. Pressure-flow relations in coronary circulation. *Physiol. Rev.* 70(2): 331-390, 1990.

59. Hogan, J.C., M.J. Lewis, and A.H. Henderson. *In vivo* EDRF activity influences platelet function. *Br. J. Pharmacol.* 94: 1020-1022, 1988.

60. Holt, J.P. The collapse factor in the measurement of venous pressure. *Am. J. Physiol.* 134: 292-299, 1941.

61. Holtz, J., U. Förstermann, U. Pohl, M. Giesler, and E. Bassenge. Flow-dependant, endothelium-mediated dilation of epicardial coronary arteries in conscious dogs: Effects of cyclooxygenase inhibition. *J. Cardiovasc. Pharmacol.* 6: 1161-1169, 1984.

62. Hutcheson, I.R. and T.M. Griffith. Release of endothelium-derived relaxing factor is modulated both by frequency and amplitude of pulsatile flow. *Am. J. Physiol.* 261: H257-H262, 1991.

63. Hutchinson, P.J.A., R.M.J. Palmer, and S. Moncada. Comparative pharmacology of EDRF and nitric oxide on vascular strips. *European J. Pharmacol.* 141: 445-451, 1987.

64. Hwa, J.J. and J.A. Bevan. A nimodipine-resistant Ca^{2+} pathway is involved in myogenic tone in a resistance artery. *Am. J. Physiol.* 251: H182-H189, 1986.

65. Ignarro, L.J. Biosynthesis and metabolism of endothelium-derived nitric oxide. *Annu. Rev. Pharmacol. Toxicol.* 30: 535-560, 1990.

66. Ignarro, L.J., G.M. Buga, K.S. Wood, R.E. Byrns, and G. Chaudhuri. Endothelium-derived relaxing factor produced and released from artery and vein is nitric oxide. *Proc. Nat. Acad. Sci. USA* 84: 9265-9269, 1987.

67. Ignarro, L.J., R.E. Byrns, G.M. Buga, K.S. Wood, and G. Chaudhuri. Pharmacological evidence that endothelium-derived relaxing factor is nitric oxide: use of pyrogallol and superoxide dismutase to study endothelium-dependant and nitric oxide-elicited vascular smooth muscle relaxation. *J. Pharmacol. Exp. Ther.* 244(1): 181-189, 1988.

68. Ignarro, L.J. and P.J. Kadowitz. The pharmacological and physiological role of cyclic GMP in vascular smooth muscle relaxation. *Annu. Rev. Pharmacol. Toxicol.* 25: 171-191, 1985.

69. Ishii, K., B. Chang, J.F. Kerwin,Jr., Z.-J. Huang, and F. Murad. N-nitro-L-arginine: a potent inhibitor of endothelium-derived relaxing factor formation. *European J. Pharmacol.* 176: 219-223, 1990.

70. Johansson, B. Determinants of vascular reactivity. *Fed. Proc.* 33: 121-126, 1974.

71. Johnson, P.C. Autoregulatory responses of cat mesenteric arterioles measured *in vivo*. *Circ. Res.* 22: 199-212, 1968.

72. Johnson, P.C. The myogenic response. In: *Handbook of Physiology. Section 2: The Cardiovascular System. Volume II. Vascular Smooth Muscle*, edited by D.F. Bohr, A.P. Somlyo and H.V. Sparks,Jr.. Bethesda, Maryland: American Physiological Society, 1980, p. 409-442.

73. Johnson, P.C. and K.M. Hanson. Effect of arterial pressure on arterial and venous resistance of intestine. *J. Appl. Physiol.* 17(3): 503-508, 1962.

74. Judd, R.M. and R.E. Mates. Coronary input impedance is constant during systole and diastole. *Am. J. Physiol.* 260: H1841-H1851, 1991.

75. Kaley, G., A. Koller, J.M. Rodenburg, E.J. Messina, and M.S. Wolin. Regulation of arteriolar tone and responses via L-arginine pathway in skeletal muscle. *Am. J. Physiol.* 262: H987-H992, 1992.

76. Kaley, G., J.M. Rodenburg, E.J. Messina, and M.S. Wolin. Endothelium-associated vasodilators in rat skeletal muscle microcirculation. *Am. J. Physiol.* 256: H720-H725, 1989.

77. Kamm, R.D. Flow through collapsible tubes. In: *Handbook of Engineering*, edited by R. Skalak and S. Chien. New York: McGraw-Hill Book Company, 1987, p. 23.1-23.19.

78. Kanatsuka, H., K. Ashikawa, T. Komaru, T. Suzuki, and T. Takishima. Diameter change and pressure-red blood cell velocity relations in coronary microvessels during long diastoles in the canine left ventricle. *Circ. Res.* 66: 503-510, 1990.

79. Katusic, Z.S., J.T. Shepherd, and P.M. Vanhoutte. Endothelium-dependent contraction to stretch in canine-basilar arteries. *Am. J. Physiol.* 252: H671-H673, 1987.

80. Kelm, M. and J. Schrader. Control of coronary vascular tone by nitric oxide. *Circ. Res.* 66: 1561-1575, 1990.

81. Klocke, F.J., I.R. Weinstein, J.F. Klocke, A.K. Ellis, D.R. Kraus, R.E. Mates, J.M. Canty, R.D. Anbar, R.R. Romanowski, K.W. Wallmeyer, and M.P. Echt. Zero-flow pressures and pressure-flow relationships during single long diastoles in the canine coronary bed before and during maximum vasodilation. *J. Clin. Invest.* 68: 970-980, 1981.

82. Knowlton, F.P. and E.H. Starling. The influence of variations in temperature and blood-pressure on the performance of the isolated mammalian heart. *J. Physiol. (Lond)* 44: 206-219, 1912.

83. Koller, A. and G. Kaley. Prostaglandins mediate arteriolar dilation to increased blood flow velocity in skeletal muscle microcirculation. *Circ. Res.* 67: 529-534, 1990.

84. Kulik, T.J., J.N. Evans, and W.J. Gamble. Stetch-induced contraction in pulmonary arteries. *Am. J. Physiol.* 255: H1391-H1398, 1988.

85. Kuo, L., W.M. Chilian, and M.J. Davis. Coronary arteriolar myogenic response is independent of endothelium. *Circ. Res.* 66: 860-866, 1990.

86. Kuo, L., W.M. Chilian, and M.J. Davis. Interaction of pressure- and flow-induced responses in porcine coronary resistance vessels. *Am. J. Physiol.* 261: H1706-H1715, 1991.

87. Kuo, L., M.J. Davis, and W.M. Chilian. Endothelial modulation of arteriolar tone. *N. I. P. S.* 7: 5-9, 1992.

88. Lamontagne, D., A. König, E. Bassenge, and R. Busse. Prostacyclin and nitric oxide contribute to the vasodilator action of acetylcholine and bradykinin in the intact rabbit coronary bed. *J. Cardiovasc. Pharmacol.* 20: 652-657, 1992.

89. Lamport, H. and S. Baez. Physical properties of small arterial vessels. *Physiol. Rev.* 42(suppl 5): 328-352, 1962.

90. Laughlin, M.H. and R.B. Armstrong. Rat muscle blood flows as a function of time during prolonged slow treadmill exercise. *Am. J. Physiol.* 244: H814-H824, 1983.

91. Lyon, C.K., J.B. Scott, and C.Y. Wang. Flow through collapsible tubes at low Reynolds numbers. *Circ. Res.* 47: 68-73, 1980.

92. Magder, S. Starling resistor versus compliance. Which explains the zero-flow pressure of a dynamic arterial pressure-flow relation? *Circ. Res.* 67: 209-220, 1990.

93. Martin, W., D.G. White, and A.H. Henderson. Endothelium-derived relaxing factor and atriopeptin II elevate cyclic GMP levels in pig aortic endothelial cells. *Br. J. Pharmacol.* 93: 229-239, 1988.

94. Meininger, G.A., C.A. Mack, K.L. Fehr, and H.G. Bohlen. Myogenic vasoregulation overrides local metabolic control in resting rat skeletal muscle. *Circ. Res.* 60: 861-870, 1987.

95. Meininger, G.A. and J.P. Trzeciakowski. Combined effects of autoregulation and vasoconstrictors on hindquarters vascular resistance. *Am. J. Physiol.* 258: H1032-H1041, 1990.

96. Mekata, F. The role of hyperpolarization in the relaxation of smooth muscle of monkey coronary artery. *J. Physiol. (Lond)* 371: 257-265, 1986.

97. Mellander, S., M. Maspers, J. Björnberg, and L.-O. Andersson. Autoregulation of capillary pressure and filtration in cat skeletal muscle in states of normal and reduced vascular tone. *Acta Physiol. Scand.* 129: 337-351, 1987.

98. Messina, E.J., D. Sun, A. Koller, M.S. Wolin, and G. Kaley. Role of endothelium-derived prostaglandins in hypoxia-elicited arteriolar dilation in rat skeletal muscle. *Circ. Res.* 71: 790-796, 1992.

99. Mitzner, W. Hepatic outflow resistance, sinusoid pressure, and the vascular waterfall. *Am. J. Physiol.* 227: 513-519, 1974.

100. Morff, R.J. and H.J. Granger. Autoregulation of blood flow within individual arterioles in the rat cremaster muscle. *Circ. Res.* 51: 43-55, 1982.

101. Morff, R.J. and H.J. Granger. Contribution of adenosine to arteriolar autoregulation in striated muscle. *Am. J. Physiol.* 244: H567-H576, 1983.

102. Nichol, J., F. Girling, W. Jerrard, E.B. Claxton, and A.C. Burton. Fundamental instability of the small blood vessels and critical closing pressures in vascular beds. *Am. J. Physiol.* 164: 330-344, 1951.

103. Oka, S. and T. Azuma. Physical theory of tension in thick-walled blood vessels in equilibrium. *Biorheology* 7: 109-117, 1970.

104. Osberg, C. and B.L. Langille. Reflex control of arterial compliance in rabbits. *Can. J. Physiol. Pharmacol.* 60: 1475-1481, 1982.

105. Palmer, R.M.J., D.S. Ashton, and S. Moncada. Vascular endothelial cells synthesize nitric oxide from L-arginine. *Nature* 333(16): 664-666, 1988.

106. Pappenheimer, J.R. and J.P. Maes. A quantitative measure of the vasomotor tone in the hindlimb muscles of the dog. *Am. J. Physiol.* 137: 187-199, 1942.

107. Permutt, S. and R.L. Riley. Hemodynamics of collapsible vessels with tone: the vascular waterfall. *J. Appl. Physiol.* 18(5): 924-932, 1963.

108. Pohl, U., J. Holtz, R. Busse, and E. Bassenge. Crucial role of endothelium in the vasodilator response to increased flow *in vivo*. *Hypertension* 8: 37-44, 1986.

109. Price, J.M., D.L. Davis, and E.B. Knauss. Length-dependent sensitivity in vascular smooth muscle. *Am. J. Physiol.* 241: H557-H563, 1981.

110. Rand, V.E. and C.J. Garland. Endothelium-dependent relaxation to acetylcholine in the rabbit basilar artery: importance of membrane hyperpolarization. *Br. J. Pharmacol.* 106: 143-150, 1992.

111. Rock, P., G.A. Patterson, S. Permutt, and J.T. Sylvester. Nature and distribution of vascular resistance in hypoxic pig lungs. *J. Appl. Physiol.* 59: 1891-1901, 1985.

112. Rosenblum, W.I. Hydroxyl radical mediates the endothelium-dependant relaxation produced by bradykinin in mouse cerebral arterioles. *Circ. Res.* 61: 601-603, 1987.

113. Rubanyi, G.M. Endothelium-dependent pressure-induced contraction of isolated canine carotid arteries. *Am. J. Physiol.* 255: H783-H788, 1988.

114. Schwartz, L.M. and J.E. McKenzie. Adenosine and active hyperemia in soleus and gracilis muscle of cats. *Am. J. Physiol.* 259: H1295-H1304, 1990.

115. Scivoletto, R. and M.H.C. Carvalho. Cardionatrin causes vasodilation *in vitro* which is not dependent on the presence of endothelial cells. *European J. Pharmacol.* 101: 143-145, 1984.

116. Segal, S.S. Microvascular recruitment in hamster striated muscle: role for conducted vasodilation. *Am. J. Physiol.* 261: H181-H189, 1991.

117. Segal, S.S. Communication among endothelial and smooth muscle cells coordinates blood flow control during exercise. *N. I. P. S.* 7: 152-156, 1992.

118. Segal, S.S. and B.R. Duling. Flow control among microvessels coordinated by intercellular conduction. *Science* 234: 868-870, 1986.

119. Shapiro, A.H. Steady flow in collapsible tubes. *J. Biomech. Eng.* 99: 126-147, 1977.

120. Sipkema, P. and N. Westerhof. Mechanics of a thin walled collapsible microtube. *Ann. Biomed. Eng.* 17: 203-217, 1989.

121. Slaaf, D.W., H.H.E. Oude Vrielink, G.-J. Tangelder, and R.S. Reneman. Effective diameter as a determinant of local vascular resistance in presence of vasomotion. *Am. J. Physiol.* 255: H1240-H1243, 1988.

122. Slaaf, D.W., R.S. Reneman, and C.A. Wiederhielm. Cessation and onset of muscle capillary flow at simultaneously reduced perfusion and transmural pressure. *Int. J. Microcirc. Clin. Exp.* 6: 215-224, 1987.

123. Slaaf, D.W., G.-J. Tangelder, H.C. Teirlinck, H.H.E. Oude Vrielink, and R.S. Reneman. Flow cessation pressures in the rabbit tenuissimus muscle. *Int. J. Microcirc. Clin. Exp.* 5: 3-9, 1986.

124. Slaaf, D.W., G.-J. Tangelder, H.C. Teirlinck, and R.S. Reneman. Arteriolar vasomotion and arterial pressure reduction in rabbit tenuissimus muscle. *Microvasc. Res.* 33: 71-80, 1987.

125. Smiesko, V., J. Kozik, and S. Dolezel. Role of endothelium in the control of arterial diameter by blood flow. *Blood Vessels* 22: 247-251, 1985.

126. Soohoo, S.L., H.S. Goldberg, R. Graham, and A.C. Jasper. Zone 2 and zone 3 pulmonary blood flow. *J. Appl. Physiol.* 62: 1982-1988, 1987.

127. Stainsby, W.N. and E.M. Renkin. Autoregulation of blood flow in resting skeletal muscle. *Am. J. Physiol.* 201(1): 117-122, 1961.

128. Sylvester, J.T., R.D. Gilbert, R.J. Traystman, and S. Permutt. Effects of hypoxia on the closing pressure of the canine systemic arterial circulation. *Circ. Res.* 49: 980-987, 1981.

129. Tonnesen, K.H. Blood-flow through muscle during rhythmic contraction measured by ^{133}Xenon. *Scandinav. J. Clin. & Lab. Investigation* 16: 646-654, 1964.

130. Urchida, E. and D.F. Bohr. Myogenic tone in isolated perfused resistance vessels from rats. *Am. J. Physiol.* 216: 1343-1350, 1969.

131. Vallance, P., J. Collier, and S. Moncada. Effects of endothelium-derived nitric oxide on peripheral arteriolar tone in man. *Lancet* 2: 997-1000, 1989.

132. Van Citters, R.L. Occlusion of lumina in small arterioles during vasoconstriction. *Circ. Res.* 18: 199-204, 1966.

133. Van Nueten, J.M. and P.M. Vanhoutte. Calcium entry blockers and vascular smooth muscle heterogeneity. *Fed. Proc.* 40: 2862-2865, 1981.

134. Whittaker, S.R.F. and F.R. Winton. The apparent viscosity of blood flowing in the isolated hindlimb of the dog, and its variation with corpuscular concentration. *J. Physiol. (Lond)* 78: 339-369, 1933.

CHAPTER 2

EFFECT OF CAROTID SINUS STIMULATION ON RESISTANCE AND CRITICAL CLOSING PRESSURE OF THE CANINE HINDLIMB

2.1. ABSTRACT

Sympathetically mediated changes in blood pressure are thought to occur through changes in arterial resistance (R_a). To test if the critical closing pressure (P_{crit}) could also play a role, we pump-perfused the vascularly isolated canine hindlimb at constant flow. Carotid sinuses were isolated and both vagus nerves cut. Carotid sinus (P_{car}), arterial (P_a), perfusion (P_{per}) and venous (P_v) pressures, and flow to the hindlimb ($\dot{Q}$, electromagnetic flow probe) were measured. By decreasing pump flow to zero over time periods of 1-10 seconds and measuring the pressure at zero-flow, it was possible to estimate arterial compliance (C_a), and P_{crit}. R_a was calculated as $(P_{per}-P_{crit})/\dot{Q}$. Venous resistance ($R_v$) was calculated as $(P_{el}-P_v)/\dot{Q}$, where P_{el} is the pressure in the compliant region obtained by the double occlusion technique. Raising P_{car} from 115±7 mmHg to 203±10 mmHg (n=6) decreased P_{crit} from 49.7±4.3 to 25.9±2.6 mmHg and R_a from 10.7±1.2 to 6.8±0.9 mmHg·min·100g·ml^{-1} ($p<0.05$). Lowering P_{car} from 119±6 mmHg to 71±6 mmHg (n=6) increased P_{crit} from 37.0±3.3 to 61.0±8.5 mmHg and R_a from 10.0±1.6 to 14.0±2.4 mmHg·min·100g·ml^{-1} ($p<0.05$). C_a increased when carotid sinus pressure was raised ($p<0.05$), and decreased when sinus pressure was decreased ($p<0.1$). Venous resistance (R_v) did not change when P_{car} was altered. In conclusion, changes in carotid sinus stimulation alters blood flow to the hindlimb through changes in both P_{crit} and R_a.

2.2. INTRODUCTION

Poiseuille's Law states that flow ($\dot{Q}$) through a tube is equal to the pressure drop across the tube, divided by the resistance [$8nl/(\pi r^4)$] between the inflow and outflow (18). Therefore, when there is no flow, the inflow pressure should equal the outflow pressure. However, many authors have shown that there is an arterial-venous pressure difference at zero flow (2,3,8,13,16,21). In 1951, Burton hypothesized that an instability in the elastic wall causes arterial vessels to suddenly collapse (i.e. resistance increases up to infinity) when the inflow pressure declines below a certain value (7). He called the perfusion pressure at zero-flow the critical closing pressure (P_{crit}). However, in 1963, Permutt and Riley showed that the pressure gradient at zero-flow (18) is better explained by a Starling resistor mechanism that creates a vascular waterfall at the level of the arterioles. The back pressure of the collapsible segment is created by the tone of the smooth muscles in the arterioles. When the intravascular pressure overcomes the tension generated by the smooth muscle, the vessel opens, but a waterfall effect is still present because the energy is lost in keeping this segment open. The arterioles thus act almost like sphincters. Flow under this condition is determined by the difference between arterial pressure (P_a), P_{crit}, and the arterial resistance (R_a) between the two. Downstream resistance and pressure have no effect on flow. Unlike Burton's model, P_{crit} affects flow throughout the pressure-flow relation, and not only at zero-flow.

There are several important implications to the presence of a Starling resistor-like mechanism in the arterial circulation (13). First, resistance calculations based on pressure-flow relations may lead to erroneous conclusions (both quantitative and qualitative) if venous pressure (P_v) is used as the downstream pressure. Hence, any inferences about changes in vessel wall diameter may also be in error. Second, P_a or flow can be altered by two mechanisms, changing P_{crit} or changing R_a. Third, capillary

pressure can be adjusted by changing downstream resistance without affecting flow into the region, since capillary pressure is below P_{crit}. Fourth, fluctuations in P_v that occur with respiration will not affect flow into the region. And finally, a sudden decrease in cardiac output will not produce as rapid or extreme a fall in P_a.

If P_{crit} is generated by smooth muscle tone, it should be affected by neuro-humoral mechanisms. Indeed, adenosine, norepinephrine (6) and reactive hyperaemia (13) have been shown to alter the critical closing pressure. However, the role of P_{crit} in the normal control of blood pressure has not been investigated. We hypothesized that the carotid sinus baroreflex alters arterial pressure through changes in P_{crit} in addition to changes in R_a. We used the method of Magder (13) to measure P_{crit} and R_a. Briefly, in a pump-perfused isolated hindlimb, P_{crit} can be estimated by slowly turning the pump flow down to zero over 5-10 seconds, and measuring the zero flow-pressure intercept (P_{zf}) (13). It should be noted that perfusion pressure continues to decline after flow has ceased. This can be explained by a small amount of collateral circulation (amounting to only 1.5% of the total conductance) which bypasses the Starling resistor (13). The P_{zf} is the pressure measured at zero-flow, and not the final plateau perfusion pressure. If the ramp time to zero-flow (t_{zf}) is less than 4 seconds (e.g. sudden stop flow, diastolic decay curve), the P_{zf} is affected by the arterial compliance (C_a) and overestimates the actual P_{crit} ($P_{zf} > P_{crit}$) (2,13,19). However, if t_{zf} is greater than 10 seconds, metabolic factors may begin to have an effect, and P_{crit} is underestimated ($P_{zf} < P_{crit}$) (4). If t_{zf} is between 5-10 seconds, P_{zf} is an approximation of P_{crit}. R_a is then calculated using P_{crit} as the downstream pressure.

2.3. METHODS

Twelve dogs weighing 18-34 kg were anaesthetized with α-chloralose (75 $mg \cdot kg^{-1}$) after initial induction with sodium pentothal (1 $mg \cdot kg^{-1}$). Supplemental

doses of α-chloralose were given as needed. The animals were intubated, ventilated (Harvard Apparatus), and given supplemental oxygen as needed. We cannulated the left carotid artery to monitor P_a and to obtain arterial blood samples. Normal saline was infused into the right jugular vein to maintain proper hydration and sodium bicarbonate was given to maintain acid-base balance. Heparin (10,000 units) was given to prevent blood clotting.

Surgical Preparation

The preparation is illustrated in figure 2.1. We isolated the carotid sinuses by ligating the lingual, external carotid, and internal carotid arteries bilaterally. Blood flow was diverted from the right common carotid artery, through a pump (Masterflex #16 Tygon tubing) and then to both carotid sinuses via the distal stumps of the common carotid arteries. Carotid sinus pressure (P_{car}) was measured via a side port on the tubing distal to the pump. A bilateral vagotomy was performed to remove the influence of aortic baroreceptors.

The vascular supply to the left hindlimb was isolated as previously described (13). In brief, all branches of the femoral artery and vein in the femoral triangle were tied. Blood flow was diverted from the right femoral artery, through an in-line electromagnetic flow probe (Carolina Medical #10), and into the left femoral artery. Perfusion pressure (P_{per}) was measured through a side port downstream from the flow probe. Two side ports upstream from the flow probe allowed blood flow to be diverted through a second pump (Masterflex #16 Tygon tubing) and back to the femoral artery. The direct line was used for measuring the natural flow of the hindlimb at a given carotid sinus pressure. During experimental runs, flow was controlled by clamping the direct line and adjusting the pump speed. We cannulated the left femoral vein and returned the outflow to the animal via the right jugular vein. Femoral venous pressure (P_v) was measured from a Y-connector close to the femoral vein cannulation site.

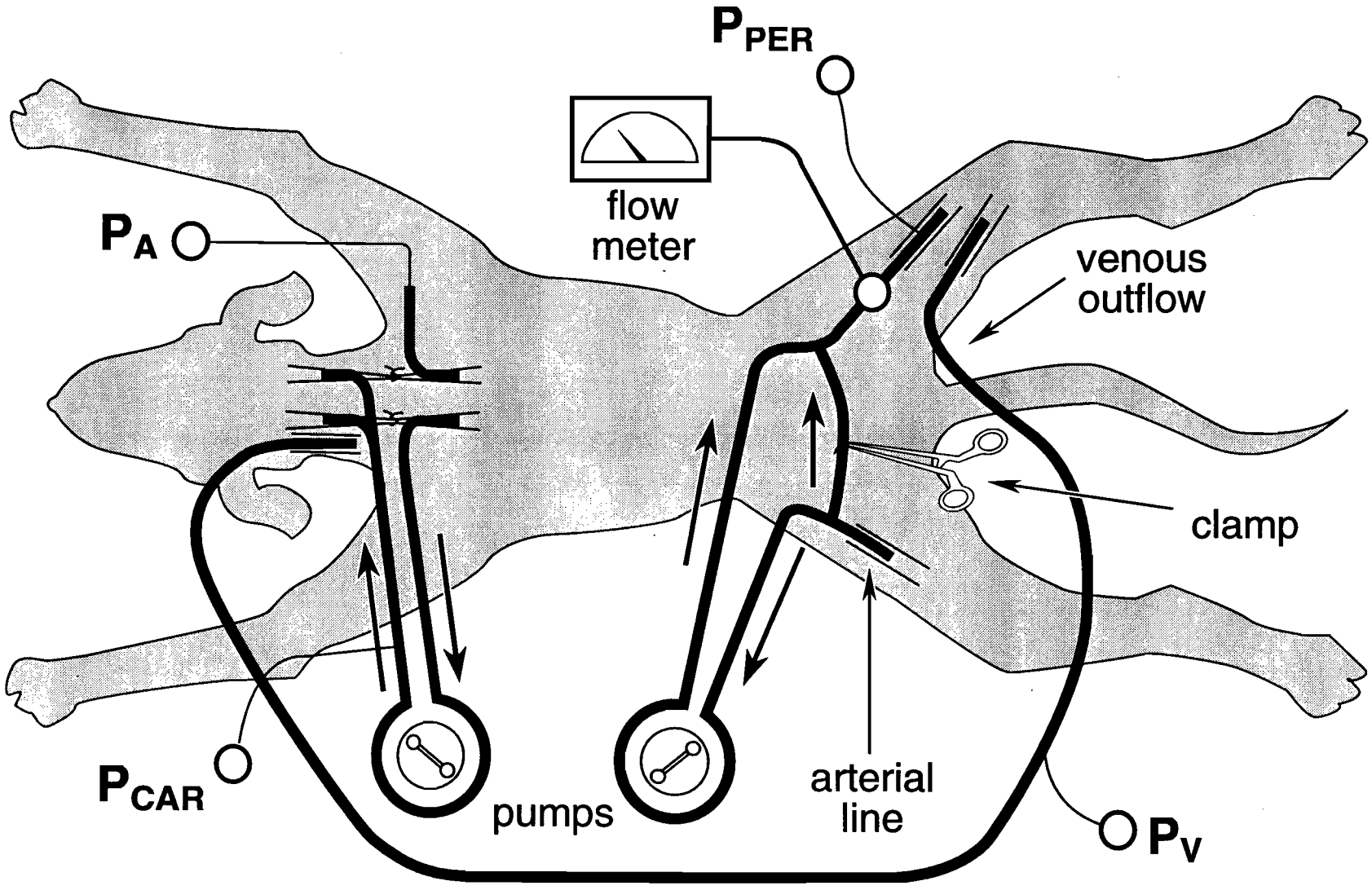

Figure 2.1: Experimental setup (see text for complete details).

We passed surgical wires through the thigh with a 12-14 gauge needle, and tied them securely around either side of the femur to eliminate any collateral flow.

Measurements

Pressures were measured with Trantec transducers. Flow ($\dot{Q}$) was measured using a square-wave electromagnetic flow meter and in-line probe (Carolina Medical). Signals were filtered at 3 Hz. All signals were processed through Gould amplifiers and simultaneously recorded on an eight-channel Graphtec recorder and on an IBM compatible computer using CODAS software program (DATAQ Instruments Inc.) for A-D conversion and analysis.

Protocol

Due to the length of the experiments, separate groups of animals (n=6 per group) were used to study the effects of raising and lowering the carotid sinus pressure. In one group, the carotid sinus was initially perfused at either normal ($P_{car} \approx P_a$, $P_{car}=115\pm7$ mmHg, mean$\pm$S.E.M.) or high ($P_{car}=203\pm10$ mmHg) pressure, and the natural flow to the hindlimb was measured. The tubing between the two side ports upstream from the flow probe was then clamped, and the pump speed adjusted to the same rate as the natural flow. To obtain the zero-flow measurements, we decreased pump flow to zero over time periods ranging from 1-10 seconds (random order). In between each run to zero-flow, the pump speed was reset to the initial flow, and perfusion pressure was allowed to return to baseline before proceeding. After a series of measurements (5-8 per carotid sinus pressure), the clamp was removed, hindlimb natural flow restored, and the carotid sinus pressure was either increased or decreased depending on the original condition. After a 15 minute equilibration period, the natural flow to the hindlimb was remeasured during the new carotid sinus pressure, and the pump flow reset to this value. Another set of zero-flow measurements was then obtained at the new carotid sinus pressure.

Statistics

We used paired t-tests to analyze changes in measured or calculated variables when the carotid sinus pressure was altered. Results were considered significant if $p<0.05$.

2.4. RESULTS

The pH and PCO_2 ranged from 7.28-7.45 and 30-46 mmHg respectively. The PO_2 ranged from 90-210 mmHg. Animals were only included if the hematocrit was above 30%. The effects of altering carotid sinus pressure on P_a and hindlimb are shown in table 2.1.

	P_{car} (mmHg)	P_a (mmHg)	P_{per} (mmHg)	$\dot{Q}$ ($ml \cdot min^{-1} \cdot 100g^{-1}$)
High Carotid Group				
Control	115±7	137±11	119±9	7.2±1.4
High Carotid	203±10	85±17*	65±11*	6.4±1.7
Low Carotid Group				
Control	119±6	122±13	111±12	8.4±1.7
Low Carotid	71±6	169±12*	164±15*	8.6±1.8

Table 2.1: Effect of carotid sinus pressure (P_{car}) on arterial pressure (P_a), perfusion pressure (P_{per}) and flow ($\dot{Q}$). Carotid sinus pressure was set ≈ arterial pressure for control runs. All values are mean±S.E.M.. (n=6 for each group). * Significantly different from value obtained at normal carotid sinus pressure for that group.

In the High Carotid Group, an increase in P_{car} from 115±7 mmHg to 203±10 mmHg resulted in a decrease in P_a from 137±11 mmHg to 85±17 mmHg ($p<0.01$). Similarly, a fall in P_{car} from 119±6 mmHg to 71±6 mmHg caused a significant rise in

P_a from 122±13 mmHg to 169±12 mmHg ($p<0.01$). P_{per} was set to the pressure measured under free flow conditions at each carotid sinus pressure. Due to the resistance of the tubing, this was always less than the P_a. Natural flow to the hindlimb was not affected by the change in P_{car}.

Figure 2.2a is a plot of the observed and predicted P_{zf} against t_{zf} from one animal.

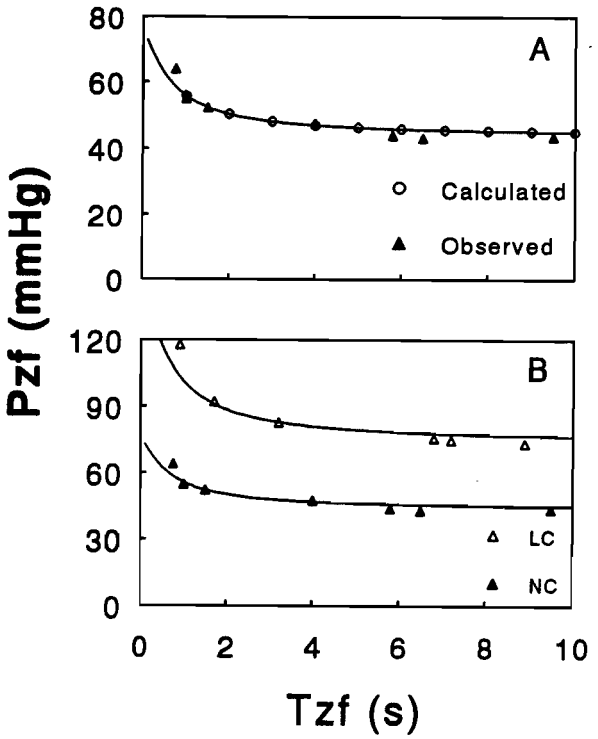

Figure 2.2: The zero-flow pressure intercept (P_{zf}) is plotted against the time taken to reach zero-flow (t_{zf}). In 2a, the closed triangles represent actual data obtained from one animal under normal carotid sinus pressure. The open circles and solid line are the values predicted using equation 2.1 (see text). Figure 2.2b, from the same experiment, shows the shift in the curve with different carotid sinus pressures. In this experiment, P_{car} was raised from a low pressure (LC) to a normal pressure (NC). The shift downwards indicates a decreased critical closing pressure.

In this animal, equation 2.1 was solved for compliance using a t_{zf} of 1.5 seconds. This value of compliance was then used to predict what the P_{zf} would be for other t_{zf} values. The data were well predicted by this approach. It can be seen that the P_{zf} initially declines with increasing t_{zf}, but reaches a plateau with t_{zf} greater than 4-5 seconds. Figure 2.2b shows a plot of the observed data from the same animal under conditions of normal carotid (NC) and low carotid (LC) sinus pressures. The solid line again represents the calculated values according to equation 2.1. At low carotid sinus pressure, the curve is shifted upwards, i.e. P_{crit} is increased.

Mean data for R_a, R_v, P_{crit}, and C_a are shown in figure 2.3.

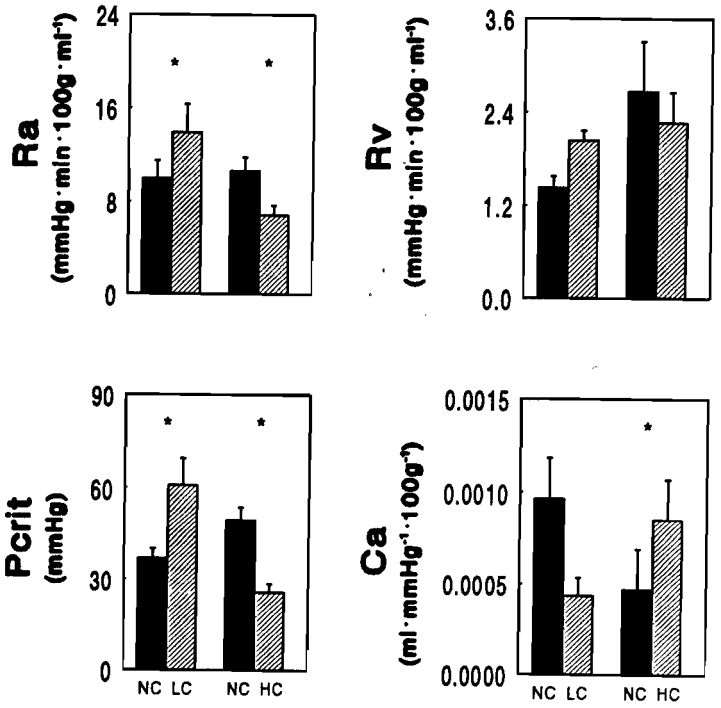

Figure 2.3: Mean±S.E.M. for arterial resistance (R_a), venous resistance (R_v), critical closing pressure (P_{crit}), and arterial compliance (C_a) in two groups of six animals (N.B. n=5 in the NC/LC group for the calculation of R_v). Each animal was studied at only two sinus pressures, i.e. at a normal carotid sinus pressure (NC), and at either low carotid sinus

pressure (LC), or high carotid sinus pressure (HC). * indicates significant differences at $p<0.05$.

When the carotid sinus pressure was lowered from 119 ± 6 mmHg to 71 ± 6 mmHg, P_{crit} increased $62\pm10\%$ and R_a increased $42\pm15\%$ ($p<0.05$). When P_{car} was raised from 115 ± 7 mmHg to 203 ± 10 mmHg, P_{crit} decreased $45\pm8\%$ and R_a decreased $34\pm9\%$ ($p<0.05$). Therefore, the changes in R_a were qualitatively similar but quantitatively smaller than the changes in P_{crit}. R_v did not change significantly with either an increase or decrease in carotid sinus pressure. C_a (expressed per 100 g) increased significantly with an increase in P_{car} ($p<0.05$). A decrease in P_{car} resulted in a decreased C_a in 5 of 6 animals but a slightly increased compliance in one animal ($p<0.1$, not significant).

Figure 2.4a shows the expected changes in P_{per} with changes in P_{car} if flow is kept constant, and one takes into account only the change in R_a or only the change in P_{crit}, or both. The left black bar represents the P_{per} at a normal P_{car}. The hatched bar shows the results if only R_a was affected when the P_{car} was changed [i.e. $P_{per}=(\dot{Q}*R_a)+P_{crit}$, where $\dot{Q}$ and P_{crit} are obtained under normal carotid conditions, and R_a is the value obtained under LC/HC conditions]. Similarly, the dotted bar shows the increased P_{per} if only P_{crit} had been affected. Under LC conditions, an isolated change of R_a would have increased P_{per} from 111 ± 12 mmHg to 142 ± 21 mmHg. An isolated change of P_{crit} would have increased P_{per} to the similar value of 135 ± 16 mmHg. The calculated P_{per} are significantly different from the initial P_{per}, but not from each other. In the HC group, the results were similar. The cross-hatched bar shows the calculated P_{per} when both R_a and P_{crit} are allowed to vary, but flow is kept at the same value as control. Finally, the right black bar shows the actual P_{per} measured when P_{car} was lowered. This is not identical to the cross-hatched bar because the

theoretical changes in P_{per} were calculated using the values for flow under control conditions, which were slightly different than the actual flow under experimental conditions.

In the previous analysis, arterial pressure (and thus the set perfusion pressure) was allowed to change when the carotid sinus pressure was altered. However, in the intact circulation, the baroreflex acts to maintain sinus pressure (and therefore arterial pressure) constant. Under these conditions, flow becomes the dependent variable. We therefore calculated what would happen to hindlimb blood flow if perfusion pressure was maintained constant (i.e. as exists in the closed-loop baroreflex of the intact circulation), and only one variable changed, i.e. either R_a or P_{crit} [$\dot{Q}=(P_{per}-P_{crit})/R_a$]. The results are presented in figure 2.4b with the same legend as in figure 2.4a.

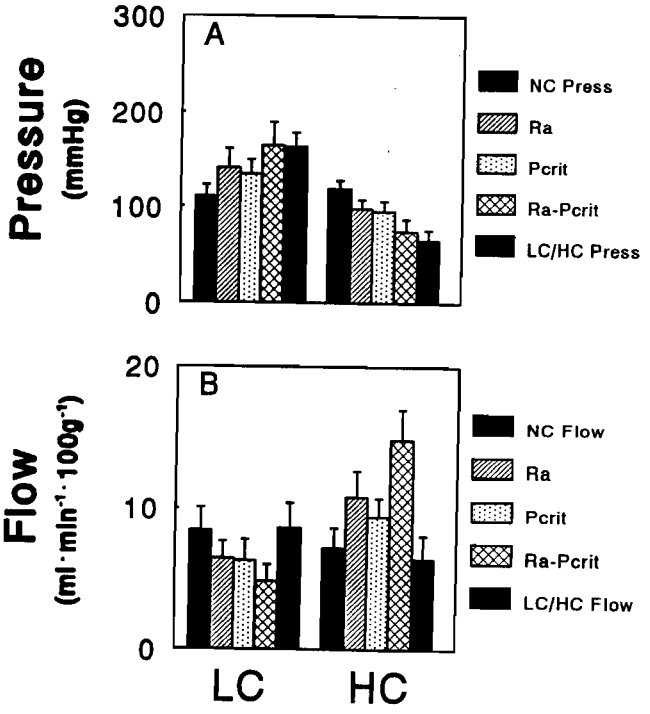

Figure 2.4: Theoretical changes in pressure (A) and flow (B) if the carotid baroreflex affected only one variable (P_{crit} or R_a). Carotid sinus pressure was lowered in one group of animals (LC), and raised in another group

of animals (HC). In A, the solid bar shows the observed data when the carotid sinus pressure is normal. The hatched bar shows the theoretical change in pressure if only R_a was affected by the baroreflex [i.e. $P_{per}=(\dot{Q}*R_a)+P_{crit}$, where $\dot{Q}$ and P_{crit} are obtained under normal carotid conditions, and R_a is the value obtained under LC/HC conditions]. Similarly, the dotted bar shows the theoretical change in pressure if only P_{crit} was affected by the baroreflex. There was no significant difference between these two values in either group. The cross-hatched bar shows the calculated change in pressure if both P_{crit} and R_a were allowed to vary. This is slightly (not significantly) different than the observed change in pressure under the new carotid sinus pressure (LC/HC) since measured flow fluctuated slightly. Figure 2.4b represents a similar analysis, except P_{per} was kept constant, and the theoretical changes in flow were calculated varying only one variable at a time. This analysis attempts to predict the changes in flow that would have occurred if we had not opened the loop of the carotid sinus baroreflex control system. The values predicted by changing either R_a or P_{crit} were not significantly different from each other.

If only R_a changed when P_{car} was lowered, then flow would have fallen from 8.4 ± 1.7 ml·min^{-1}·100g^{-1} to 6.4 ± 1.3 ml·min^{-1}·100g^{-1}. If only P_{crit} changed when P_{car} was lowered, then flow would have fallen to the similar value of 6.3 ± 1.5 ml·min^{-1}·100g^{-1}. If changes in flow are calculated when both R_a and P_{crit} are altered but with the control value for P_{per}, flow would have been 4.8 ± 1.2 ml·min^{-1}·100g^{-1}. This is very different than the cross-hatched bar because the theoretical changes in flow were calculated using the control values of P_{per} which were very different than P_{per} under

experimental conditions. Therefore, a fall in arterial pressure activates the carotid baroreflex, which restores systemic arterial pressure to normal by increasing both P_{crit} and R_a. This results in a large decrease in flow to the hindlimb. When theoretical changes in flow with a high carotid sinus pressure are examined, the results are again similar.

2.5. DISCUSSION

Our results indicate that R_a, P_{crit}, and C_a in the hindlimb are altered by carotid sinus mediated changes in sympathetic drive, whereas R_v is not. Therefore, when the carotid sinus pressure is low, the baroreflex increases blood pressure by increasing P_{crit} in addition to increasing R_a. Whereas the relative changes in R_a and P_{crit} are qualitatively similar, quantitatively P_{crit} changed more than R_a. Before discussing these results in detail, some technical factors need to be considered, including the influence of other baroreceptors, the completeness of the hindlimb isolation, and the effects of compliance on the measurement of P_{crit}.

Carotid sinus pressure was controlled with a pump, and the bilateral vagotomy should have removed most of the thoracic baroreceptor reflexes. If any baroreflexes still remained, they would only have blunted the responses we observed.

Complete hindlimb isolation is necessary to obtain accurate values for P_{zf} (9). When pump speed is decreased, the perfusion pressure measured at the femoral artery declines. However, any arterial inflow bypassing the hindlimb isolation would remain equal to arterial pressure. When femoral pressure becomes less than this collateral arterial pressure, flow through the flow probe will stop even though the hindlimb is being perfused. This results in an artificially high P_{zf}. Collateral venous flow should not affect the P_{zf}, but must be eliminated to obtain accurate recordings of P_{el} (and hence accurate calculations of R_v). As discussed in the Methods section, we used the double

occlusion technique (14) to ensure isolation, and did not proceed unless isolation was confirmed.

The zero-flow pressure intercept of a dynamic pressure flow relation can also be affected by vessel compliance (2,8,13,19). The reasoning is similar to how collateral inflow can yield artificially high values. For instance, if inflow is instantaneously decreased to the value in the compliant region, the pressure gradient decreases to zero. Flow measured at the femoral artery would therefore cease, even though flow continues downstream from the compliant region. Thus, an artificially high P_{zf} would be recorded. Magder recognized this problem and compared the observed results for the relationship of P_{zf} versus ramp time with several different models of the circulation (13). The plateau in the relationship (figure 2.2) could not be explained by modelling the region as a single compliant region, nor as two compliant regions in series with resistances, but could only be explained if a Starling resistor-like mechanism was operative. On the other hand, the decrease in P_{zf} when ramp time is increased from 1-4 seconds indicates that compliance effects cannot be ignored. This effect is minimized if t_{zf} is long enough to allow the compliant regions to empty (i.e. >5 time constants, τ). The τ of discharge of a region can be described by the product of its compliance and downstream resistance. In this experiment, the compliance is the arterial compliance, and the resistance is the arterial resistance located above the Starling resistor. The average τ thus calculated was 0.34 ± 0.27 seconds (mean$\pm$S.D.) and therefore compliance effects on P_{crit} (i.e. the P_{zf} when $t_{zf} > 5$ seconds) could be considered negligible. τ was not affected by the carotid sinus pressure (i.e. the change in resistance was matched by the change in compliance), which is in agreement with observations made by Osberg and Langille (17).

The τ in our experiment is considerably less than the arterial τ estimated in other experiments (e.g. 0.76 seconds in whole body rat (12), 1.15-1.59 seconds in

pressure reported by other authors (22), and must therefore occur upstream from the capillaries. Second, an increase in carotid sinus pressure induced vasodilatation which theoretically, should have increased tissue edema and increased P_{crit}. However, we observed a decrease. Our results are more consistent with Permutt and Riley's model of the circulation where the back pressure of the Starling resistor mechanism (P_{crit}) is generated by the arteriolar smooth muscle tone (18). A decrease in vasomotor tone (vasodilation) is then expected to result in a decrease of P_{crit}.

Work from other laboratories has suggested that P_{crit} may be controlled through neural and/or hormonal mechanisms. In 1962, Ashton measured pressure and flow in the human forearm and finger (1). By decreasing local perfusion pressure in steps and waiting for a steady-state flow to develop each time, she was able to plot the steady-state pressure-flow relation and obtain a steady-state P_{zf}. Ashton found the steady-state pressure-flow relation was shifted to the right with cooling of the forearm (i.e. an increase in P_{zf} due to vasoconstriction), and shifted to the left with heating. In two subjects, vasodilation to the finger was induced by nerve block, and the pressure-flow relation was again shifted to the left. Later, Braakman et al. showed that vasoactive drugs can affect the pressure-flow relation and the steady-state P_{zf} in the isolated, pump-perfused canine iliac periphery (5).

The usefulness of steady-state measurements for assessing P_{crit} is limited since they include changes from autoregulation. As flow is decreased in steps and the tissue becomes hypoxic, one would expect P_{crit} and R_a to decrease. Therefore, the P_{crit} obtained using these methods does not reflect the instantaneous P_{crit} that exists at higher flows. If the value of P_{crit} is unreliable, then resistance calculations ($R_a=(P_{per}-P_{crit})/\dot{Q}$) are also unreliable. Therefore, inferences on vessel diameter changes may be in error. Recently however, Braakman et al. (6) used dynamic conditions to assess the effects of norepinephrine and adenosine. Their method was to decrease P_{per} in multiples of

7.5 mmHg (over <200 ms), and measure the flow response. When flow became zero, the set P_{per} was considered the P_{crit}. As noted in the introduction, and confirmed by our results, this method overestimates P_{crit} due to the effects of compliance. Acknowledging these limitations, their results still suggest that adenosine and norepinephrine affect the critical closing pressure. Since norepinephrine is released during increased sympathetic drive, the results support our conclusions that P_{crit} can be controlled by neural activity.

The value for arterial compliance that we obtained is in the same range as that obtained by Magder (13). Our study also confirms previous results that arterial compliance is affected by the carotid sinus baroreflex (17). When we increased the carotid sinus pressure, C_a increased, and when we decreased carotid sinus pressure, C_a tended to decrease (The non-significant result in the low carotid group most likely represents a ß-error in statistical analysis). Two possibilities exist to explain this. Since increasing carotid sinus pressure causes smooth muscle relaxation in response to the increased sinus pressure, one would expect that the vessel wall would be more compliant. However, it is also possible to model the vessel as having smooth muscle in series with an elastic component in the wall. In this model, the compliance of the elastic component is much greater than the compliance of the smooth muscle. Therefore changes in smooth muscle tone would have negligible effects on the overall wall compliance. Compliance changes in our experiment could then be considered secondary to the observed changes in arterial pressure. Since arterial pressure fell (and therefore our set perfusion pressure fell) during increased carotid sinus pressure, the elastic component would be less stretched, and therefore more compliant (assuming a non-linear compliance). Our study was not designed to answer this question.

Venous resistance of the hindlimb did not change when carotid sinus pressure was varied. This is in agreement with Magder and Deschamps (15). Therefore, if there is neural control of venous tone, it is limited to the small venules.

Our main finding was that the %change in P_{crit} was greater than the %change in R_a. However, each of the variables contributed equally to the observed change in pressure, and to the theoretical changes in flow (figure 2.4). It is important to realize that when flow is kept constant and P_{per} allowed to vary, it is the absolute changes in P_{crit}, and not the relative changes that are important. Regardless of its initial value, a 5 mmHg increase in P_{crit} causes a 5 mmHg increase in P_{per} [$P_{per}=P_{crit}+(R_a*\dot{Q})$].

The analysis of theoretical changes in flow is more complex. The rationale for the analysis was to estimate changes in an intact circulation (i.e. P_a constant), rather than the open-loop control system created by carotid sinus isolation. Our results indicate that the relative effects of changing R_a and P_{crit} are again, approximately equal. In this analysis however, the effect of any given absolute change in P_{crit} affects flow only in relation to how the driving pressure is changed [$\dot{Q}=(P_{per}-P_{crit})/R_a$]. Expressing changes in P_{crit} as a percentage increase does not solve the problem. For instance, it can be shown mathematically that the effects of a 25% increase in P_{crit} can result in less than, equal, or greater than a 25% decrease in flow depending on the initial values of P_{per} and P_{crit}. Therefore, the results may have been different if we set the P_{per} to another value. However, it is also possible that P_{per} and P_{crit} are linked to each other through the myogenic response of the vasculature. If so, raising P_{per} artificially might also raise P_{crit}, and keep the ratio constant. Our study does not resolve this question.

In conclusion, when the transmural carotid sinus pressure is increased, arterial pressure is lowered by a decrease in the tone of the Starling resistor mechanism in the hindlimb in addition to a decrease in the arterial resistance. Conversely, a decrease in carotid sinus transmural pressure results in an increase in both R_a and P_{crit}. Whereas %changes in P_{crit} were quantitatively greater than %changes in R_a, they both contributed equally to the observed changes in pressure.

2.6. REFERENCES

1. Ashton, H. Critical closing pressure in human peripheral vascular beds. *Clin. Sci.* 22: 79-87, 1962.

2. Aversano, T., F.J. Klocke, R.E. Mates, and J.M. Canty,Jr.. Preload-induced alterations in capacitance-free diastolic pressure-flow relationships. *Am. J. Physiol.* 246: H410-H417, 1984.

3. Bellamy, R.F. Diastolic coronary artery pressure-flow relations in the dog. *Circ. Res.* 43(1): 92-101, 1978.

4. Björnberg, J., U. Albert, and S. Mellander. Resistance responses in proximal arterial vessels, arterioles and veins during reactive hyperaemia in skeletal muscle and their underlying regulatory mechanisms. *Acta Physiol. Scand.* 139: 535-550, 1990.

5. Braakman, R., P. Sipkema, and N. Westerhof. Pressure-flow relationships of the canine iliac periphery and systemic hemodynamics: Effects of sodium nitroprusside and adenosine. *Pflügers Arch.* 407: 432-439, 1986.

6. Braakman, R., P. Sipkema, and N. Westerhof. Two zero-flow pressure intercepts exist in autoregulating isolated skeletal muscle. *Am. J. Physiol.* 258: H1806-H1814, 1990.

7. Burton, A.C. On the physical equilibrium of small blood vessels. *Am. J. Physiol.* 164: 319-329, 1951.

8. Eng, C., J.H. Jentzer, and E.S. Kirk. The effects of the coronary capacitance on the interpretation of diastolic pressure-flow relationships. *Circ. Res.* 50: 334-341, 1982.

9. Green, H.D., C.E. Rapela, and M.C. Conrad. Resistance (conductance) and capacitance phenomena in terminal vascular beds. In: *Handbook of Physiology. Circulation. Section 2, Volume II.* Washington, D.C.: American Physiological Society, 1963, p. 935-960.

10. Johnson, P.C. Review of previous studies and current theories of autoregulation. *Circ. Res.* 14-15 (Suppl. 1): I2-I9, 1964.

11. Laskey, W.K., H.G. Parker, V.A. Ferrari, W.G. Kussmaul, and A. Noordergraaf. Estimation of total systemic arterial compliance in humans. *J. Appl. Physiol.* 69(1): 112-119, 1990.

12. Levy, B.I., J. Benessiano, P. Poitevin, L. Lukin, and M.E. Safar. Systemic arterial compliance in normotensive and hypertensive rats. *J. Cardiovasc. Pharmacol.* 7(Suppl 2): S28-S32, 1985.

13. Magder, S. Starling resistor versus compliance. Which explains the zero-flow pressure of a dynamic arterial pressure-flow relation? *Circ. Res.* 67: 209-220, 1990.

14. Magder, S. Vascular mechanics of venous drainage in dog hindlimbs. *Am. J. Physiol.* 259: H1789-H1795, 1990.

15. Magder, S. and A. Deschamps. Role of regional blood flow distribution, venous resistance and unstressed volume in the vascular volume mobilization by the baroreceptor reflex. *FASEB J.* 5(4): A774, 1991.(Abstract)

16. Nichol, J., F. Girling, W. Jerrard, E.B. Claxton, and A.C. Burton. Fundamental instability of the small blood vessels and critical closing pressures in vascular beds. *Am. J. Physiol.* 164: 330-344, 1951.

17. Osberg, C. and B.L. Langille. Reflex control of arterial compliance in rabbits. *Can. J. Physiol. Pharmacol.* 60: 1475-1481, 1982.

18. Permutt, S. and R.L. Riley. Hemodynamics of collapsible vessels with tone: the vascular waterfall. *J. Appl. Physiol.* 18(5): 924-932, 1963.

19. Spaan, J.A.E. Coronary diastolic pressure-flow relation and zero flow pressure explained on the basis of intramyocardial compliance. *Circ. Res.* 56: 293-309, 1985.

20. Sylvester, J.T., R.D. Gilbert, R.J. Traystman, and S. Permutt. Effects of hypoxia on the closing pressure of the canine systemic arterial circulation. *Circ. Res.* 49: 980-987, 1981.

21. Van Huis, G.A., P. Sipkema, and N. Westerhof. Instantaneous and steady-state pressure-flow relations of the coronary system in the canine beating heart. *Cardiovasc. Res.* 19: 121-131, 1985.

22. Zweifach, B.W. Local regulation of capillary pressure. *Circ. Res.* 28-29 (Suppl. I): I-129-I-134, 1971.

CHAPTER 3

RESPONSE OF ARTERIAL RESISTANCE AND CRITICAL PRESSURE TO CHANGES IN PERFUSION PRESSURE IN THE CANINE HINDLIMB

3.1. ABSTRACT

The dynamic pressure-flow relationship in the canine hindlimb at normal arterial pressure is best explained by modelling a Starling resistor (critical pressure, P_{crit}) at the level of the arterioles. Regulation of flow can therefore occur at the Starling resistor through changes in P_{crit}, or along the length of the vessel through changes in arterial resistance (R_a). We hypothesized that increasing perfusion pressure (P_{per}) would increase P_{crit} due to the myogenic response, but decrease R_a due to flow-mediated vasodilation and passive effects. We pump-perfused vascularly isolated hindlimbs of anaesthetized dogs and measured P_{crit} and calculated R_a over P_{per} range of 75-175 mmHg. When P_{per} was increased from 75 to 175 mmHg, P_{crit} increased from 33 ± 2 mmHg to 48 ± 6 mmHg (mean$\pm$S.E.M.), whereas R_a decreased from 10.1 ± 1.2 mmHg·min·100g·ml^{-1} to 7.86 ± 0.7 mmHg·min·100g·ml^{-1} ($p<0.01$). Thus, the responses of P_{crit} and R_a to an increase in P_{per} were dissociated. In a second part of the study, we lowered carotid sinus pressure to determine the effects of central factors on local autoregulation. A decrease in carotid sinus pressure increased P_{crit} and R_a at each P_{per} ($p<0.05$). We conclude that an increase in P_{per} causes the arterial vasculature to constrict at the level of the Starling resistor, and dilate more proximally. The carotid baroreflex causes an increase in tone throughout the arterial vasculature, but does not alter the local response to increases in perfusion pressure.

3.2. INTRODUCTION

Poiseuille's Law states that flow ($\dot{Q}$) through a tube is equal to the pressure drop across the tube, divided by the resistance between inflow and outflow (32). Therefore, inflow pressure and outflow pressure should be equal when flow is zero. However, many authors have shown that arterial pressure is greater than venous pressure at zero flow (2,5,11,27,31,39). In 1951, Burton hypothesized that an instability in the elastic wall causes arterial vessels to collapse when the inflow pressure declines below a critical value (P_{crit}) (9). Permutt and Riley later showed that the zero-flow pressure gradient is better explained by a Starling resistor-like mechanism at the level of arterioles that behaves like a vascular "waterfall" (32). The collapsible segment of the Starling resistor exists at the arteriolar level, and the "external pressure" is due to smooth muscle tone. Flow under these conditions is similar to a natural waterfall in which flow is determined by the difference in altitude between the upstream lake and the waterfall, divided by the river's resistance. It is not affected by the actual height of the falls nor by the resistance to flow in the river below the falls. Similarly, when a vascular waterfall is present, the appropriate downstream pressure to calculate arterial resistance (R_a) is P_{crit}, and not venous pressure (P_v). Unlike Burton's model, the critical pressure due to a vascular waterfall determines flow throughout the pressure-flow relation (as long as P_{crit} is greater than the downstream pressure), and not only at zero-flow.

A Starling resistor-like mechanism created by arteriolar tone in the circulation has several important implications (27). First, resistance calculations (and therefore inferences about changes in vessel diameter) which are based on arterial-venous pressure gradients may lead to erroneous conclusions (both quantitative and qualitative). For instance, when P_{per} is increased, flow increases and peripheral resistance calculated as $(P_{per}-P_v)/\dot{Q}$ has been shown to decrease (5,6). However, small

arterioles exhibit a myogenic response and constrict in response to increased pressure (21). Therefore, classical calculations of resistance do not correlate with direct microvascular observations. Second, arterial blood pressure (P_a) or flow can be altered by two mechanisms, i.e. a change in P_{crit} or a change in R_a. Third, fluctuations in P_v or venous resistance (R_v) that occur with respiration or reflexes will not affect flow into a vascular region, although they will still affect capillary pressure, microcirculatory flow distribution, and venous return. Finally, a sudden decrease in cardiac output will not produce as rapid or extreme a fall in P_a.

If P_{crit} is due to arteriolar smooth muscle tone, it should be affected by mechanisms that affect vascular tone. In support of this, we have shown that changes in carotid sinus pressure alter P_{crit} and R_a (34). However, arterial pressure in that study increased when carotid sinus pressure was lowered. Therefore, it is possible that P_{crit} and R_a increased due to a local myogenic response (the constriction of a vessel when exposed to increased transmural pressure), and not directly due to the carotid baroreflex. *In vivo*, Meininger et al. showed that 3rd and 4th order cremasteric arterial vessels constrict in response to increased P_{per}, whereas 1st and 2nd order vessels dilate (30). Since P_{crit} is thought to be at the level of arterioles (32)), we hypothesized that raising perfusion pressure would cause an increase in P_{crit}, but a decrease in R_a.

Perfusion pressure is not the only variable that can affect arterial tone. The final vessel diameter depends on the integration of all the vasodilator and vasoconstrictor forces present (i.e. passive, myogenic, metabolic, neurogenic, and endothelial-derived factors). Since lowering P_{car} increases sympathetic tone, we further hypothesized that lowering P_{car} would increase both P_{crit} and R_a at any given perfusion pressure.

Theoretical Analysis of a Starling Resistor

Since Permutt and Riley's analysis, many authors have investigated the properties of flow through collapsible tubing using Penrose drains. Most studies have

concentrated on why flow becomes limited when the downstream pressure is decreased below the pressure surrounding the tube (P_{crit}). One theory proposes that flow is supersonic at the constriction of the collapsible tubing, but becomes subsonic at some downstream point (16). The transition from supersonic to subsonic flow is abrupt and creates a hydraulic jump which dissociates the energy and pressure gradients. This theory is similar to the wave-speed hypothesis and choke-point analysis (22). However, although these hypotheses adequately explain the dissociation between flow and changes in venous pressure observed in the circulation (14,27), they do not explain the large arterial-venous pressure gradient which is observed at zero-flow (2,27). In the *in vitro* penrose drain studies, flow occurs even when inflow pressure is less than P_{crit} (through side channels that had remained open) (10,16). Although one might suggest that this is an artifact due to the low compliance of penrose tubing, no one has yet shown that higher pressures or more compliant tubing will eliminate the effect. Therefore, the zero-flow pressure gradient requires further analysis.

In 1980, Lyon et al. demonstrated that the mechanics of flow through collapsible tubing is dependent on the maximum Reynolds number (26). When they used a low viscosity fluid (high Reynolds number), flow initially occurred through side channels, and they obtained the same relationship as previous authors. When the viscosity of the fluid was increased, the steepness of the initial portion of the curve was increased (Reynolds number of 40), but side-channel flow still occurred. However, when very viscous fluids were used (maximum Reynolds number of 2), two different observations were noted. First, flow did not occur through side-channels and only began once the inflow pressure exceeded P_{crit}. Therefore a true zero-flow pressure gradient was present. Second, oscillations in the tubing that occurred at higher Reynolds number were absent. These results suggest that the mechanics of flow through collapsible tubes is dependent on the Reynolds number. Since the Reynolds

number in the arterioles is less than 2 (26), a Starling resistor-like mechanism at this level will cause both a flow-limitation and a zero-flow pressure gradient.

A repeated concern about the Starling resistor hypothesis has been the lack of microcirculatory data to support the existence of vascular closure. We therefore feel that it is important to cite the work of Baez and co-workers who stated that "closure at positive pressure values occurred often in precapillary sphincters and metarterioles" (3). In their work, the internal diameter of vessels which closed was 16 μ (as measured during P_{per}=50 mmHg) and occurred at an arterial pressure of 25 mmHg. One would predict that closure would occur at higher pressures if the vascular tone was increased. This was observed by Van Citters (38) by infusing epinephrine into the mesentery of the dog, and by Baez during stimulation of sympathetic nerves to the rat mesoappendix and cremasteric muscles (4).

3.3. METHODS

Twelve dogs weighing 18-34 kg were anaesthetized with α-chloralose (75 $mg \cdot kg^{-1}$) after initial induction with sodium pentothal (1 $mg \cdot kg^{-1}$). Supplemental doses of α-chloralose were given as needed. The animals were intubated, ventilated (Harvard Apparatus), and given supplemental oxygen as needed. We cannulated the left carotid artery to monitor P_a and to obtain arterial blood samples. Normal saline was infused into the left jugular vein to maintain proper hydration and sodium bicarbonate was given to maintain acid-base balance. Heparin (10,000 units) was given to prevent blood clotting.

Surgical Preparation

The preparation is illustrated in figure 3.1. We isolated the carotid sinuses by ligating the lingual, external carotid, and internal carotid arteries bilaterally. Blood flow was diverted from the right common carotid artery, through a pump (Masteflex

#16 Tygon tubing) and then to both carotid sinuses via the distal stumps of the common carotid arteries. We measured P_{car} via a side port on the tubing distal to the pump. A bilateral vagotomy was performed to remove the influence of aortic baroreceptors.

The vascular supply to the left hindlimb was isolated as previously described (27,34). In brief, we tied all branches of the femoral artery and vein in the femoral triangle. Blood flow was diverted from the right femoral artery, through an in-line electromagnetic flow probe (Carolina Medical #10), and into the left femoral artery. A side port placed distal to the flow probe was used to measure the pressure perfusing the limb (P_{per}). We placed two side ports proximal to the flow probe so that blood flow could be diverted through a second pump (Masterflex #16 Tygon tubing) during the experimental runs. The direct line was used for measuring the natural flow of the hindlimb at a given carotid sinus pressure. During experimental runs, flow was controlled by clamping the direct line and adjusting the pump speed. We cannulated the left femoral vein and returned the outflow to the animal via the right jugular vein. P_v was measured from a side port close to the cannulation site.

We passed surgical wires through the proximal thigh with a 12-14 gauge needle. The wires were tied securely around either side of the femur to eliminate any collateral flow.

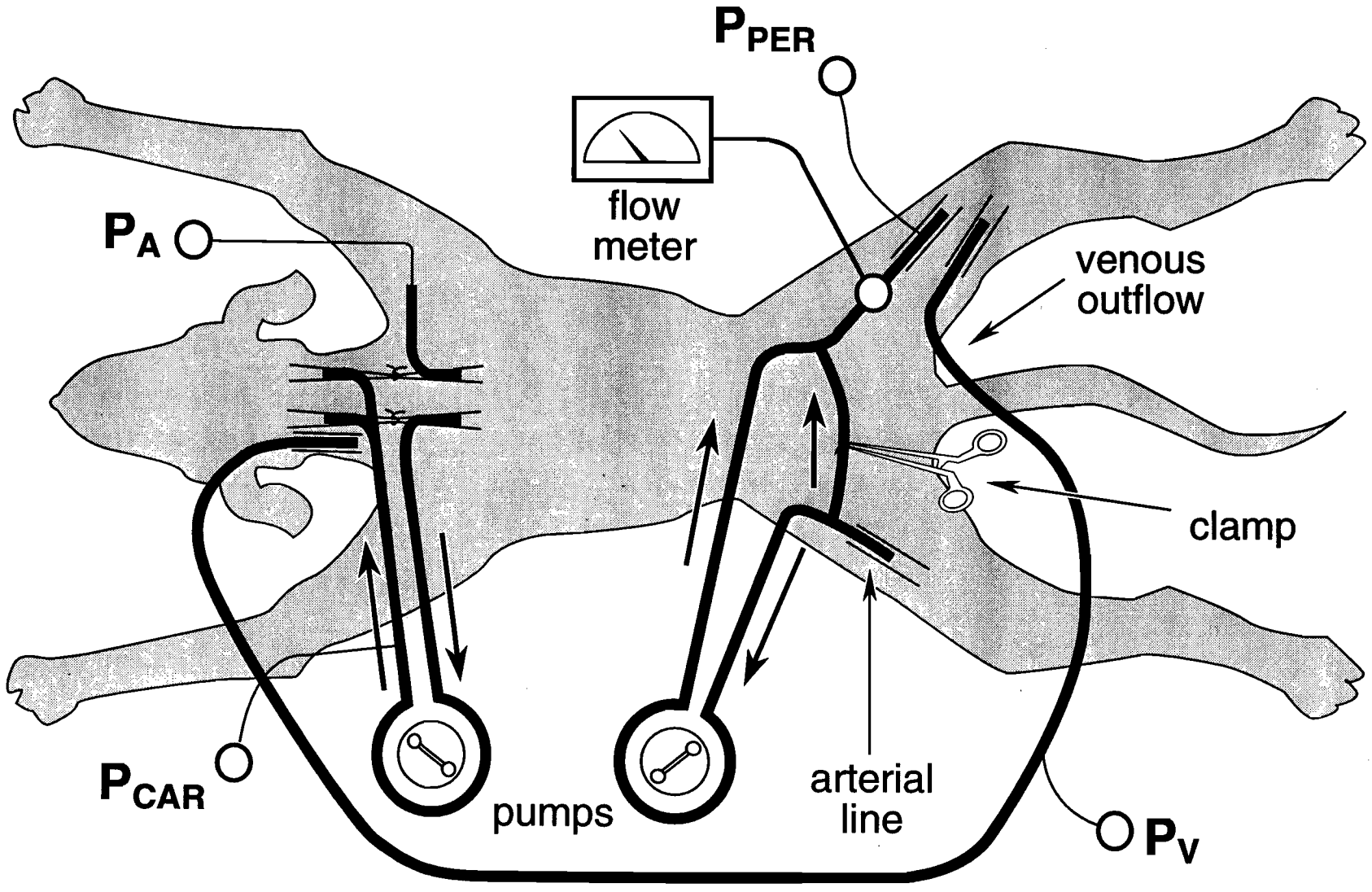

Figure 3.1: Experimental setup.

Measurements

Pressures were measured with Trantec transducers. We measured flow ($\dot{Q}$) with a Carolina Medical electromagnetic flow meter and an in-line probe. Signals were filtered at 3 Hz. All signals were processed through Gould amplifiers and simultaneously recorded on an eight-channel Graphtec recorder and on an IBM compatible computer using CODAS software program (DATAQ Instruments Inc.) for A-D conversion and analysis. Lactate levels were measured on a YSI Model 23L lactate analyzer (Yellow Springs Instrument Co. Inc) and oxygen content on an Instrumentation Laboratory 282 Co-oximeter.

Protocol

Experimental runs were performed at both normal carotid pressure ($P_{car} \approx P_a$, mean of 129 mmHg), and low carotid pressure (mean P_{car} of 65 mmHg) in random order. P_{car} was set by changing carotid sinus perfusion rate, and the natural flow to the hindlimb was measured. The tubing was then clamped between the two proximal side ports, and pump flow adjusted to give the same perfusion pressure as natural flow conditions. Pump flow was then manually turned down to zero over a ramp-time period ranging from 5-10 seconds (The pressure-flow intercept under these conditions approximates P_{crit} (27)). This was repeated a second time at the same perfusion pressure. Perfusion pressure was then changed, and we allowed the pressure to stabilize before continuing (approximately 5 minutes). The pump flow was again decreased to zero over two separate runs at the new P_{per}. We repeated this procedure at perfusion pressures 75, 100, 125, 150 and 175 mmHg in random order. To assess the metabolic contributions to vasomotor tone, arterial and venous blood samples for oxygen content and lactate levels were taken from the femoral vessels of the perfused hindlimb during perfusion at the two lowest pressures in three animals.

Hindlimb inflow and outflow were simultaneously occluded (double occlusion) before and after each series of measurements to ensure isolation (28). A continuous rise in venous pressure indicates collateral arterial inflow, and a continuous fall in venous pressure indicates collateral venous outflow. The surgical wires were then tightened and another double occlusion performed. We continued the experiment only after complete isolation was obtained.

At the end of the experiment, the hindlimb was amputated at the level of the surgical wires and weighed. Flow and resistance are expressed per 100 g of hindlimb.

Data Analysis

The data were digitized and sampled using the CODAS software program at 50 Hz per channel. Mean P_{car}, P_a, P_{per}, P_v, and $\dot{Q}$ were obtained before each zero-flow pressure measurement.

In general, the relation between flow and perfusion pressure during a ramp to zero flow was linear. In a few experimental runs, a curvilinear phase convex to the pressure axis occurred at high flows. This was most likely due to passive stretching of the arterial walls, and has been noted by other authors (8,27). Occasionally, a curvilinear phase convex to the pressure axis occurred at low flows. Two possibilities may account for this. First, reactive vasodilation may have occurred in response to the decreased flow, even though the time to zero-flow was less than ten seconds. Second, the rate of decrease in pump speed may have slowed as flow approached zero (due to human or mechanical factors). In this case, pressure would continue to decline below P_{crit} due to the small collateral vessels around the Starling resistor. To avoid the influence of these factors and to be consistent with runs not exhibiting a curvilinear phase, we plotted the regression line for the linear phase, and used the calculated x-intercept as the zero-flow pressure intercept. The two P_{crit} values obtained for each P_{per} were averaged. R_a was calculated as $(P_{per}-P_{crit})/\dot{Q}$.

Statistics

The changes in P_{crit} and R_a, with varying carotid sinus pressures were compared using ANOVA for Repeated Measures: Two factor design (P_{per} x P_{car}) and the Newman-Keuls' Multiple-Range Test. Results were considered significant if $p<0.05$. In one animal there was no flow at P_{per}=75 mmHg during carotid sinus hypoperfusion, and we therefore imputed the mean value of P_{crit} and R_a from the other five animals for the purposes of statistical analysis. Since the results are presented as the mean of six animals, this method of analysis means P_{crit} is slightly underestimated at 75 mmHg, and R_a is slightly overestimated.

3.4. RESULTS

PCO_2 was 38.1±5.3 mmHg (mean±S.D.) and PO_2 was 143±45 mmHg. Rectal temperature was 36±2°C and hematocrit was 41.4±5.9%. The $[H]^+$ was $4.68x10^{-8}\pm0.65x10^{-8}$ M (pH=7.33). When P_{car} was lowered from 129±3.1 mmHg (mean±S.E.M.) to 65±3 mmHg, P_a increased from 122±13 mmHg to 169±12 mmHg indicating that the carotid sinus preparation was functional.

Figure 3.2a is a plot of P_{crit} versus P_{per} at normal and low carotid sinus pressures. At normal carotid pressures, the P_{crit} increased as P_{per} was raised from 75 mmHg to 175 mmHg ($p<0.001$). In two animals, we lowered P_{per} to 25 mmHg and the P_{crit} continued to decrease. At low carotid sinus pressure, P_{crit} also increased as P_{per} increased, and the absolute value was higher at any given perfusion pressure when compared to normal carotid pressures ($p<0.025$). The slope of the relationship was not different ($p>0.2$).

Figure 3.2b is a plot of R_a against P_{per}. At normal P_{car}, resistance declined with increasing P_{per} ($p<0.05$). At low P_{car}, there was a parallel upward shift in the curve similar to the relationship between P_{crit} and perfusion pressure.

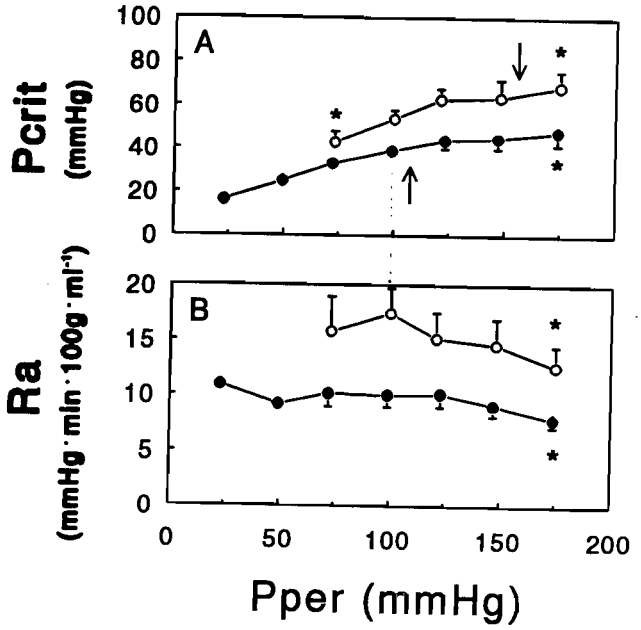

Figure 3.2: In A, the relationship between critical pressure (P_{crit}) (±S.E.M.) and perfusion pressure (P_{per}) (±S.E.M.) over the range of 75-175 mmHg is shown (n=6). The O represent the data during carotid sinus perfusion at low pressure, whereas the ● represent the data when the carotid sinus is perfused at a normal pressure. In two dogs, P_{crit} was also measured at perfusion pressures of 25 and 50 mmHg. The average (without S.E.M.) of these two animals is also plotted on the graph. The arrows indicate the working points of the hindlimb at the different carotid sinus pressures. In B, arterial resistance (R_a) is plotted against P_{per} for the same animals, with the same legend. There is a significant increase in P_{crit} ($p<0.005$) and a significant decrease in R_a ($p<0.05$) as P_{per} is increased. In addition, there is a significant increase in both P_{crit} and R_a when the carotid sinus pressure was lowered ($p<0.05$). There was no interaction between the carotid sinus pressure and either

dependent variable, i.e. no change in the slope of the relationships ($p>0.2$). * indicates significantly different from P_{per} of 100 mmHg.

Table 3.1 shows the values for blood samples of arterial and venous oxygen content, as well as arterial-venous differences in lactate concentration obtained in three dogs during perfusion at low pressures (under both normal and low P_{car} conditions). There was always a large reserve of oxygen in the venous sample, and the arterial-venous difference in lactate concentration was negligible. Therefore, the autoregulatory responses that occurred were unlikely to be of metabolic origin (see discussion).

Experiment	Condition	P_{per}	Oxygen Content (ml $O_2 \cdot 100ml^{-1}$ blood) Art	Ven	A-V diff	Lactate ($mmole \cdot L^{-1}$) A-V diff
1	NC	75	20.1	17.5	2.6	0.1
	LC	75	not applicable			
	NC	100	20.2	17.6	2.6	n/a
	LC	100	23.6	18.9	4.7	0.2
2	NC	75	14.2	12.8	1.4	0.0
	LC	75	18.6	16.3	2.3	0.1
	NC	100	13.7	12.8	0.9	0.1
	LC	100	22.1	18.7	3.4	0.0
3	NC	75	16.5	8.7	7.8	0.5
	LC	75	20.8	8.9	11.9	0.5
	NC	100	15.8	10.7	5.1	0.9
	LC	100	20.8	13.6	7.2	0.2

Table 3.1. Arterial and venous oxygen content, and arterio-venous lactate differences in three animals at perfusion pressures (P_{per}) of 75 and 100 mmHg. Blood samples were drawn during carotid sinus perfusion at

normal pressure (NC), and at low pressure (LC). In experiment 1, the critical pressure during LC condition was higher than 75 mmHg, and there was no flow at this pressure.

3.5. DISCUSSION

We found that P_{crit} increases in response to 1) an increase in perfusion pressure, and 2) an increase in sympathetic tone induced by lowering carotid sinus pressure. Before discussing these results in detail, some technical factors need to be considered. These include the influence of other baroreceptors, the completeness of the hindlimb isolation, and the effects of vascular compliance on the measurement of P_{crit}.

We controlled the carotid sinus pressure with a pump. Input from the aortic arch baroreceptors and the pulmonary circuit should have been removed by the bilateral vagotomy. If any baroreflexes still remained, they should have blunted the responses we observed.

If the hindlimb is not completely isolated from the systemic circulation, P_{crit} is overestimated (15). We used the double occlusion technique described in the methods section to ensure isolation (28), and did not proceed unless isolation was confirmed. This collateral flow needs to be distinguished from "collateral" channels that do not have a critical pressure and "bypass" the Starling resistor. The flow around the Starling resistor is responsible for the decrease in perfusion pressure below P_{crit} following arterial occlusion, and necessitates the ramp technique for measuring P_{crit} (27).

Changes in resistance and P_{crit} have been studied with steady-state pressure-flow relations (1,7). However, steady-state measurements are of limited value since they include adjustments from autoregulatory mechanisms. When flow is decreased in steps, metabolic vasodilation may decrease the tone of the vessels responsible for the

Starling resistor-like mechanism, and thus lower P_{crit}. In addition, the decrease in P_{per} could result in further vasodilation due to the myogenic response (19). Therefore, the values from steady-state measurements might not reflect the instantaneous P_{crit} that exists at higher flows or higher pressures. If P_{crit} is unreliable, then resistance calculations [$R_a=(P_{per}-P_{crit})/\dot{Q}$] are also unreliable.

In order to estimate P_{crit} at each P_{per}, we used the dynamic pressure-flow relation. These however, can be affected by vessel compliance (2,11,27,35). If inflow is instantaneously decreased to the value in the compliant region, the inflow pressure gradient decreases to zero and inflow ceases even though flow downstream from the compliant region continues. Thus, an artificially high P_{crit} is recorded. This effect is minimized if the ramp time to zero-flow is long enough to allow the compliant region to empty. Compliance effects are negligible for ramp times greater than 5 seconds (27,34).

Finally, it should be noted that P_{crit} is the pressure when flow ceases, but arterial pressure continues to decline if the occlusion is maintained (27). This is because the volume above the site of P_{crit} can escape through channels which bypass the Starling resistor-like mechanism. We have previously shown that if only 1.5% of the total conductance goes through these channels, P_{crit} will be significantly underestimated if the final arterial pressure is used instead of the actual pressure when zero flow occurs (27). In our previous study, we showed that this problem can be avoided by ramping the inflow down to zero with times to zero flow of 4-10 sec. The arterial pressure will continue to fall as soon as the inflow stops, but the value just before this is a very close approximation of P_{crit}. This is supported by the fact that there is very little change in the measured P_{crit} with times to zero flow of 5-10 seconds (27). In fact, the plateau in this measurement with different times to zero flow supports the existence of a true physiological phenomenon and is very difficult to explain with any other

model (27). The second advantage of the ramp technique is that it eliminates the effects of capacitance flow mentioned above, which are present when the flow is rapidly decreased and which produce an artificially high P_{crit} (2,11,27,35).

P_{crit}, R_a, and Autoregulation

To explain the increase in P_{crit} with an increase in P_{per}, it is best to separate the local control systems into vasodilating and vasoconstricting factors. Metabolic and myogenic regulation should result in vasoconstriction with an increase in P_{per}, whereas passive forces and flow-induced vasodilation (endothelial-derived relaxing factor, EDRF) would cause vasodilation. Thus, EDRF release and passive distention may have attenuated the magnitude of the observed response, but the major control system of this vascular segment had to be either metabolic or myogenic. It is unlikely that metabolic factors were important since oxygen consumption of resting skeletal muscle is low (5-6 μl $O_2 \cdot g^{-1} \cdot min^{-1}$, (36,37)), and metabolites would not be expected to accumulate. Furthermore, the oxygen content of the venous effluent was high in the three animals in which it was measured, and there was minimal lactate production, even at the lowest flows. Therefore, the changes in P_{crit} were most likely due to a myogenic response, i.e. smooth muscle contraction in response to an increased transmural pressure (20).

Our results support those of Braakman et al. who showed the P_{crit} in isolated skeletal muscle increases from 3 to 6 kPa (22.5-45 mmHg) when P_{per} is increased from 5 to 20 kPa (37.5-150 mmHg) (8). Braakman et al. however, did not examine the relation between P_{per} and R_a. Contrary to the increase in P_{crit}, we found that R_a decreases with increasing P_{per}. This could be explained by constriction of the terminal arterioles or metarterioles and a vasodilation of the vessels located more proximally. In support of this, Meininger et al. (30) used intra-vital microscopy and showed that third and fourth order rat cremasteric arterioles constrict when P_{per} is increased, whereas the more proximal vessels dilate. This does not imply that the myogenic response is

limited to third order arterioles, for the proximal vessels may simply be more sensitive to passive factors and/or EDRF. If the more proximal vessels were completely unresponsive to increased transmural pressure, then the dilation may have been greater. Similarly, the Starling resistor mechanism may have been influenced by EDRF, but the effect was presumably overshadowed by the myogenic response.

Interestingly, although Meininger (30) showed that first order vessels dilate *in vivo* when P_{per} is increased (N.B. since flow decreased in their experiment, this was not EDRF mediated), he has also shown that the same stimulus on the same sized vessels *in vitro* results in vasoconstriction (13). Furthermore, Kuo et al. studied 40-80 um porcine coronary arterioles *in vitro* and also found that the myogenic response is greater than the flow-induced vasodilation (24). The difference between *in vitro* and *in vivo* results most likely reflects the different relative strengths of the myogenic and flow-induced responses in the different preparations, perhaps due to circulating hormones or sympathetic tone. Our results correspond well with the *in vivo* data.

The decrease in resistance that we observed is different from the observation of Braakman et al. who found that resistance of the canine abdominal peripheral bed increased when P_{per} was increased (6). However, since the abdominal peripheral bed has numerous anastomotic sites between vessels of origin above and below the renal vessels (12), it is possible their preparation was not completely isolated. Without proper isolation, any conclusions about changes in resistance become questionable (15).

Carotid Sinus Baroreflex

The second part of our study examined the interaction of the central and local control of vascular tone. Our hypothesis that lowering carotid sinus pressure would result in a higher P_{crit} and R_a for any given P_{per} was confirmed. In addition, the rate of rise in P_{crit} (and fall in R_a) was similar at both carotid sinus pressures, indicating that the myogenic response operates independently of central control. This could arise for

example, if the different control systems affect cytosolic calcium levels through different channels.

Our conclusion that P_{crit} and R_a are increased during activation of the carotid sinus baroreflex independently from the myogenic response conflicts with the results of Lash and Shoukas (25). These authors used intra-vital microscopy and observed minimal vessel diameter changes (i.e. no change in resistance) in the rat spinotrapezius bed during carotid occlusion whenever arterial pressure was maintained constant (accomplished by bleeding the animal). They therefore concluded that most of the vasoconstrictor response to carotid occlusion was due to the local myogenic response. However, these results are contradicted by several other studies. Hébert and Marshall studied the same vascular bed and found that increasing carotid sinus pressure to 240-250 mmHg caused an immediate vasodilation in the arterial tree, and that the effect was abolished with local sympathetic blockade (guanethidine or crushing of paravascular sympathetic nerves) (18). A local metabolic component probably occurred as some vessels began to vasoconstrict 8-12 seconds after the arterial pressure began to fall. This effect was not abolished by local sympathetic blockade. Marshall also showed that stimulation of the sympathetic nerves to the rat spinotrapezius muscle causes arteriolar vasoconstriction, and the effect is abolished if the paravascular nerves distal to the stimulating electrode are crushed (29). Finally, Hainsworth et al. kept P_{per} constant and found that flow to the canine hindlimb was affected by changes in carotid sinus pressure (17).

The results of Lash and Shoukas could be explained by damage of the nerve supply to the muscle during dissection, or failure to fully activate the baroreceptor reflex. In addition, since the spinotrapezius muscle is a postural muscle, its vasomotor regulation might be different than the hindlimb. If so, it is possible that vasoconstriction of this bed only occurs when the sympathetic nervous system is strongly activated. Lash and Shoukas (25) used carotid occlusion which does not result

in a maximum response, whereas our animals were vagotomized and P_{car} lowered below 75 mmHg to achieve a maximal effect (23,33). Marshall's results suggest that Lash and Shoukas would have observed a neurogenic reflex involving the spinotrapezius vascular bed if the baroreflex had been fully activated.

Implications

We previously showed that lowering carotid sinus pressure from 119±6 mmHg to 71±6 mmHg (allowing P_{per} to increase from 111±12 mmHg to 164±15 mmHg), increased P_{crit} by 62±10%, and R_a by 42±15% (34). Normally however, carotid sinus pressure and arterial pressure decrease together (e.g. hemorrhage). Our present results suggest that this would result in a higher R_a, and a lower P_{crit} than noted above. For instance, the P_{crit} at a P_{per} of 111 mmHg under normal carotid sinus perfusion is approximately 41 mmHg. If arterial pressure declines from 125 mmHg to 75 mmHg, the carotid baroreflex should cause P_{crit} to increase from 44 mmHg to 63 mmHg. However, without the carotid baroreflex, the overall effect of local factors (passive, EDRF, metabolic, and myogenic) would normally cause P_{crit} to decrease to 33 mmHg. If both effects are combined, the new P_{crit} value would be 43 mmHg, i.e. unchanged. Under the same circumstances, arterial resistance would increase from 10.1 $mmHg \cdot min \cdot ml^{-1} \cdot 100g^{-1}$ to 15.2 $mmHg \cdot min \cdot ml^{-1} \cdot 100g^{-1}$ due to the carotid baroreflex, and increase further to 15.8 $mmHg \cdot min \cdot ml^{-1} \cdot 100g^{-1}$ due to the local effects. The net effect would therefore be a decrease in flow to the hindlimb as a result of a decreased arterial pressure and an increased resistance, with no change in P_{crit}.

If no waterfall is present, arterial pressure after hemorrhage can only be increased by increasing total resistance. Since the vasculature can be modelled as several resistances in series, the total resistance can be increased by increasing the resistance in any of the regions, presumably through an increase in sympathetic activity. However, the sympathetic nervous system would require an extremely sensitive feedback system to accurately return blood pressure to normal. This is

because the proportional change in resistance (R_2/R_1) is equal to r_1^4/r_2^4 where R_1 is the original resistance, R_2 is the new resistance, r_1 is the original radius, and r_2 is the new radius. Therefore, a small change in radius would have a large effect on blood pressure. This type of control system is appropriate for coarse changes, but is not appropriate for a system requiring fine control. A Starling resistor-like mechanism however, allows both fine control (through P_{crit}), and coarse control through R_a. This is because P_{crit} is controlled through changes in smooth muscle tension, and is not dependent on the vessel diameter. For instance, if arterial pressure should be increased by 5 mmHg, the sympathetic activity is increased and augments smooth muscle tension by the equivalent of 5 mmHg. The actual change in vessel diameter is not important because the increased tone is acting as a back pressure to flow, and not as a change in resistance.

In conclusion, an increase in P_{per} causes an increase in P_{crit} and a decrease in the resistance of the upstream vessels. The carotid baroreflex however, causes increased tone throughout the arterial system.

3.6. REFERENCES

1. Ashton, H. Critical closing pressure in human peripheral vascular beds. *Clin. Sci.* 22: 79-87, 1962.

2. Aversano, T., F.J. Klocke, R.E. Mates, and J.M. Canty,Jr.. Preload-induced alterations in capacitance-free diastolic pressure-flow relationships. *Am. J. Physiol.* 246: H410-H417, 1984.

3. Baez, S. Bayliss response in the microcirculation. *Fed. Proc.* 27: 1410-1415, 1968.

4. Baez, S., S.M. Feldman, and P.M. Gootman. Central neural influence on precapillary microvessels and sphincter. *Am. J. Physiol.* 233: H141-H147, 1977.

5. Bellamy, R.F. Diastolic coronary artery pressure-flow relations in the dog. *Circ. Res.* 43(1): 92-101, 1978.

6. Braakman, R., P. Sipkema, and N. Westerhof. Steady-state and instantaneous pressure-flow relationships: characterisation of the canine abdominal periphery. *Cardiovasc. Res.* 17: 577-588, 1983.

7. Braakman, R., P. Sipkema, and N. Westerhof. Pressure-flow relationships of the canine iliac periphery and systemic hemodynamics: Effects of sodium nitroprusside and adenosine. *Pflügers Arch.* 407: 432-439, 1986.

8. Braakman, R., P. Sipkema, and N. Westerhof. Two zero-flow pressure intercepts exist in autoregulating isolated skeletal muscle. *Am. J. Physiol.* 258: H1806-H1814, 1990.

9. Burton, A.C. On the physical equilibrium of small blood vessels. *Am. J. Physiol.* 164: 319-329, 1951.

10. Conrad, W.A. Pressure-flow relationships in collapsible tubes. *IEEE Trans. Biomed. Eng.* 16: 284-295, 1969.

11. Eng, C., J.H. Jentzer, and E.S. Kirk. The effects of the coronary capacitance on the interpretation of diastolic pressure-flow relationships. *Circ. Res.* 50: 334-341, 1982.

12. Evans, H.E. and G.C. Christensen. *Miller's Anatomy of the Dog*, Philadelphia:W.B.Saunders Company, 1979.

13. Falcone, J.C., M.J. Davis, and G.A. Meininger. Endothelial independence of myogenic response in isolated skeletal muscle arterioles. *Am. J. Physiol.* 260: H130-H135, 1991.

14. Farhi, E.R., F.J. Klocke, R.E. Mates, K. Kumar, R.M. Judd, J.M. Canty,Jr., S. Satoh, and B. Sekovski. Tone-dependent waterfall behaviour during venous pressure elevation in isolated canine hearts. *Circ. Res.* 68: 392-401, 1991.

15. Green, H.D., C.E. Rapela and M.C. Conrad. Resistance (conductance) and capacitance phenomena in terminal vascular beds. In: *Handbook of Physiology. Circulation. Section 2, Volume II*, Washington, D.C.: American Physiological Society, 1963, p. 935-960.

16. Griffiths, D.J. Hydrodynamics of male micturition - I. Theory of steady flow through elastic-walled tubes. *Med. Biol. Engng.* 9: 581-588, 1971.

17. Hainsworth, R., F. Karim, K.H. McGregor, and L.M. Wood. Hind-limb vascular-capacitance responses in anaesthetized dogs. *J. Physiol. (Lond)* 337: 417-428, 1983.

18. Hébert, M.T. and J.M. Marshall. Direct observation of the effects of baroreceptor stimulation on skeletal muscle circulation of the rat. *J. Physiol. (Lond)* 400: 45-59, 1988.

19. Johnson, P.C. Autoregulatory responses of cat mesenteric arterioles measured *in vivo*. *Circ. Res.* 22: 199-212, 1968.

20. Johnson, P.C. The myogenic response. In: *Handbook of Physiology. Section 2: The Cardiovascular System. Volume II. Vascular Smooth Muscle*, edited by D.F. Bohr, A.P. Somlyo and H.V. Sparks,Jr.. Bethesda, Maryland: American Physiological Society, 1980, p. 409-442.

21. Johnson, P.C. and M. Intaglietta. Contributions of pressure and flow sensitvity to autoregulation in mesenteric arterioles. *Am. J. Physiol.* 231: 1686-1698, 1976.

22. Kamm, R.D. Flow through collapsible tubes. In: *Handbook of Engineering*, edited by R. Skalak and S. Chien. New York: McGraw-Hill Book Company, 1987, p. 23.1-23.19.

23. Kirchheim, H.R. Systemic arterial baroreceptor reflexes. *Physiol. Rev.* 56: 100-176, 1976.

24. Kuo, L., W.M. Chilian, and M.J. Davis. Interaction of pressure- and flow-induced responses in porcine coronary resistance vessels. *Am. J. Physiol.* 261: H1706-H1715, 1991.

25. Lash, J.M. and A.A. Shoukas. Pressure dependence of baroreceptor-mediated vasoconstriction in rat skeletal muscle. *J. Appl. Physiol.* 70: 2551-2558, 1991.

26. Lyon, C.K., J.B. Scott, and C.Y. Wang. Flow through collapsible tubes at low Reynolds numbers. *Circ. Res.* 47: 68-73, 1980.

27. Magder, S. Starling resistor versus compliance. Which explains the zero-flow pressure of a dynamic arterial pressure-flow relation? *Circ. Res.* 67: 209-220, 1990.

28. Magder, S. Vascular mechanics of venous drainage in dog hindlimbs. *Am. J. Physiol.* 259: H1789-H1795, 1990.

29. Marshall, J.M. The influence of the sympathetic nervous system on individual vessels of the microcirculation of skeletal muscle of the rat. *J. Physiol. (Lond)* 332: 169-186, 1982.

30. Meininger, G.A., C.A. Mack, K.L. Fehr, and H.G. Bohlen. Myogenic vasoregulation overrides local metabolic control in resting rat skeletal muscle. *Circ. Res.* 60: 861-870, 1987.

31. Nichol, J., F. Girling, W. Jerrard, E.B. Claxton, and A.C. Burton. Fundamental instability of the small blood vessels and critical closing pressures in vascular beds. *Am. J. Physiol.* 164: 330-344, 1951.

32. Permutt, S. and R.L. Riley. Hemodynamics of collapsible vessels with tone: the vascular waterfall. *J. Appl. Physiol.* 18(5): 924-932, 1963.

33. Sagawa, K. and M. Watanabe. Summation of bilateral carotid sinus signals in the barostatic reflex. *Am. J. Physiol.* 209(6): 1278-1286, 1965.

34. Shrier, I., S.N.A. Hussain, and S. Magder. Effect of carotid sinus stimulation on resistance and critical closing pressure of the canine hindlimb. *Am. J. Physiol.* 1992.(In Press)

35. Spaan, J.A.E. Coronary diastolic pressure-flow relation and zero flow pressure explained on the basis of intramyocardial compliance. *Circ. Res.* 56: 293-309, 1985.

36. Stainsby, W.N. Oxygen uptake for isotonic and isometric twitch contractions of dog skeletal muscle in situ. *Am. J. Physiol.* 219(2): 435-439, 1970.

37. Stainsby, W.N. and A.B. Otis. Blood flow, blood oxygen tension, oxygen uptake, and oxygen transport in skeletal muscle. *Am. J. Physiol.* 206(4): 858-866, 1964.

38. Van Citters, R.L. Occlusion of lumina in small arterioles during vasoconstriction. *Circ. Res.* 18: 199-204, 1966.

39. Van Huis, G.A., P. Sipkema, and N. Westerhof. Instantaneous and steady-state pressure-flow relations of the coronary system in the canine beating heart. *Cardiovasc. Res.* 19: 121-131, 1985.

CHAPTER 4

L-NITRO-ARGININE AND PHENYLEPHRINE HAVE SIMILAR EFFECTS ON THE VASCULAR WATERFALL IN THE CANINE HINDLIMB

4.1. ABSTRACT

Hindlimb pressure-flow relationships are well characterized by modelling a vascular waterfall at the arteriolar level. Under these conditions, $\dot{Q}=(P_{per}-P_{crit})/R_a$, where $\dot{Q}$ is blood flow, P_{per} is perfusion pressure, P_{crit} is waterfall pressure, and R_a is the resistance upstream from the waterfall. To determine the effects of endothelium-derived relaxing factor (EDRF) on P_{crit}, R_a, and venous resistance (R_v), we varied P_{per} in the canine hindlimb between 100-200 mmHg before and after L-nitro-arginine infusion (L-NNA, an inhibitor of EDRF synthesis). Pre L-NNA, P_{crit} increased with increasing P_{per} ($p<0.001$). Post L-NNA, P_{crit} was higher at each P_{per}, and the increase in P_{crit} with increases in P_{per} was greater than under control conditions ($p<0.001$). In contrast to P_{crit}, R_a decreased with increasing P_{per} pre L-NNA ($p<0.001$). Post L-NNA, R_a was higher at each P_{per} ($p<0.001$), and no longer decreased with increasing P_{per} ($p>0.05$). R_v was not affected by P_{per} under control conditions, but decreased with increasing P_{per} post L-NNA ($p<0.05$). In a second group of animals, we infused phenylephrine to control for increased tone produced by L-NNA. Results were similar to those seen with L-NNA. In conclusion, blocking EDRF synthesis increases both P_{crit} and R_a, but the response of these variables to changes in P_{per} is through a non-specific increase in vascular tone.

4.2. INTRODUCTION

In 1980, Furchgott and Zawadzki demonstrated that acetylcholine-induced smooth muscle relaxation is dependent on the presence of an intact endothelium (11). Later studies showed that flow-induced vasodilation was also endothelium-dependent (24), and that both effects were due to a diffusible substance which became known as endothelial-derived relaxing factor (EDRF) (10). Blocking EDRF synthesis during constant flow conditions results in an increase in hindlimb perfusion pressure (P_{per}), which suggests that there is a basal release of EDRF *in vivo* (4).

Traditionally, the increase in P_{per} with EDRF blockers is interpreted as an increase in resistance. This is based on Poiseuille's Law which states that flow is proportional to the difference between inflow and outflow pressures. However, two observations raise questions about the application of this model to the circulation. First, whereas Poiseuille's Law predicts that arterial and venous pressure should be equal when flow is zero, it has been repeatedly shown that an arterial-venous pressure gradient remains at zero-flow (2,3,18). Second, it is difficult to explain the observation that small increases in venous pressure do not affect inflow into the region until a critical value is reached (8,18,28). Therefore, some authors have postulated that arteriolar tone creates a back pressure to flow, or vascular waterfall (8,18,22,28). In this model, flow is determined by the difference between P_{per} and P_{crit}, divided by the resistance between the two (R_a). Whereas P_{crit} is directly related to tone, R_a is dependent on the diameter of the vessel, and reflects the balance between tone and intravascular pressure. Both P_{crit} and R_a are increased with vasoconstrictor drugs and increases in sympathetic tone, and decreased with vasodilator drugs and decreases in sympathetic tone (6,26).

A change in P_{per} also affects vascular tone and diameter but the overall effect depends on the interaction between vasoconstrictor forces (myogenic response, removal

of metabolites) and vasodilator forces (EDRF, passive). We have previously found P_{crit} increases with increases in P_{per}, whereas R_a is constant at lower P_{per} (50-150 mmHg) but decreases at higher P_{per} (27,30). Since neurogenic factors were controlled and metabolic factors were negligible (9,26), the increased P_{crit} is best explained by a myogenic effect in response to the increased P_{per} (perhaps attenuated by EDRF). The decrease in R_a may have been due to the release of EDRF secondary to the increased flow, or by passive factors (perhaps attenuated by a myogenic response).

The purpose of this study was therefore to isolate the role of EDRF in the control of P_{crit} and R_a. We hypothesized that blockade of EDRF synthesis with L-nitro-arginine (L-NNA) (14,31) would increase vascular tone and thereby increase both P_{crit} and R_a. In addition, we hypothesized the decrease in R_a previously seen with increasing perfusion pressure was EDRF mediated, and would be abolished by L-NNA infusion. Our method also allowed us to examine the effects of EDRF on venous resistance (R_v). In a second group of animals, we controlled for effects mediated solely by increased vascular tone by giving phenylephrine to produce the same increase in P_{per} as observed with L-NNA.

We estimated P_{crit} and R_a from dynamic pressure-flow relations in which the time taken to decrease flow to zero was between 5-10 seconds. Under these conditions, the zero-flow pressure intercept approximates P_{crit} (18,26,27). Arterial resistance is then calculated as $(P_{per}-P_{crit})/\dot{Q}$, where P_{per} is perfusion pressure and $\dot{Q}$ is inflow into the region.

4.3. METHODS

Eleven dogs weighing 18-31 kg were anaesthetized with α-chloralose (75 $mg \cdot kg^{-1}$) after initial induction with sodium pentothal (1 $mg \cdot kg^{-1}$). Supplemental doses of α-chloralose were given as needed. The animals were intubated, ventilated

(Harvard Apparatus), and given supplemental oxygen to maintain PO_2 greater than 100 mmHg. We cannulated the left carotid artery to monitor arterial blood pressure (P_a) and to obtain arterial blood samples. Normal saline was infused into the left jugular vein to maintain proper hydration and sodium bicarbonate was given to maintain acid-base balance. Heparin (10,000 units bolus) was given to prevent blood clotting.

Surgical Preparation

The vascular supply to the left hindlimb was isolated as in previous studies (18,26,30). We tied all branches of the femoral artery and vein in the femoral triangle. Blood flow was diverted from the proximal end of the left femoral artery, through an in-line electromagnetic flow probe (Carolina Medical #10), and back into the distal end of the left femoral artery. Perfusion pressure (P_{per}) was measured through a side port close to the distal femoral artery segment. We placed two side ports upstream from the flow probe so that blood flow could be diverted through a pump (Masterflex #16 or #14 Tygon tubing) and controlled by clamping the direct line and adjusting the pump speed. A third side port was placed between the pump and flow probe for infusion of L-NNA or phenylephrine. We cannulated the left femoral vein and allowed the blood to flow into a reservoir. A Y-connector on the venous tubing had one end open to atmosphere to create a waterfall, thereby allowing us to control venous pressure. Reservoir blood was returned to the animal via the right jugular vein. Venous pressure (P_v) was measured from a side port close to the cannulation site.

We passed surgical wires through the proximal thigh with a 14 gauge needle. The wires were tied securely around either side of the femur to eliminate any collateral flow. A simultaneous occlusion of hindlimb inflow and outflow (double occlusion) was performed to ensure that isolation was maintained (18,19). Isolation was rechecked before and after each protocol. In addition, the level at which the venous pressure plateaus during the double occlusion is the pressure of the compliant region of the

vascular bed (elastic recoil pressure, P_{el}), and was used as the upstream pressure in the calculation of venous resistance (R_v) (19).

Measurements

Pressures were measured with Trantec transducers. We measured flow ($\dot{Q}$) using a Carolina Medical electromagnetic flow meter and an in-line probe. Signals were filtered at 3 Hz. All signals were processed through Gould amplifiers and simultaneously recorded on an eight-channel Graphtec recorder and on an IBM compatible computer using CODAS software program (DATAQ Instruments Inc.) for A-D conversion. Analysis was performed using the Codas and Anadat (RHT-Infodat Inc.) software programs.

Drug Concentrations

L-NNA was dissolved in HCl and saline to yield a concentration of $6x10^{-2}$ M (0.76N HCl). Hindlimb blood flow during drug infusion was fixed to yield an initial perfusion pressure of 100 mmHg. The drug infusion rate was set at 1/100 of the blood flow rate to give a L-NNA blood concentration of $6x10^{-4}$ M. In preliminary experiments, it was found that infusion for 20 minutes at this concentration increased P_{per} from 100 mmHg to approximately 175-200 mmHg during constant flow and that the effect lasted for more than 2 hours.

In experiments using phenylephrine, we dissolved 10 mg in 250 ml 5% dextrose (D_5W) and started the infusion at 1 $ml \cdot min^{-1}$ during conditions of constant flow (P_{per}=100 mmHg). The infusion rate was slowly increased every 2-3 minutes until $P_{per} \approx$175-200 mmHg. This infusion rate was kept constant throughout the remainder of the experiment.

Protocol

We tested the effect of L-NNA and phenylephrine on the response of P_{crit} and R_a to increasing P_{per} as in our previous studies (27,30). Under control conditions, the

pump flow rate was set at a given P_{per} between 100 and 200 mmHg. Pump flow was then manually turned down to zero over 5 to 10 seconds to obtain P_{crit}. We call this time the "ramp time". Two measurements were obtained at each perfusion pressure. The perfusion pressure was then changed, and the pump flow again decreased to zero in two separate runs. Isolation was rechecked with double occlusions at each P_{per}. We measured P_{crit} and calculated R_a at perfusion pressures of 100, 125, 150, 175, and 200 mmHg in random order. The procedure was then repeated following L-NNA administration in one group of animals (n=6), or with a continuous phenylephrine infusion (infusion was stopped during the experimental run, i.e. for 10 seconds) in another group of animals (n=5).

At the end of the experiment, the hindlimb was amputated at the level of the surgical wires and weighed. Flow and resistance are expressed per 100 g of hindlimb.

Data Analysis

Mean P_a, P_{per}, P_v and $\dot{Q}$ were obtained before each zero-flow pressure measurement. P_{el} was considered equal to the venous pressure during the double occlusion.

In general, the dynamic pressure-flow relation was linear. Under the conditions of our experiment, the zero-flow pressure intercept (calculated from least-squares linear regression analysis), is an excellent approximation of P_{crit} (18,26,27). The two P_{crit} values obtained for each P_{per} were averaged. R_a was calculated as $(P_{per}-P_{crit})/\dot{Q}$. R_v was calculated as $(P_{el}-P_v)/\dot{Q}$.

Statistics

The relationship between P_{crit} and P_{per} pre and post L-NNA infusion, and pre and post phenylephrine, were analyzed using ANOVA for Repeated Measures: Two factor design (P_{per} x L-NNA, or P_{per} x phenylephrine). In addition, the Two-Factor Mixed Design: Repeated Measures on one Factor was used to compare the L-NNA

group with the phenylephrine group, and the Newman-Keuls' Multiple-Range Test was used as the post-hoc test where appropriate. Results were considered significant if $p<0.05$. A similar analysis was performed for arterial resistance and venous resistance.

4.4. RESULTS

There was no difference in $[H^+]$, PCO_2, PO_2, temperature, or hemoglobin concentration between the L-NNA and phenylephrine groups. The PCO_2 was 36.9 ± 6.2 mmHg (mean$\pm$S.D.) and PO_2 was 167 ± 47 mmHg. Rectal temperature was 37 ± 1°C and hemoglobin concentration was 12.7 ± 2.5 $g\cdot dl^{-1}$. The $[H^+]$ was $4.26x10^{-8}\pm0.66x10^{-8}$ M (pH=7.37).

There was no difference in the hemodynamics between L-NNA and phenylephrine groups for any of the variables examined ($\dot{Q}$, P_{crit}, R_a, or R_v) ($p>0.2$). This is illustrated in each figure where all four conditions are plotted [pre-L-NNA (closed circles), post-L-NNA (open circles), pre-phenylephrine (closed squares), and post-phenylephrine (open squares)].

In figure 4.1, steady-state flow is plotted against P_{per}. Vasoconstriction induced by either L-NNA or phenylephrine resulted in lower flows at each P_{per}, and less change in flow for a given change in pressure.

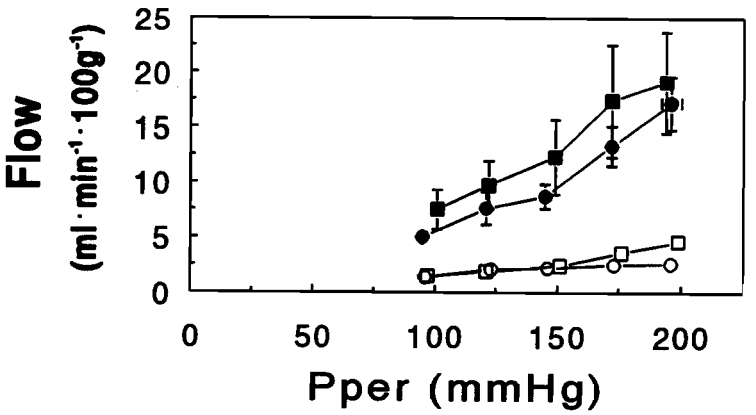

Figure 4.1: A plot of flow versus pressure during steady-state perfusion. The L-nitro-arginine group (L-NNA) is represented by circles [pre-L-NNA (●), post-L-NNA (○)], and the phenylephrine group is represented by squares [pre-phenylephrine (■), post-phenylephrine (□)]. Results are expressed as mean±S.E.M. with error bars in both X and Y directions. The error bars for some data points are too small to be visualized. There was no difference between L-NNA and phenylephrine groups, but each experimental group had a lower flow than during the control period.

Figure 4.2a is a plot of P_{crit} versus P_{per}. Blocking EDRF synthesis with L-NNA increased the value of P_{crit} at each P_{per} ($p<0.001$). As P_{per} was increased from approximately 100 mmHg to 200 mmHg, P_{crit} increased from 39.9±1.7 mmHg (mean±S.E.M.) to 60.5±3.9 mmHg before L-NNA infusion ($p<0.001$), and from 56.4±4.7 mmHg to 107.6±6.6 mmHg following L-NNA infusion ($p<0.001$). The slope of the relationship P_{crit} versus P_{per} was increased following L-NNA infusion ($p<0.001$). Results were similar between the L-NNA and phenylephrine groups ($p>0.2$).

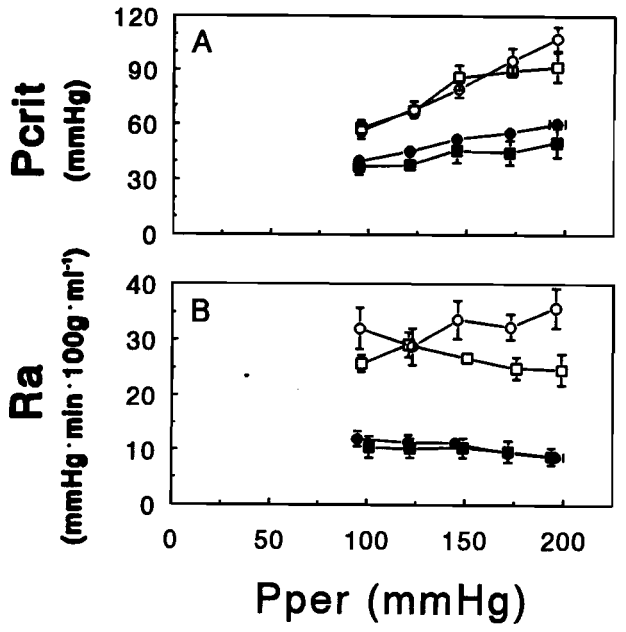

Figure 4.2: In A, the pressure at the waterfall (P_{crit}) is plotted against the perfusion pressure (P_{per}) for both L-NNA and phenylephrine groups. The legend is the same as figure 4.1, [pre-L-NNA (●), post-L-NNA (○), pre-phenylephrine (■), post-phenylephrine (□)]. There was no difference between the groups during control conditions, nor after vasoconstriction ($p>0.2$). Both L-NNA and phenylephrine resulted in an increased P_{crit} at each P_{per} ($p<0.001$). In addition, there was an increase in P_{crit} with increasing P_{per} both pre and post vasoconstriction ($p<0.001$). The slope of the relationship P_{crit} versus P_{per} was increased during vasoconstriction ($p<0.001$). In B, arterial resistance (R_a) is plotted against P_{per}. As in 4.2a, there was no difference between L-NNA and phenylephrine groups ($p>0.2$), and both drugs resulted in an increased R_a at each P_{per} ($p<0.001$). Before the infusions, R_a was constant between 100 and 150 mmHg, and decreased when P_{per} was

increased to 200 mmHg ($p<0.001$). Unlike control conditions, R_a was not affected by P_{per} after drug-induced vasoconstriction ($p>0.05$).

In figure 4.2b, R_a is plotted against P_{per}. Similar to the observations with P_{crit}, EDRF blockade increased the value of R_a at any given P_{per} ($p<0.001$). Prior to L-NNA infusion, R_a was constant at low perfusion pressures (100-150 mmHg) but declined at higher perfusion pressures (175-200 mmHg). Overall, resistance decreased from 12.0 ± 1.4 mmHg·min·100g·ml^{-1} at 100 mmHg, to 8.7 ± 1.1 mmHg·min·100g·ml^{-1} at 200 mmHg ($p<0.001$). After L-NNA infusion however, R_a did not change when P_{per} was increased (32.1 ± 3.7 mmHg·min·100g·ml^{-1} at 100 mmHg versus 35.8 ± 3.5 mmHg·min·100g·ml^{-1} at 200 mmHg, $p>0.05$). The results for the phenylephrine group were similar to the L-NNA group ($p>0.2$).

Figure 4.3 shows the changes in R_v with increasing P_{per} for both groups of animals. Once again, R_v was higher at all P_{per} after L-NNA infusion ($p<0.05$). R_v did not change with changes in P_{per} during control conditions ($p>0.05$). Post-L-NNA, R_v decreased when P_{per} increased from 100 mmHg to 125 mmHg ($p<0.05$), but did not significantly decrease any further with higher pressures. The response of R_v to changes in P_{per} with the phenylephrine group was similar to the L-NNA group ($p>0.2$).

Finally, P_{el} decreased at each P_{per} following L-NNA infusion. Furthermore, P_{el} increased with increasing P_{per} in each group. For instance, when perfusion pressure was increased from 100 to 125 mmHg, P_{el} increased from 11.6 ± 1.7 to 14.6 ± 1.3 mmHg during control conditions, and from 9.1 ± 2.5 to 10.2 ± 2.4 mmHg after L-NNA infusion ($p<0.05$). The results were similar for the phenylephrine group.

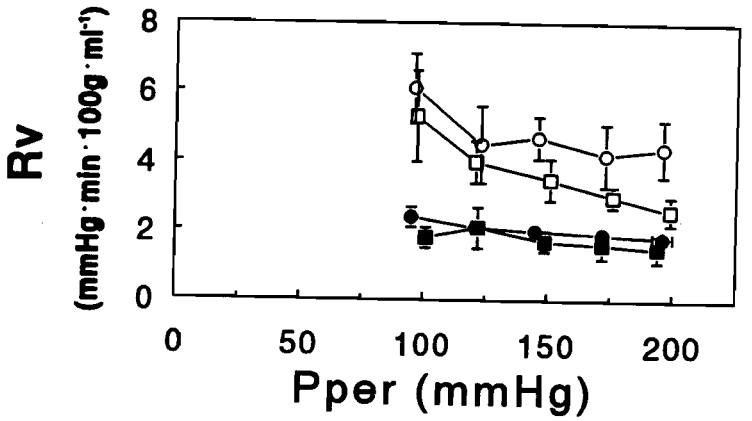

Figure 4.3: Venous resistance (R_v) is plotted against P_{per}. The legend is the same as figure 4.1, [pre-L-NNA (●), post-L-NNA (O), pre-phenylephrine (■), post-phenylephrine (□)]. Similar to figures 4.1 and 4.2, there was no difference between L-NNA and phenylephrine groups before or after drug infusion ($p>0.2$). The value of R_v at each P_{per} was significantly increased by both experimental interventions ($p<0.05$). R_v was significantly higher at $P_{per}=100$ mmHg when compared to $P_{per}=200$ mmHg for both experimental groups ($p<0.05$), but not during control conditions ($p>0.05$).

4.5. DISCUSSION

We found that both L-NNA (a blocker of EDRF synthesis) (14,31) and phenylephrine (an α_1-adrenoceptor stimulator) increased P_{crit} at any given perfusion pressure, in addition to increasing arterial resistance. Furthermore, both agents increased the slope of the relationship between P_{crit} and P_{per}, and abolished the decrease in R_a that occurred with increases in P_{per} under control conditions. These results suggest that the effects of L-NNA on P_{crit} and R_a are mediated by an increase in basal

tone and are not specific for EDRF inhibition. Before discussing these results in detail, some technical factors should be considered.

The hindlimb must be completely isolated from the systemic circulation or an artificially high P_{crit} will be recorded (12). As discussed in the Methods section, we used the double occlusion technique (19) to ensure isolation, and did not proceed unless isolation was confirmed.

Changes in resistance and critical pressure have been studied with steady-state pressure-flow relations (1,5). However, steady-state measurements are of limited value since they include adjustments from autoregulatory mechanisms and do not reflect the instantaneous P_{crit} that exists at higher flows or higher pressures (6,26). If P_{crit} is unreliable, then resistance calculations $[R_a=(P_{per}-P_{crit})/\dot{Q}]$ and inferences about vessel diameter changes are also unreliable. In order to estimate P_{crit} at each P_{per}, we used the dynamic pressure-flow relation. Dynamic pressure-flow relations, however, can be affected by vessel compliance if the flow is decreased too rapidly (2,18). This effect is minimal if the ramp time is greater than 5 seconds (18,26,27).

The duration of vasoconstriction produced by phenylephrine and L-NNA is different. Whereas L-NNA induced vasoconstriction persists for more than two hours (31), phenylephrine induced vasoconstriction does not last for long and the drug must continuously be infused during the experiment. We therefore titrated the phenylephrine dose so that perfusion pressure increased the same as with L-NNA, and then fixed the infusion rate at this level. However, this means the blood concentration of phenylephrine increased as flow was decreased during perfusion at lower pressures. This could have resulted in phenylephrine-induced vasoconstriction being greater than L-NNA-induced vasoconstriction at low P_{per}. The fact that steady-state pressure-flow relations post L-NNA and post phenylephrine are almost identical (figure 4.1) suggests this effect was minimal.

EDRF and P_{crit}

L-NNA increased P_{crit} at each P_{per}. This supports the notion that EDRF is released under control conditions, and affects small vessel tone (7,29). We also found that P_{crit} increases when P_{per} is increased, and that the slope of the relationship is even greater after blocking EDRF synthesis with L-NNA.

When P_{per} was increased, several factors were altered that could affect P_{crit}. First, the higher perfusion pressure could have induced a myogenic response which would have increased tone (15). Second, the increase in P_{per} was accompanied by an increase in flow. This effect might have increased EDRF release and decreased smooth muscle tone (23). Third, the increased flow may have led to increased removal of vasodilator metabolites which would have decreased the metabolic signal and increased tone, but this is not likely to be important in the resting hindlimb (9). Since P_{crit} increased when P_{per} increased and metabolic factors are negligible in our preparation, one must conclude that myogenic factors predominated. Since the slope of the relationship P_{crit} versus P_{per} was increased following EDRF synthesis blockade, the results support the notion that EDRF normally attenuates the response of the arterioles to a myogenic stimulus (17). However, phenylephrine also increased the slope of the relationship between P_{crit} and P_{per}, indicating the mechanism is not specific for EDRF inhibition but may be due to a non-specific increase in basal tone.

EDRF and R_a

EDRF blockade with L-NNA infusion increased R_a at each P_{per}. This supports previous results which indicate that EDRF is released under basal conditions and affects large vessel tone in addition to small vessel tone (7,24). Furthermore, as in our previous study, R_a decreased at high P_{per} under control conditions, whereas P_{crit} increased (27,30). However, following vasoconstriction with either L-NNA or phenylephrine, R_a remained constant with increasing P_{per}.

The effect of increasing P_{per} on R_a can be analyzed in a similar manner to its effect on P_{crit}. Since R_a decreased with increasing P_{per} under control conditions, it appears that vasodilator forces (EDRF and passive factors) predominate. Following EDRF blockade with L-NNA, R_a did not decrease with increasing P_{per}, which indicates that the decrease in R_a under control conditions was not due to a passive effect. Furthermore, phenylephrine produced the same results as L-NNA, which suggests that decreases in R_a with increases in P_{per} cannot be explained by an increase in EDRF release. Rather, it seems vasoconstriction with either drug increases the myogenic response of the vessels responsible for R_a in the same way it increases the myogenic response of the vessels responsible for P_{crit}.

EDRF and R_v

Similar to the effects on P_{crit} and R_a, L-NNA and phenylephrine increased R_v at each P_{per}. This finding supports other studies which have shown an increase in R_v with increases in sympathetic tone (25), and supports the role of EDRF in the venous circulation (21).

A second observation was that R_v increased when P_{per} was decreased from 125 to 100 mmHg under vasoconstricted conditions but not under control conditions. However, the venous system should not have been directly exposed to the high arterial P_{per} because of the vascular waterfall. It is therefore more appropriate to examine the relationship between R_v and P_{el} (i.e. the pressure in the venous compliant region). P_{el} was obtained by the plateau in P_v during a stop-flow procedure (19). In our experiments, R_v was unaffected by changes in P_{el} until P_{el} decreased below 10 mmHg (i.e. P_{per}=100 mmHg). These results are supported by previous studies. For instance, Shoukas and Bohlen found that R_v did not change when P_{el} varied from 10 to 30 mmHg (25). In addition, Johnson and Hanson found that R_v increased when P_{per} was decreased to 60-80 mmHg (16). Although P_{el} was not measured in their study, our

results indicate that P_{el} would likely decrease below 10 mmHg at these perfusion pressures.

The mechanism for the increased venous resistance at low P_{el} is not well understood. It cannot be due to metabolic or direct myogenic effects because vasoconstriction occurs when flow or pressure are decreased. It cannot be due to EDRF effects, since it occurred equally in L-NNA and phenylephrine groups. One possibility is a local capillary-venous reflex (causing venoconstriction) which occurs when capillary pressure falls below a critical value. Other possibilities include passive narrowing of the vessels at low pressures, derecruitment of vessels, or increased blood viscosity at low flows (13). Finally, the increased venous resistance may be important in maintaining capillary pressure constant during decreased arterial pressure (13,20,32).

In conclusion, P_{crit}, arterial resistance, and venous resistance are all increased when EDRF synthesis is blocked with L-NNA. Furthermore, there is a potentiated myogenic response of P_{crit} that is not specific to EDRF inhibition, but is a result of increased tone. Our results also suggest that the normal decrease in arterial resistance observed with increasing P_{per} is abolished during conditions of increased vascular tone due to an enhanced myogenic response of the proximal vessels. Finally, our results show that venous resistance is increased at low perfusion pressures if vessel tone is increased by phenylephrine or L-NNA.

4.6. REFERENCES

1. Ashton, H. Critical closing pressure in human peripheral vascular beds. *Clin. Sci.* 22: 79-87, 1962.

2. Aversano, T., F.J. Klocke, R.E. Mates, and J.M. Canty,Jr.. Preload-induced alterations in capacitance-free diastolic pressure-flow relationships. *Am. J. Physiol.* 246: H410-H417, 1984.

3. Bellamy, R.F. Diastolic coronary artery pressure-flow relations in the dog. *Circ. Res.* 43(1): 92-101, 1978.

4. Bellan, J.A., R.K. Minkes, D.B. McNamara, and P.J. Kadowitz. N-nitro-L-arginine selectively inhibits vasodilator responses to acetylcholine and bradykinin in cats. *Am. J. Physiol.* 260: H1025-H1029, 1991.

5. Braakman, R., P. Sipkema, and N. Westerhof. Pressure-flow relationships of the canine iliac periphery and systemic hemodynamics: Effects of sodium nitroprusside and adenosine. *Pflügers Arch.* 407: 432-439, 1986.

6. Braakman, R., P. Sipkema, and N. Westerhof. Two zero-flow pressure intercepts exist in autoregulating isolated skeletal muscle. *Am. J. Physiol.* 258: H1806-H1814, 1990.

7. Faraci, F.M. Role of endothelium-derived relaxing factor in cerebral circulation: large arteries vs. microcirculation. *Am. J. Physiol.* 261: H1038-H1042, 1991.

8. Farhi, E.R., F.J. Klocke, R.E. Mates, K. Kumar, R.M. Judd, J.M. Canty,Jr., S. Satoh, and B. Sekovski. Tone-dependent waterfall behaviour during venous pressure elevation in isolated canine hearts. *Circ. Res.* 68: 392-401, 1991.

9. Folkow, B. Intravascular pressure as a factor regulating the tone of the small vessels. *Acta Physiol. Scand.* 17: 289-310, 1949.

10. Furchgott, R.F. The role of endothelium in the responses of vascular smooth muscle to drugs. *Annu. Rev. Pharmacol. Toxicol.* 24: 175-197, 1984.

11. Furchgott, R.F. and J.V. Zawadzki. The obligatory role of endothelial cells in the relaxation of arterial smooth muscle by acetylcholine. *Nature* 288: 373-376, 1980.

12. Green, H.D., C.E. Rapela and M.C. Conrad. Resistance (conductance) and capacitance phenomena in terminal vascular beds. In: *Handbook of Physiology. Circulation. Section 2, Volume II*, Washington, D.C.: American Physiological Society, 1963, p. 935-960.

13. House, S.D. and P.C. Johnson. Microvascular pressure in venules of skeletal muscle during arterial pressure reduction. *Am. J. Physiol.* 250: H838-H845, 1986.

14. Ishii, K., B. Chang, J.F. Kerwin,Jr., Z.-J. Huang, and F. Murad. N-nitro-L-arginine: a potent inhibitor of endothelium-derived relaxing factor formation. *European J. Pharmacol.* 176: 219-223, 1990.

15. Johnson, P.C. Autoregulatory responses of cat mesenteric arterioles measured *in vivo*. *Circ. Res.* 22: 199-212, 1968.

16. Johnson, P.C. and K.M. Hanson. Effect of arterial pressure on arterial and venous resistance of intestine. *J. Appl. Physiol.* 17(3): 503-508, 1962.

17. Kuo, L., W.M. Chilian, and M.J. Davis. Interaction of pressure- and flow-induced responses in porcine coronary resistance vessels. *Am. J. Physiol.* 261: H1706-H1715, 1991.

18. Magder, S. Starling resistor versus compliance. Which explains the zero-flow pressure of a dynamic arterial pressure-flow relation? *Circ. Res.* 67: 209-220, 1990.

19. Magder, S. Vascular mechanics of venous drainage in dog hindlimbs. *Am. J. Physiol.* 259: H1789-H1795, 1990.

20. Mellander, S., M. Maspers, J. Björnberg, and L.-O. Andersson. Autoregulation of capillary pressure and filtration in cat skeletal muscle in states of normal and reduced vascular tone. *Acta Physiol. Scand.* 129: 337-351, 1987.

21. Miller, V.M. and P.M. Vanhoutte. Is nitric oxide the only endothelium-derived relaxing factor in canine femoral veins? *Am. J. Physiol.* 257: H1910-H1916, 1989.

22. Permutt, S. and R.L. Riley. Hemodynamics of collapsible vessels with tone: the vascular waterfall. *J. Appl. Physiol.* 18(5): 924-932, 1963.

23. Pohl, U., K. Herlan, A. Huang, and E. Bassenge. EDRF-mediated shear-induced dilation opposes myogenic vasoconstriction in small rabbit arteries. *Am. J. Physiol.* 261: H2016-H2023, 1991.

24. Pohl, U., J. Holtz, R. Busse, and E. Bassenge. Crucial role of endothelium in the vasodilator response to increased flow *in vivo*. *Hypertension* 8: 37-44, 1986.

25. Shoukas, A.A. and H.G. Bohlen. Rat venular pressure-diameter relationships are regulated by sympathetic activity. *Am. J. Physiol.* 259: H674-H680, 1990.

26. Shrier, I., S.N.A. Hussain, and S. Magder. Effect of carotid sinus stimulation on resistance and critical closing pressure of the canine hindlimb. *Am. J. Physiol.* 1992.(In Press)

27. Shrier, I. and S. Magder. A zero-flow pressure intercept still exists in the canine hindlimb during maximal vasodilation. *Clin. Invest. Med.* 15 (Suppl): A13, 1992.(Abstract)

28. Soohoo, S.L., H.S. Goldberg, R. Graham, and A.C. Jasper. Zone 2 and zone 3 pulmonary blood flow. *J. Appl. Physiol.* 62: 1982-1988, 1987.

29. Sun, D., E.J. Messina, A. Koller, M.S. Wolin, and G. Kaley. Endothelium-dependent dilation to L-arginine in isolated rat skeletal muscle arterioles. *Am. J. Physiol.* 262: H1211-H1216, 1992.

30. Vanelli, G., I. Shrier, and S. Magder. Critical closing pressure and arterial resistance have opposing responses to increases in perfusion pressure. *FASEB J.* 6(4): A1472, 1992.(Abstract)

31. Wang, Y.-X., T. Zhou, and C.C.Y. Pang. Pressor effects of L and D enantiomers of N-nitro-arginine in conscious rats are anatagonized by L- but not D-arginine. *European J. Pharmacol.* 200: 77-81, 1991.

32. Zweifach, B.W. Local regulation of capillary pressure. *Circ. Res.* 28-29 (Suppl. I): I-129-I-134, 1971.

CHAPTER 5

MAXIMAL VASODILATION DOES NOT ELIMINATE THE VASCULAR WATERFALL IN THE CANINE HINDLIMB

5.1. ABSTRACT

The dynamic pressure-flow relationship in skeletal muscle at normal arterial pressure can be explained by modelling a vascular waterfall (critical pressure, P_{crit}) at the arteriolar level. Regulation of flow can therefore occur through changes in P_{crit} at the waterfall, or changes in upstream resistance (R_a). To determine if P_{crit} still exists during maximal vasodilation, we pump-perfused vascularly isolated canine hindlimbs. We kept venous pressure (P_v) constant and measured P_{crit}, perfusion pressure (P_{per}), the regional elastic recoil pressure (P_{el}, by a stop-flow technique), and calculated both R_a and venous resistance (R_v) during control and vasodilated conditions. Maximal vasodilation with adenosine and nitroprusside decreased P_{crit} from 56.4 ± 5.1 to 11.0 ± 0.6 mmHg. R_a decreased to $10.2\pm2.6\%$, and R_v to $41\pm6\%$ of control. P_{el} at zero arterial flow was always less than P_{crit}, but close to normal flow, P_{el} was always greater than P_{crit}. In a second protocol we raised P_v during maximal vasodilation and found that P_{per} was immediately affected. We conclude that a small P_{crit} is still present in the maximally dilated hindlimb but is less than the downstream pressure, and does not affect flow at normal perfusion pressures. We also found that P_{crit} increases when P_{per} is increased during vasodilated conditions indicating that myogenic activity is still present, but the rate of increase was less than during normal conditions. R_a was not affected by increases in P_{per}.

5.2. INTRODUCTION

According to Poiseuille's Law, inflow and outflow pressure should be equal when flow is decreased to zero (20). However, many authors have shown a large arterial-venous pressure gradient at zero flow (2,3,10,16,19,24). In 1951, Burton hypothesized that an instability in the elastic wall causes arterial vessels to collapse when inflow pressure declines below a critical value (P_{crit}) (8). However, in 1963, Permutt and Riley showed that the zero-flow pressure gradient is better explained by a vascular "waterfall" at the arteriolar level (20). Flow over a waterfall is determined by the difference in altitude between the upstream lake and the waterfall, divided by the resistance of the river in between. It is not affected by the actual height of the falls nor by the resistance to flow in the river below the falls. Similarly, when a vascular waterfall is present, flow is determined by the difference between perfusion pressure (P_{per}) and P_{crit}, divided by the resistance between the two (arterial resistance, R_a). Venous pressure (P_v) does not affect inflow until the downstream pressure exceeds P_{crit}. Unlike Burton's model, a vascular waterfall affects flow throughout the pressure-flow relation and not only at zero-flow.

A vascular waterfall is created when there is a sudden increase in the pressure surrounding a vessel, thereby dissociating the energy and hydraulic gradients for flow (9). In Permutt and Riley's model, the pressure is supplied by arteriolar smooth muscle tone (20). In support of this theory, Braakman et al. found that P_{crit} obtained from dynamic pressure-flow relations in isolated skeletal muscle (28.5 ± 9.5 mmHg) is affected by norepinephrine and adenosine (tone-dependent) (7). However, when the authors suddenly occluded arterial inflow and maintained zero-flow for one minute, P_{per} was only 8.8 ± 2.2 mmHg above P_v. They called this zero-flow pressure the steady-state P_{crit}. Since the steady-state P_{crit} was less than the estimated skeletal muscle small venular pressure of 15 mmHg (5), they reasoned that the vessels responsible must be

located in the venous circulation. In contrast, the dynamic P_{crit} was 28 mmHg which they attributed to an arteriolar waterfall. Furthermore, Braakman et al. showed that unlike the dynamic P_{crit}, the steady-state P_{crit} is not affected by norepinephrine or adenosine (tone-independent). Therefore, Braakman et al. concluded that a tone-dependent waterfall exists in the arterial circulation, and a tone-independent waterfall exists in the venous circulation.

The venous waterfall hypothesis was based on a comparison between capillary pressure at normal P_{per}, and the perfusion pressure one minute after arterial occlusion (steady-state P_{crit}). However, during the arterial occlusion used to measure the steady-state P_{crit}, venous outflow continued and capillary pressure must have decreased. After one minute of arterial occlusion, capillary pressure might have decreased to less than 9 mmHg, which would mean the steady-state P_{crit} was greater than capillary pressure and therefore located in the arterioles. In fact, the steady-state P_{crit} might simply represent the tone-dependent arteriolar waterfall after smooth muscle tone is decreased by ischemic metabolites. The purpose of our investigation was therefore to test the hypothesis that P_{crit} is located at the arteriolar level even under conditions of maximal vasodilation. We defined maximal vasodilation as the loss of reactive hyperemia.

The method of estimating P_{crit} is essential to our experiment. Emptying of the arterial compliance can cause an artificially high pressure at zero flow when arterial pressure is rapidly decreased (2,16,23). Vasodilation from the myogenic response (15) or the release of metabolic factors (4) might produce an artificially low P_{crit} if the arterial pressure is decreased too slowly. In our previous studies, we showed these problems can be avoided by using ramp times (the time taken to decrease flow to zero) between 4-10 seconds (16,22). In order to know if P_{crit} is due to venous or arterial vessels, we estimated small venular pressure (elastic recoil pressure of the vascular bed, P_{el}) by a double occlusion technique (17). If P_{crit} is greater than P_{el}, the waterfall must be upstream from the small venules.

We have also recently shown that P_{crit} increases when perfusion pressure is increased, implying an increased tone at the waterfall possibly due to myogenic mechanisms (25). Therefore, we further hypothesized that maximal vasodilation (as defined by loss of reactive hyperemia) will lower P_{crit} at any given P_{per}, but that P_{crit} will still increase when P_{per} is increased.

Finally, we gave a bolus of indomethacin before inducing maximal vasodilation to remove prostaglandin-mediated effects. In another series of experiments, P_{crit} and R_a were measured over a range of perfusion pressures before and after a bolus of indomethacin to examine the role of prostaglandins.

5.3. METHODS

Six dogs weighing 18-24 kg were anaesthetized with α-chloralose (75 $mg \cdot kg^{-1}$) after initial induction with sodium pentothal (1 $mg \cdot kg^{-1}$). Supplemental doses of α-chloralose were given as needed. The animals were intubated, ventilated (Harvard Apparatus), and given supplemental oxygen to maintain PO_2 greater than 100 mmHg. We cannulated the left carotid artery to monitor arterial blood pressure (P_a) and to obtain arterial blood samples. Normal saline was infused into the left jugular vein to maintain proper hydration and sodium bicarbonate was given to maintain acid-base balance. Heparin (10,000 units) was given to prevent blood clotting.

Surgical Preparation

The vascular supply to the left hindlimb was isolated as in previous studies (16,22) (figure 5.1). We tied all branches of the femoral artery and vein in the femoral triangle. Blood flow was diverted from the proximal end of the left femoral artery, through an in-line electromagnetic flow probe (Carolina Medical #10), and back into the distal end of the left femoral artery. A side port placed downstream from the flow probe was used to measure the pressure perfusing the limb (P_{per}). We placed two

side ports upstream from the flow probe so that blood flow could be diverted through a pump (Masterflex #16 tubing) during experimental runs. The direct line was used for measuring the natural flow of the hindlimb and looking for the presence of reactive hyperemia. During experimental runs, we clamped the direct line and controlled flow by adjusting the pump speed. A third side port was placed between the pump and flow probe for infusion of vasodilator drugs. We cannulated the left femoral vein and allowed the blood to flow into a reservoir. We created an external waterfall in the venous tubing by including a Y-connector with one end open to atmosphere. Venous pressure (P_v) was controlled by adjusting the height of the Y-connector. Reservoir blood was returned to the animal via the right jugular vein. P_v was measured from a side port close to the cannulation site.

We passed surgical wires through the proximal thigh with a 14 gauge needle. The wires were tied securely around either side of the femur to eliminate any collateral flow. A simultaneous occlusion of hindlimb inflow and outflow (double occlusion) was performed to ensure complete vascular isolation (16,17). A continuous rise in venous pressure implies that arterial inflow still exists and a continuous decrease in venous pressure implies that venous outflow exists. If either was observed, the surgical wires were tightened and the double occlusion repeated. We only continued the experiment after complete isolation was obtained. Isolation was rechecked before and after each protocol. The venous plateau pressure is also the pressure of the compliant region of the vascular bed (elastic recoil pressure, P_{el}), and is used to calculate venous resistance (R_v) (17).

Although we infused vasoactive drugs locally, there was some systemic hypotension due to recirculation of blood. To maintain P_a constant, we connected the right femoral artery to a large reservoir suspended from the ceiling so that the height of the reservoir determined P_a. The reservoir was filled with Dextran and/or saline.

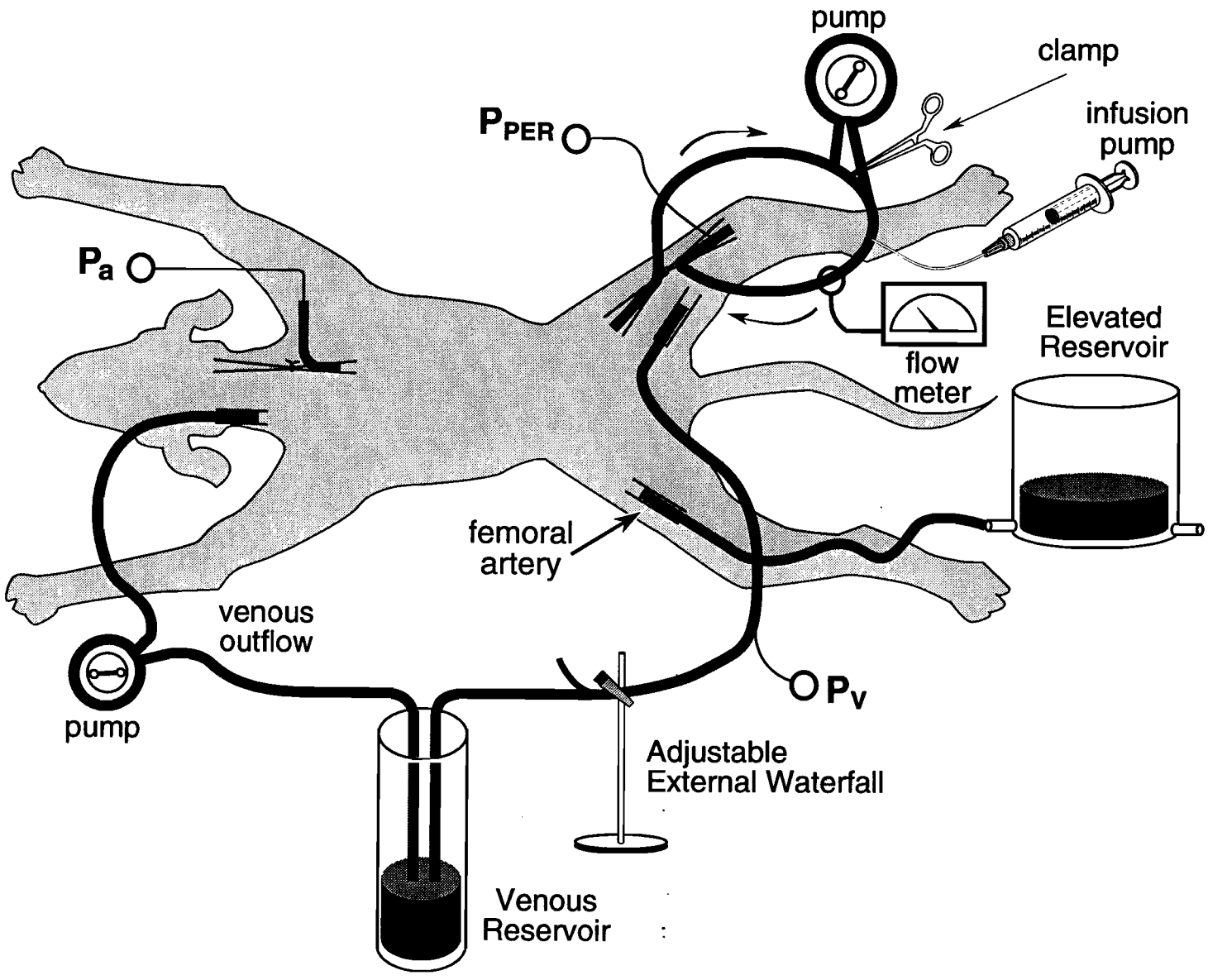

Figure 5.1: Experimental Setup

Measurements

Pressures were measured with Trantec transducers. We measured flow ($\dot{Q}$) using a Carolina Medical electromagnetic flow meter and an in-line probe. Signals were filtered at 3 Hz. All signals were processed through Gould amplifiers and simultaneously recorded on an eight-channel Graphtec recorder and on an IBM compatible computer using CODAS software program (DATAQ Instruments Inc.) for A-D conversion. Analysis was performed using Codas and Anadat (RHT-Infodat Inc.) software programs.

Drug Concentrations

After control measurements were completed, we eliminated prostaglandin effects with a bolus injection of indomethacin (5 $mg \cdot kg^{-1}$) (14). Vasodilation was achieved with a solution of 2.5 $mg \cdot ml^{-1}$ of adenosine and 0.2$\mu g \cdot ml^{-1}$ of nitroprusside dissolved in 5% dextrose (D_5W), and protected from light with silver wrapping. The infusion rate was increased until reactive hyperemia to a 30-60 second occlusion was abolished. In two animals, we doubled the infusion rate after no reactive hyperemia was observed and no further vasodilation occurred.

Protocol

Protocol 1: In five animals, we determined if P_{crit} still exists when the hindlimb is maximally vasodilated (16,22). We first measured the natural flow to the hindlimb. The tubing between the two proximal side ports was then clamped, and the pump speed adjusted to give the same flow rate. We obtained zero-flow pressure intercepts (P_{zf}) by decreasing pump flow to zero over time periods ranging from 0.5-10 seconds (random order). After each run to zero-flow, the pump speed was reset to the initial flow, and perfusion pressure was allowed to return to baseline. Approximately 5-10 different ramp times were used in each animal. The same procedure was repeated after reactive hyperemia was abolished (maximal vasodilated conditions).

Waterfall behaviour only occurs when P_{crit} is greater than downstream pressure. We therefore compared P_{crit} with the small venular pressure (P_{el}) obtained from the double occlusion method (17). In addition, we measured small venular pressure at the time we measured P_{crit} (P_{el2}) by occluding venous outflow when arterial inflow reached zero.

Protocol 2: The results from protocol 1 suggested that waterfall behaviour would not be present during maximal vasodilation because the downstream pressure was greater than P_{crit} when perfusion pressure was close to normal. If true, changes in venous pressure should immediately affect P_{per} during constant flow conditions (16). We tested this hypothesis by raising P_v in small steps and measuring the changes in P_{per} during constant flow conditions in the maximally vasodilated hindlimb (n=3).

Protocol 3: We have previously found that P_{crit} increases with increases in P_{per}, presumably due to a myogenic response (25). To determine if myogenic activity is still present in the maximally vasodilated bed, we measured P_{crit} at several different P_{per} in five animals. Under control conditions the pump flow rate was set at a given P_{per} and then manually turned down to zero over a ramp time period ranging from 5-10 seconds, which from Protocol 1, gives a good estimate of P_{crit}. Two measurements were obtained at each perfusion pressure. The perfusion pressure was then changed, and the pump flow again decreased to zero in two separate runs. We measured P_{crit} at perfusion pressures of 50, 75, 100, 125, and 150 mmHg in random order. The procedure was then repeated in the vasodilated hindlimb. However, following maximal vasodilation, the maximal capacity of the pump (approximately 500 $ml \cdot min^{-1}$) could not generate pressures above 75 mmHg in the majority of animals. The range of perfusion pressures studied was therefore 10-125 mmHg, depending on the animal. A minimum of four perfusion pressures were studied in each animal.

Protocol 4: To isolate the role of indomethacin, we repeated protocol 3 in a separate group of animals, before and after a 5 $mg \cdot kg^{-1}$ bolus of indomethacin (n=6). The range of perfusion pressures studied was 100-200 mmHg.

At the end of the experiment, the hindlimb was amputated at the level of the surgical wires and weighed. Flow and resistance are expressed per 100 g of hindlimb.

Data Analysis

Mean P_a, P_{per}, P_v and $\dot{Q}$ were obtained before each zero-flow pressure measurement. Double occlusion venous plateau pressures before and after each series of measurements were averaged to obtain P_{el} (17).

In general, the relation between flow and perfusion pressure during a ramp to zero flow was linear and the calculated x-intercept from a least-squares linear regression analysis was used as the zero-flow pressure intercept (16,22).

Protocol 1 was used to determine if a vascular waterfall exists when the hindlimb is maximally vasodilated (16). We compared the observed results with those predicted by two different models of the circulation (figure 5.2). In the first model, two compliant regions are in series with three resistances and the total resistance R_{tot} is calculated as $(P_{per}-P_v)/\dot{Q}$. Since P_{el} was obtained from the double occlusion method (i.e. the pressure in the second compliant region) and P_v was measured, R_3 could be calculated and expressed as a percentage of R_{tot}. The first resistance was estimated to be 5% of the total, and the middle resistance was calculated as $R_{tot}-(R_1+R_3)$. Venous compliance was varied between 0.4 and 3.2 $ml \cdot mmHg^{-1} \cdot 100g^{-1}$, and arterial compliance was varied between 1/320 and 1/5 of venous compliance. In the second model, a vascular waterfall placed after the first compliant region.

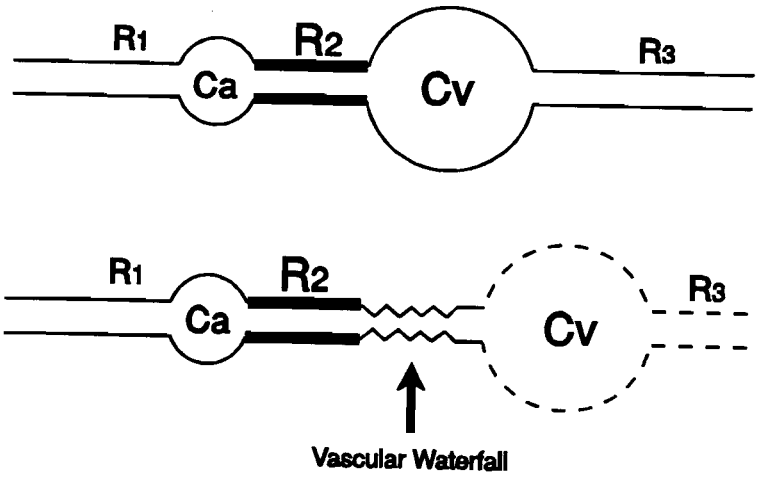

Figure 5.2: Theoretical models of the hindlimb circulation. In A, the vascular bed is composed of an arterial compliant region (C_a) and a venous compliant region (C_v), separated by resistances (R_1, R_2, R_3). The major site of resistance is in the arteries distal to the arterial compliant region. In B, a vascular waterfall is added to the arterial side of the vasculature, downstream from R_2. The double occlusion technique (see Methods) measures the elastic recoil pressure in the most compliant region of the bed, i.e. C_v.

The mathematical basis for the analysis of the second model is fully described elsewhere (16). Briefly, P_{crit} is calculated as the average of the P_{zf} values obtained for ramp times greater than 5 seconds (16). R_a is calculated as $(P_{per}-P_{crit})/\dot{Q}$, where $\dot{Q}$ is the mean flow per 100 g. Venous resistance (R_v) is calculated as $(P_{el}-P_v)/\dot{Q}$ (17). Arterial compliance was calculated according to the equation

$$P_{zf} = P_{crit} - \beta R_a^2 C_a \left(1 - e^{\frac{Q_{I(0)}}{\beta R_a C_a}}\right) \quad \text{.....(5.1)}$$

where the P_{zf} used was that experimentally obtained with a ramp time of approximately 2 seconds, ß is the rate of change of inflow, and $Q_{I(0)}$ is the initial inflow (16). Using this calculated value of compliance, P_{zf} values can then be predicted for ramp times varying from 1-20 seconds, and the results compared with the experimentally obtained values.

In protocols 3 and 4, the two P_{crit} values obtained for each P_{per} were averaged. R_a was again calculated as $(P_{per}-P_{crit})/\dot{Q}$.

Statistics

In protocol 1, we used paired t-tests to analyze differences in measured or calculated variables (P_a, P_{crit}, R_a, and R_v) under control and vasodilated conditions. Results were considered significant if $p<0.05$.

In protocols 3 and 4, we calculated the least squares linear regression for the relationship P_{crit} x P_{per} for each experiment individually, and then compared the mean of the slopes using a paired t-test. Results were considered significant if $p<0.05$. A similar analysis was performed for arterial resistance.

5.4. RESULTS

The PCO_2 was 35.7±4.4 mmHg (mean±S.D.) and PO_2 was 185±50 mmHg. Rectal temperature was 37.7±1.6 °C and hematocrit was 39.9±7.1%. The $[H]^+$ was $4.93x10^{-8}\pm0.57x10^{-8}$ M (pH=7.31). P_a decreased during vasodilation from 143±12 mmHg to 108±22 mmHg.

Infusion of vasodilator drugs increased the slope of the steady-state pressure-flow relation and shifted the curve to the left (figure 5.3). There was no apparent autoregulation during vasodilated conditions.

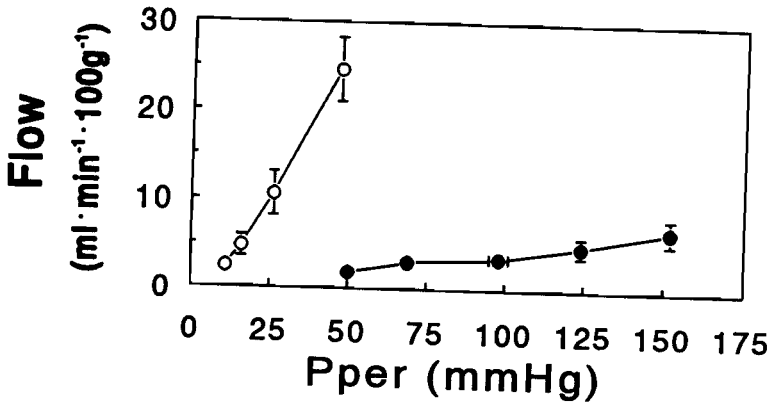

Figure 5.3: The steady-state pressure-flow relationships are plotted for control (●) and vasodilated (O) conditions. Autoregulation was present under control conditions, but not under vasodilated conditions. Data were obtained from four animals which were studied over the same pressure ranges. Results are expressed as mean±S.E.M. with error bars in both X and Y directions. The error bars for some data points are too small to be visualized.

Figure 5.4a is a plot of the zero-flow pressure intercept against the time taken to reach zero-flow for one animal before (●) and after (O) maximal vasodilation. The dotted lines represent the best results that could be predicted if the circulation consisted of two compliant regions in series (arterial and venous) with three resistances (figure 5.2a). Values for R_1, R_2, R_3, C_a, and C_v used are described in the Methods section. The best results under control conditions were obtained with C_a=0.02 and C_v=0.2, and under maximal vasodilation with C_a=0.02 and C_v=0.8. Even using these values, the P_{zf} at long ramp times was underestimated, and there was no indication of a plateau in the predicted values. If we increased either arterial or venous compliance to raise the values corresponding to longer ramp times, then the model was unable to predict P_{zf}

values obtained with shorter ramp times. The same results were obtained for every animal studied.

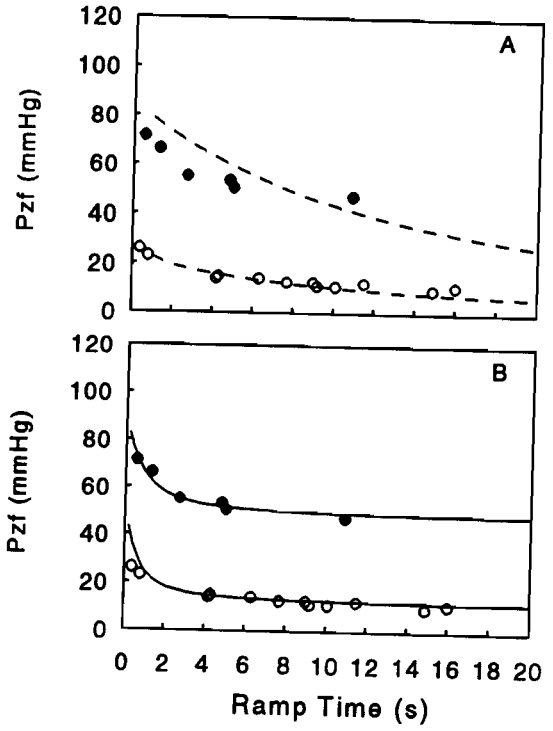

Figure 5.4: The zero-flow pressure intercept (P_{zf}) is plotted against the time taken to reach zero flow for both the control (●) and vasodilated (O) conditions. The dotted lines in A represent the best predicted results based on the two-compliant model of the vasculature represented in figure 5.2a for control (C_a=0.02, C_v=0.2) and vasodilated (C_a=0.02, C_v=0.8) conditions. This model overestimates P_{zf} with short ramp times, and underestimates P_{zf} with long ramp times. In B, the same data points are plotted, but the solid lines show the predicted results if a vascular waterfall is present at the arteriolar level (figure 5.2b). This model accurately predicts the observed fall in P_{zf} with ramp times between 1-4 seconds, and the plateau in the relationship with ramp times greater than 5 seconds.

Figure 5.4b shows the same data, but the solid lines represent predicted values using a model that incorporates a vascular waterfall on the arterial side (figure 5.2b). In contrast to the simple two-compartment model, the vascular waterfall model accurately predicts that P_{zf} for ramp times of 5 seconds will be almost equal to those of 10 or 20 seconds. In previous studies, we used ramp times between 5-10 seconds to avoid any vasodilation due to metabolites (16,22). This should not be a concern during maximal vasodilation, and figure 5.4b shows that P_{zf} only slightly decreased with ramp times up to 20 seconds. Extended ramp times were necessary during maximal vasodilation because under these conditions, the two-compartment model predicts only a slow fall in P_{zf} with longer ramp times. This might be interpreted as a plateau in the P_{zf} versus ramp time relationship if the plot is limited to 10 seconds. However, the longer ramp times used show that the predicted P_{zf} from the two-compartment model continues to decline and underestimates the observed P_{zf}, whereas the vascular waterfall model accurately predicts the plateau in the relationship.

The mean values for P_{crit}, R_a, and R_v for the five animals studied (n=4 for R_v) are shown in figure 5.5.

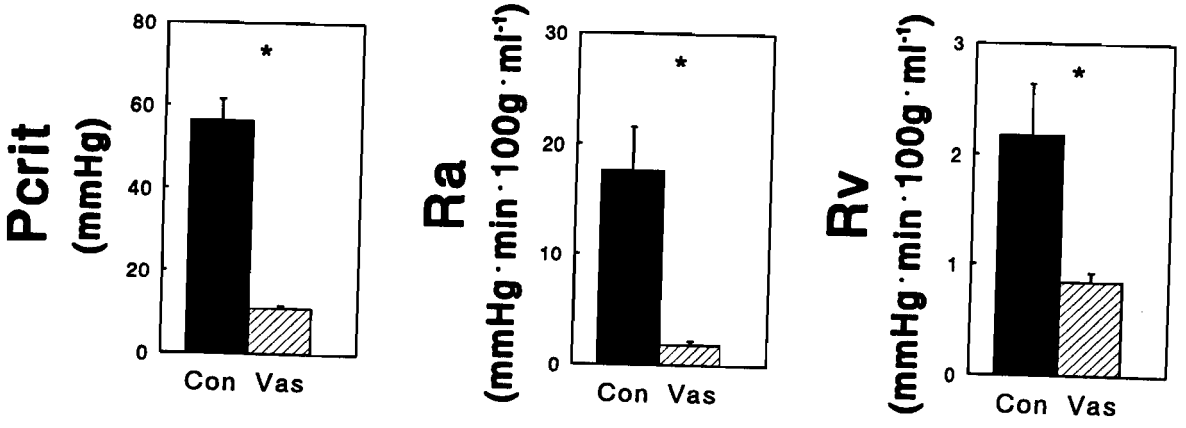

Figure 5.5: Values of waterfall pressure (P_{crit}), arterial resistance (R_a), and venous resistance (R_v) under control (Con) and vasodilated (Vas)

conditions. There was a significant decrease in all variables with vasodilation ($p<0.001$ for P_{crit}, $p<0.02$ for R_a, and $p<0.05$ for R_v).

Maximal vasodilation decreased P_{crit} from 56.4±5.1 to 11.0±0.6 mmHg ($p<0.001$), decreased R_a from 17.6±3.9 to 1.8±0.3 mmHg·min·100g·ml^{-1} ($p<0.02$), and decreased R_v from 2.2±0.5 to 0.8±0.1 mmHg·min·100g·ml^{-1} ($p<0.05$).

In order to determine if the vascular waterfall is upstream or downstream from the venous compliant region, we performed a double occlusion when the inflow reached zero during runs greater than 5 seconds. These venous plateau pressures represent the pressure in the venous compliant region after it has partially discharged and were recorded as P_{el2}. Table 5.1 shows P_v and P_{el} prior to the ramp down, as well as P_{crit} and P_{el2} for the four animals in which it was studied. Since P_{el2} was always less than P_{crit}, the venous compliant region must have been downstream from P_{crit}. However, P_{el} was always greater than P_{crit} indicating that downstream pressure was greater than P_{crit} when the hindlimb was perfused at close to normal perfusion pressures.

Experiment	Maximal Vasodilation			
	P_v	P_{el}	P_{crit}	P_{el2}
910925	1.6	20.0	11.3	6.7
911002	3.6	20.9	9.0	7.0
911004	0.8	18.5	11.1	3.4
911126	-0.1	18.5	10.7	7.5

Table 5.1: Comparison of venous pressure (P_v), small venule pressure during normal flow (P_{el}), the waterfall pressure (P_{crit}), and the small venule pressure at the time P_{crit} is measured (P_{el2}) during the maximally vasodilated condition.

Figure 5.6 shows the effect of raising P_v on P_{per} in the three animals studied (Protocol 2). Perfusion pressure increased with the first increase in P_v in two animals, and after the second increase in the third animal. The lack of an immediate response in the third animal was due to a single point, and is within the limits of experimental error.

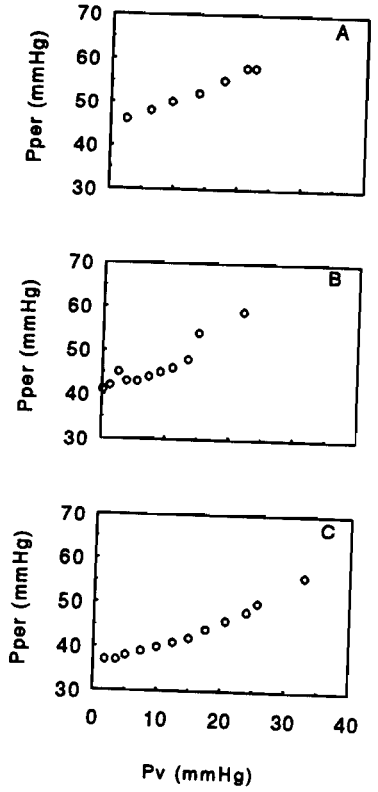

Figure 5.6: Perfusion pressure (P_{per}) is plotted against venous pressure (P_v) for the three animals in which it was studied (vasodilated conditions only). P_{per} is immediately affected by increases in P_v. Although there is no apparent increase in P_{per} for the first increase in P_v in C, this is within the limits of experimental error.

Figure 5.7a is a plot of P_{crit} values obtained at their respective P_{per} for all animals before and after maximal vasodilation. The solid lines represent the equations derived from the mean of the slopes and intercepts of the individual animals. In each

animal there was a linear relationship between P_{crit} and P_{per} (r values ranged from 0.87-0.99). The slopes are significantly different from each other ($p<0.01$).

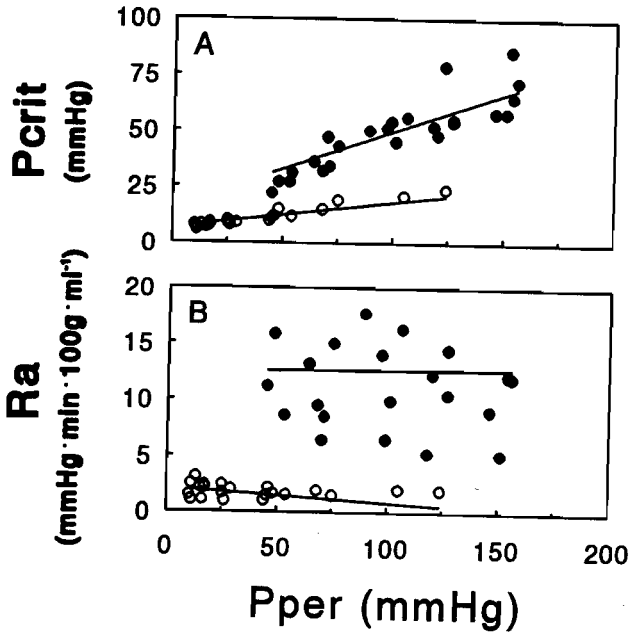

Figure 5.7: In A, P_{crit} is plotted against P_{per} for the five animals in which it was studied. All data points are plotted for control (●) and vasodilated (O) conditions. The equation for the solid lines are derived from the means of the slopes and intercepts of individual animals. The slopes are significantly different from each other and from zero ($p<0.01$). In B, R_a is plotted against P_{per}. Neither slope is significantly different from zero ($p>0.5$).

Figure 5.7b shows the same relationship for arterial resistance. Individual relationships were mostly linear (r values ranged from 0.77-0.99 in 7/10 experiments and 0.54, 0.38, and 0.25 in the remaining three). The slope of the R_a/P_{per} relationship

for individual animals was positive in 4/10 experiments, and negative in 6/10 experiments. The mean of the slopes was not different from zero ($p > 0.5$).

Figure 5.8 is the same as figure 5.7 except the conditions are pre and post indomethacin infusion ($n=6$). There was no significant difference between the two conditions for either variable. The results for R_a suggest a decreased variability after indomethacin. This is due to an unusually high resistance that was present in two dogs during control conditions.

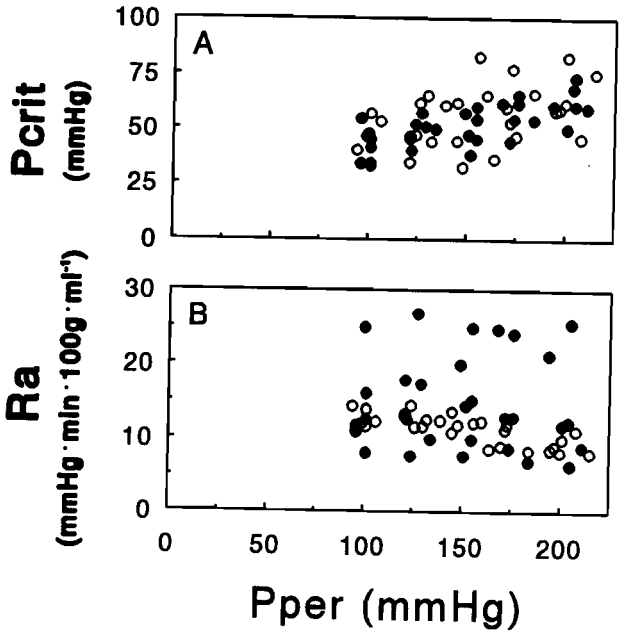

Figure 5.8: The relationship between P_{crit} and P_{per}, and between R_a and P_{per} are shown before (●) and after (O) indomethacin. There was no significant difference between the two conditions ($p > 0.5$).

5.5. DISCUSSION

We found that under the appropriate experimental conditions, an arterial P_{crit} can be observed during maximal vasodilation, but it is less than the elastic recoil pressure of the downstream compliant region and therefore not affect flow when the vascular bed is perfused at normal perfusion pressures. Increases in P_{per} under maximally vasodilated conditions still results in increases in P_{crit} whereas R_a is unaffected. This suggests that myogenic tone is still operative at the site of P_{crit}. Finally, prostaglandins do not affect P_{crit} or R_a in the canine hindlimb under normal conditions. Before discussing these results in detail, some technical considerations have to be discussed.

Technical Considerations:

Complete hindlimb isolation is necessary to obtain accurate values of P_{crit} (12). When pump flow is decreased, the perfusion pressure measured at the femoral artery declines. Any collateral vessels which bypass the hindlimb isolation would continue to maintain flow and pressure distally even when flow through the flow probe stops, thus resulting in an artificially high P_{crit}. As discussed in the Methods section, we used the double occlusion technique (17) and did not proceed unless isolation was confirmed.

Changes in resistance and P_{crit} have been studied with steady-state pressure-flow relations (1,6). However, under control conditions, steady-state measurements are of limited value because P_{crit} is tone-dependent and would therefore be affected by any autoregulatory mechanisms that might occur (7,16). Since P_{crit} increased with increasing P_{per}, our results indicate this is also true for maximally vasodilated conditions. Therefore, P_{crit} must be measured with dynamic pressure-flow relations. Although compliance may affect the measurement of P_{crit} if the flow is decreased too rapidly, this effect is negligible for ramp times greater than 5 seconds (16,22).

In order to fully dilate the hindlimb, we used sodium nitroprusside to activate the cGMP pathway, adenosine to activate the cAMP pathway, and indomethacin to block prostaglandin-mediated effects. We defined maximal vasodilation by the absence of reactive hyperemia. Björnberg et al (4) showed that a 20 second occlusion resulted in maximal vasodilation whereas longer occlusions affected only the duration of vasodilation. Therefore, we only continued the experiment if there was no reactive hyperemia after 30-60 seconds of complete ischemia. Furthermore, there was no further vasodilation even when we doubled the infusion rate after reactive hyperemia was abolished.

P_{crit} and Vasodilation

As shown in figure 5.4a, the two-compliant model alone failed to predict P_{zf} when ramp time to zero-flow was varied under control or maximally vasodilated conditions. However, when a vascular waterfall was incorporated into the model (figure 5.4b), the data were well predicted. This implies that a vascular waterfall was operating even after reactive hyperemia was abolished. As discussed in the methods section, P_{crit} is equal to the average zero-flow pressure intercept for ramp times greater than 5 seconds.

To determine if the vessels responsible for P_{crit} during maximal vasodilation were still arteriolar as previously shown under control conditions (16), we measured the pressure in the venous compliant region by the double occlusion method (17). The value of P_{crit} (11.0 ± 0.6 mmHg) was below P_{el} (19.5 ± 0.6 mmHg) which might suggest that P_{crit} is downstream from this region (i.e. in the venous circulation). Indeed, this was the conclusion of Braakman et al. who found that P_{per} declined to 8.9 mmHg if an arterial occlusion was maintained for one minute (7). However, in our experimental approach, and that of Braakman et al.'s, venous outflow continues while the arterial inflow is decreased to zero. Therefore, P_{el} declines during the measurement of P_{crit} and may be less than P_{crit} when arterial inflow is zero. Indeed, when we measured the

elastic recoil pressure at zero-flow (P_{el2}) by clamping venous outflow as soon as arterial inflow reached zero, P_{el2} was always less than P_{crit}. Therefore, the small venules must be downstream from the waterfall.

If a vascular waterfall is present, then increases in P_v should not affect P_{per} under constant flow conditions until the downstream pressure becomes greater than P_{crit}. This has been confirmed previously in the hindlimb (16), heart (11), lung (21), and liver (18) under normal tone conditions. However, when the hindlimb was maximally vasodilated, the downstream pressure (P_{el}) during normal flow was greater than P_{crit}, suggesting waterfall behaviour would not occur. The results of protocol 2 support this hypothesis in that small increases in venous pressure had an immediate effect on P_{per} under maximally vasodilated conditions (figure 5.6). Even though the waterfall is inactive during perfusion at normal pressures, P_{crit} can still be measured if the intravascular pressure is decreased below the residual tone of the arteriolar vessels, as shown by the plateau in figure 5.4.

If the waterfall is not active during normal flow, equation 5.1 should not be able to predict the relationship between P_{zf} and ramp time (figure 5.4). In fact, P_{zf} at ramp times less than 1 second were consistently less than predicted by the model for the vasodilated condition, but not for the control condition. Since our equation assumes the waterfall present at the end of the dynamic pressure-flow relation is also operative at the beginning, the P_{zf} with ramp times of 1 second are calculated based on the presence of a vascular waterfall. In the vasodilated hindlimb, the waterfall is inactive at the beginning of the run due to the high downstream pressure. The pressure drop during sudden occlusions is therefore greater than the equation predicts, and P_{zf} for ramp times under 1 second are overestimated by the equation. This does not occur under control conditions because the waterfall is always active.

R_a, R_v, and C_a

Under control conditions, R_a is calculated as $(P_{per}-P_{crit})/\dot{Q}$. During vasodilation however, there is no longer an active P_{crit} during normal P_{per}. In order to see how vasodilation affected the segment representing R_a under control conditions, one needs to know the intravascular pressure at the waterfall. The P_{crit} obtained under vasodilated conditions is less than the actual intravascular pressure at this site during normal flow since the waterfall is not active. Therefore, the pressure drop across the segment is exaggerated in our calculations, and the calculated resistance of 1.8 ± 0.3 mmHg·min·100g·ml^{-1} is an overestimation for the segment referred to under control conditions. On the other hand, the intravascular pressure at the waterfall during normal flow must be greater than the downstream pressure, P_{el}. R_a calculated using P_{el} as the downstream pressure (i.e. underestimating the pressure drop and R_a) is 1.2 ± 0.3 mmHg ·min·100g·ml^{-1}. Therefore, arterial resistance decreased to a value between 6.8% and 10.2% of its control value.

R_v also decreased with vasodilator drugs, but not as much as R_a. Under control conditions, R_v is approximately $8.4\pm0.9\%$ of R_{tot} but does not affect flow into the region because it is downstream from P_{crit}. With maximal vasodilation however, R_v was 43.3% R_{tot} and contributed significantly to overall resistance. Since flow increased, and the resistance downstream from P_{el} increased as a percentage of R_{tot}, P_{el} should have increased. Indeed, P_{el} increased from 11.5 ± 1.6 mmHg under control conditions to 19.5 ± 0.6 mmHg under vasodilated conditions despite the lower perfusion pressures ($p<0.05$). This implies an increase in capillary pressure and an increase in filtration forces.

The Myogenic Response

In protocol 3, we increased P_{per} and observed an increase in P_{crit} under control conditions. When we repeated the protocol with the hindlimb vasodilated, P_{crit} again

increased but the slope of the relationship was less. In the control condition, the change in P_{crit} is due to the interaction of vasoconstricting (myogenic, removal of metabolites) and vasodilating (endothelial-derived relaxing factor, EDRF) factors. In the vasodilated condition, metabolic and EDRF pathways should be abolished, leaving only myogenic mechanisms to affect P_{crit}. Our results suggest two conclusions. First, maximal vasodilation does not abolish the myogenic response of P_{crit}. Second, the change in the slope of the relationship during vasodilation (change in gain) means the myogenic response is affected by either cAMP or cGMP levels or both, but is not dependent on them.

The effect of increased P_{per} on R_a is also due to the interaction of vasoconstricting and vasodilating factors. In contrast to our previous findings that R_a decreases with increases in P_{per} under both control and vasoconstricted conditions (25), the present results did not show any effect of P_{per} on R_a (figure 5.7b). The difference is most likely because a higher range of P_{per} was used in the previous work. There was no significant effect in the previous study over the pressure range 75-150 mmHg.

Since P_{crit} is affected by P_{per} under maximally vasodilated conditions, occlusions of 30-60 seconds might cause myogenic relaxation and hence, "reactive hyperemia". This was not observed because P_{crit} is less than the downstream pressure during normal flow. Under the conditions of an inactive waterfall, flow is determined by the total resistance (R_a+R_v) of the circuit. Since total resistance did not change with changes in P_{per}, reactive hyperemia was not present.

Finally, indomethacin did not affect P_{crit} or R_a in our preparation. Therefore, the results during vasodilation are due to the combination of adenosine and nitroprusside, and are not due to prostaglandins. Prostaglandins have previously been shown to affect the myogenic response in rat cremasteric muscle (13). These differing results may represent species or regional differences.

In conclusion, maximal vasodilation decreases P_{crit} to a value below the downstream venous pressure. This eliminates the vascular waterfall effect and flow becomes dependent on the arterial-venous pressure difference divided by the resistance between the two. However arteriolar tone is still present and responds to changes in P_{per}. A vascular waterfall can still become active if the intravascular pressure is reduced sufficiently.

5.6. REFERENCES

1. Ashton, H. Critical closing pressure in human peripheral vascular beds. *Clin. Sci.* 22: 79-87, 1962.

2. Aversano, T., F.J. Klocke, R.E. Mates, and J.M. Canty,Jr.. Preload-induced alterations in capacitance-free diastolic pressure-flow relationships. *Am. J. Physiol.* 246: H410-H417, 1984.

3. Bellamy, R.F. Diastolic coronary artery pressure-flow relations in the dog. *Circ. Res.* 43(1): 92-101, 1978.

4. Björnberg, J., U. Albert, and S. Mellander. Resistance responses in proximal arterial vessels, arterioles and veins during reactive hyperaemia in skeletal muscle and their underlying regulatory mechanisms. *Acta Physiol. Scand.* 139: 535-550, 1990.

5. Björnberg, J., P.-O. Grände, M. Maspers, and S. Mellander. Site of autoregulatory reactions in the vascular bed of cat skeletal muscle as determined with a new technique for segmental vascular resistance recordings. *Acta Physiol. Scand.* 133: 199-210, 1988.

6. Braakman, R., P. Sipkema, and N. Westerhof. Pressure-flow relationships of the canine iliac periphery and systemic hemodynamics: Effects of sodium nitroprusside and adenosine. *Pflügers Arch.* 407: 432-439, 1986.

7. Braakman, R., P. Sipkema, and N. Westerhof. Two zero-flow pressure intercepts exist in autoregulating isolated skeletal muscle. *Am. J. Physiol.* 258: H1806-H1814, 1990.

8. Burton, A.C. On the physical equilibrium of small blood vessels. *Am. J. Physiol.* 164: 319-329, 1951.

9. Duomarco, J.L. and R. Rimini. Energy and hydraulic gradients along systemic veins. *Am. J. Physiol.* 178: 215-219, 1954.

10. Eng, C., J.H. Jentzer, and E.S. Kirk. The effects of the coronary capacitance on the interpretation of diastolic pressure-flow relationships. *Circ. Res.* 50: 334-341, 1982.

11. Farhi, E.R., F.J. Klocke, R.E. Mates, K. Kumar, R.M. Judd, J.M. Canty,Jr., S. Satoh, and B. Sekovski. Tone-dependent waterfall behaviour during venous pressure elevation in isolated canine hearts. *Circ. Res.* 68: 392-401, 1991.

12. Green, H.D., C.E. Rapela and M.C. Conrad. Resistance (conductance) and capacitance phenomena in terminal vascular beds. In: *Handbook of Physiology. Circulation. Section 2, Volume II*, Washington, D.C.: American Physiological Society, 1963, p. 935-960.

13. Hill, M.A., M.J. Davis, and G.A. Meininger. Cyclooxygenase inhibition potentiates myogenic activity in skeletal muscle arterioles. *Am. J. Physiol.* 258: H127-H133, 1990.

14. Holtz, J., U. Förstermann, U. Pohl, M. Giesler, and E. Bassenge. Flow-dependant, endothelium-mediated dilation of epicardial coronary arteries in conscious dogs: Effects of cyclooxygenase inhibition. *J. Cardiovasc. Pharmacol.* 6: 1161-1169, 1984.

15. Johnson, P.C. Autoregulatory responses of cat mesenteric arterioles measured in vivo. *Circ. Res.* 22: 199-212, 1968.

16. Magder, S. Starling resistor versus compliance. Which explains the zero-flow pressure of a dynamic arterial pressure-flow relation? *Circ. Res.* 67: 209-220, 1990.

17. Magder, S. Vascular mechanics of venous drainage in dog hindlimbs. *Am. J. Physiol.* 259: H1789-H1795, 1990.

18. Mitzner, W. Hepatic outflow resistance, sinusoid pressure, and the vascular waterfall. *Am. J. Physiol.* 227: 513-519, 1974.

19. Nichol, J., F. Girling, W. Jerrard, E.B. Claxton, and A.C. Burton. Fundamental instability of the small blood vessels and critical closing pressures in vascular beds. *Am. J. Physiol.* 164: 330-344, 1951.

20. Permutt, S. and R.L. Riley. Hemodynamics of collapsible vessels with tone: the vascular waterfall. *J. Appl. Physiol.* 18(5): 924-932, 1963.

21. Rock, P., G.A. Patterson, S. Permutt, and J.T. Sylvester. Nature and distribution of vascular resistance in hypoxic pig lungs. *J. Appl. Physiol.* 59: 1891-1901, 1985.

22. Shrier, I., S.N.A. Hussain, and S. Magder. Effect of carotid sinus stimulation on resistance and critical closing pressure of the canine hindlimb. *Am. J. Physiol.* 1992.(In Press)

23. Spaan, J.A.E. Coronary diastolic pressure-flow relation and zero flow pressure explained on the basis of intramyocardial compliance. *Circ. Res.* 56: 293-309, 1985.

24. Van Huis, G.A., P. Sipkema, and N. Westerhof. Instantaneous and steady-state pressure-flow relations of the coronary system in the canine beating heart. *Cardiovasc. Res.* 19: 121-131, 1985.

25. Vanelli, G., I. Shrier, and S. Magder. Critical closing pressure and arterial resistance have opposing responses to increases in perfusion pressure. *FASEB J.* 6(4): A1472, 1992.(Abstract)

CHAPTER 6

THE EFFECTS OF NIFEDIPINE ON THE VASCULAR WATERFALL AND ARTERIAL RESISTANCE IN THE CANINE HINDLIMB

6.1. ABSTRACT

Pressure-flow relations in the canine hindlimb are well explained by a vascular waterfall at the arteriolar level. Under these conditions, $P_a = P_{crit} + \dot{Q} * R_a$, where P_a is the arterial pressure, P_{crit} is the waterfall pressure, $\dot{Q}$ is regional blood flow, and R_a is the arterial resistance of the vessels upstream from the waterfall. To determine whether nifedipine affects P_{crit} in addition to R_a, we pump-perfused canine hindlimbs and measured both variables over a range of perfusion pressures (P_{per}) before (50 to 150 mmHg) and after (25 to 100 mmHg) nifedipine infusion. Nifedipine significantly decreased P_{crit} and R_a at P_{per}=75 mmHg ($p<0.01$). Increasing P_{per} under control conditions increased P_{crit} from 24.2 ± 1.5 to 42.5 ± 2.2 mmHg ($p<0.001$). During nifedipine infusion, increasing P_{per} still increased P_{crit} from 14.5 ± 1.5 to 20.2 ± 1.9 mmHg ($p<0.001$), but the rate of increase was less ($p<0.001$). In contrast to the rise in P_{crit} with increasing P_{per}, R_a decreased from 10.7 ± 1.1 to 8.1 ± 1.2 mmHg·min·100g·ml^{-1} before nifedipine infusion, and from 5.7 ± 0.4 to 2.2 ± 0.1 mmHg·min·100g·ml^{-1} after nifedipine infusion ($p<0.01$). These results suggest that nifedipine decreases the waterfall pressure and also decreases the resistance of the more proximal vessels. Nifedipine also affects the response of both variables to increasing P_{per}.

6.2. INTRODUCTION

Traditionally, arterial pressure is said to be determined by the product of cardiac output and total vascular resistance. This is based on Poiseuille's Law which states that flow is proportional to the pressure drop across a tube. Theoretically, pressure-lowering agents such as nifedipine, may act along any segment of the vasculature to decrease total resistance. More recently however, investigators have shown that a vascular waterfall exists in several vascular beds (7,17,19). Under these conditions, Poiseuille's Law cannot be applied across the *entire* vascular bed and pressure-flow relationships are governed by the same physics that apply to a natural waterfall. In nature, flow over a waterfall is not determined by the difference in height between the upstream lake and the river downstream from the waterfall, but instead, flow is dependent on the difference in altitude between the upstream lake and the top of the waterfall, as well as the resistance in the river between the two. It is important to note that flow is not affected by the actual height of the falls nor by the resistance to flow in the river below the falls. Similarly, when a vascular waterfall is present, flow is determined by the difference between arterial pressure and the pressure at the waterfall (critical pressure, P_{crit}), divided by the resistance between the two as determined by Poiseuille's Law (arterial resistance, R_a) (24). The vascular waterfall can also be considered a back pressure to flow and is presumed to be due to a Starling resistor-like mechanism created by the force of the constricting smooth muscle at the arteriolar level. The tone-dependent nature of the waterfall is supported by experiments showing that it is affected by both vasoactive drugs (5) and the carotid sinus baroreflex (27).

If a vascular waterfall is present, arterial pressure can be controlled by changes in either P_{crit} or R_a. The goal of the present study was to determine the effect of the commonly used calcium channel blocker nifedipine, on both these variables, as well as the downstream venous resistance.

We have previously found that P_{crit} increases with increases in P_{per} (33), which most likely reflects an increase in smooth muscle tone in response to increased transmural pressure (i.e. a myogenic response (13)). It has been suggested that the myogenic response may be due to increased calcium entry (20), and we therefore hypothesized that nifedipine would block the increase in P_{crit} with increasing P_{per}.

The method of estimating P_{crit} is essential to our experiment, and is based on our previous work (17,27). Briefly, flow will stop when the perfusion pressure is lowered below the waterfall pressure. Therefore, the pressure at zero-flow should reflect P_{crit}. However, if arterial pressure is rapidly decreased, the discharging arterial compliance can cause an artificially high pressure at zero flow (2,17,29). On the other hand, if the arterial pressure is decreased too slowly, vasodilation from the myogenic response (12), or from the release of metabolic factors (3), could produce an artificially low P_{crit}. Finally, it should be noted that P_{crit} is the pressure when flow ceases, even though arterial pressure continues to decline if the occlusion is maintained (17). This is because the volume above the waterfall can escape through channels which bypass the vascular waterfall. If only 1.5% of the total conductance goes through these channels, P_{crit} will be significantly underestimated if the final arterial pressure is used instead of the actual pressure when zero flow occurs (17).

Problems in estimating P_{crit} can be avoided by ramping the inflow down to zero with times to zero flow of 4-10 sec (17). Under these conditions, the arterial capacitance has time to fully discharge and therefore has a negligible effect on P_{crit} (2,17). Second, the ramp period needs to be short enough so that metabolic (3) and myogenic (12) factors do not have enough time to cause vasodilation. Finally, the ramp method keeps the bypass channels filled and prevents the loss of pressure observed with sudden occlusions. Therefore, by decreasing flow to zero over 5-10

seconds, we can approximate the back pressure at the waterfall. R_a is then calculated as P_{per}-$P_{crit}/\dot{Q}$, where P_{per} is perfusion pressure and $\dot{Q}$ is inflow into the region.

6.3. METHODS

Six dogs weighing 18-24 kg were anaesthetized with α-chloralose (75 mg·kg^{-1}) after initial induction with sodium pentothal (1 mg·kg^{-1}). Supplemental doses of α-chloralose were given as needed. The animals were intubated, ventilated (Harvard Apparatus), and given supplemental oxygen to maintain PO_2 greater than 100 mmHg. We cannulated the left carotid artery to monitor arterial blood pressure (P_a) and to obtain arterial blood samples. Normal saline was infused into the left jugular vein to maintain proper hydration and sodium bicarbonate was given to maintain acid-base balance. Heparin (10,000 unit bolus) was given to prevent blood clotting.

Surgical Preparation

The vascular supply to the left hindlimb was isolated as in previous studies (17,33) (figure 6.1). We tied all branches of the femoral artery and vein in the femoral triangle. Blood flow was diverted from the proximal end of the left femoral artery, through an in-line electromagnetic flow probe (Carolina Medical #10), and back into the distal end of the left femoral artery. A side port placed downstream from the flow probe was used to measure the pressure perfusing the limb (P_{per}). We placed two side ports upstream from the flow probe so that blood flow could be diverted through a pump (Masterflex #16 tubing) and controlled by clamping the direct line and adjusting the pump speed. A third side port was placed between the pump and the flow probe for infusion of nifedipine. We cannulated the left femoral vein and allowed the blood to flow into a reservoir. A Y-connector on the venous tubing had one end open to atmosphere, and therefore created a waterfall to control venous pressure (P_v).

Reservoir blood was returned to the animal via the right jugular vein. P_v was measured from a side port close to the cannulation site.

We passed surgical wires through the proximal thigh with a 14 gauge needle. The wires were tied securely around either side of the femur to eliminate any collateral flow. A simultaneous occlusion of hindlimb inflow and outflow (double occlusion) was performed to ensure that isolation was maintained (17,18). A continuous rise in venous pressure implies that arterial inflow still exists and a continuous decrease in venous pressure implies that venous outflow exists. If either case was observed, the surgical wires were tightened and another double occlusion performed. We continued the experiment only after complete isolation was obtained. Isolation was rechecked before and after each protocol. The pressure at which the venous pressure plateaus is also the pressure of the compliant region of the vascular bed (elastic recoil pressure, P_{el}), and is used as the upstream pressure in the calculation of venous resistance (R_v) (18).

In preliminary experiments, infusion of 10^{-7} M nifedipine into the femoral artery had no effect on P_a. However, femoral arterial infusion of 10^{-6} M nifedipine caused a significant decrease in P_a due to recirculation of the blood. We therefore maintained P_a constant during 10^{-6} M infusion by connecting a large Dextran-filled reservoir suspended from the ceiling, to the right femoral artery. Under these conditions, the height of the fluid in the reservoir determined P_a.

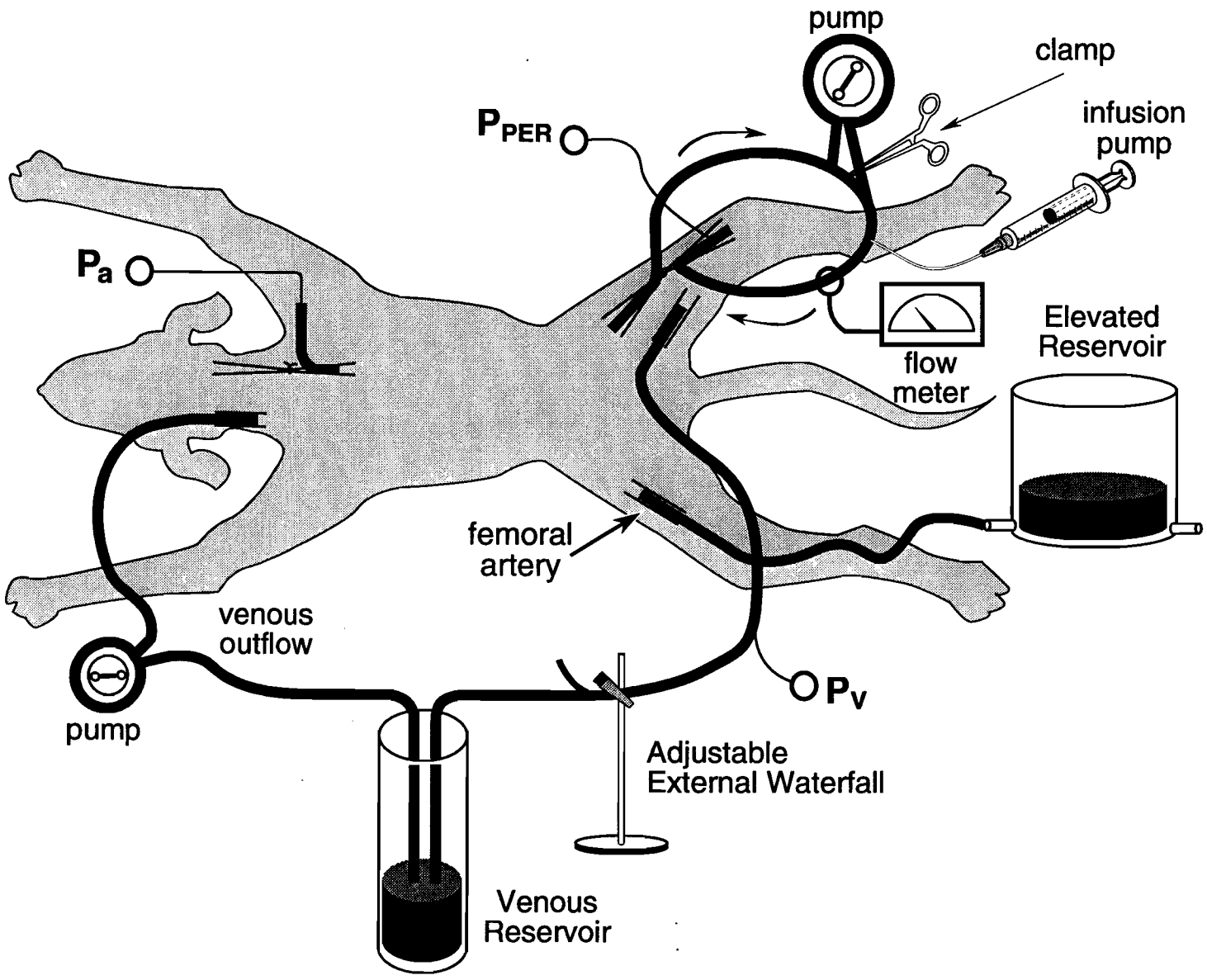

Figure 6.1: Experimental Setup

Measurements

Pressures were measured with Trantec transducers. We measured flow ($\dot{Q}$) using a Carolina Medical electromagnetic flow meter and an in-line probe. Signals were filtered at 3 Hz. All signals were processed through Gould amplifiers and simultaneously recorded on an eight-channel Graphtec recorder and on an IBM compatible computer using CODAS software program (DATAQ Instruments Inc.) for A-D conversion. Analysis was performed using the Codas and Anadat (RHT-Infodat Inc.) software programs.

Drug Concentrations

Nifedipine was first dissolved in acetone, and then diluted to a concentration of 10^{-5} M with saline. The solution was protected from light with silver foil, and infused into the femoral artery at 1/100 of the flow rate (blood concentration of 10^{-7} M). In preliminary experiments, femoral perfusion pressure during constant flow decreased from 125 mmHg to 60 mmHg with 10^{-7} M nifedipine. This dose of nifedipine decreases reactive hyperemia substantially, but does not eliminate it. The infusion rate was changed each time the pump flow to the hindlimb was changed so that nifedipine blood concentration was constant at 10^{-7} M. In three dogs, we infused a solution of 10^{-4} M nifedipine at 1/100 the flow rate (10^{-6} M blood concentration). There was no further drop in P_{per} at this dose and reactive hyperemia was still present.

Protocol

We used a protocol similar to our previous study (33). Briefly, the pump flow rate was initially set at a P_{per} between 50 and 150 mmHg. Pump flow was then manually turned down to zero over a ramp-time period ranging from 5-10 seconds to obtain P_{crit}. Two measurements were obtained at this perfusion pressure. We then changed P_{per} to a different value, and again decreased pump flow to zero in two separate runs. We measured P_{crit} at perfusion pressures of 50, 75, 100, 125, and 150

mmHg in random order. The procedure was then repeated during nifedipine infusion. Following nifedipine-induced vasodilation, the maximal capacity of the pump (approximately 500 ml·min^{-1}) could not generate pressures above 100 mmHg in the majority of animals. The perfusion pressures studied during nifedipine infusion were therefore 25, 50, 75, and 100 mmHg. In three animals, we then increased the nifedipine concentration to 10^{-6} M blood concentration, waited 30 minutes for the preparation to stabilize, and repeated the protocol.

At the end of the experiment, the hindlimb was amputated at the level of the surgical wires and weighed. Flow and resistance are expressed per 100 g of hindlimb.

Data Analysis

Mean P_a, P_{per}, P_v and $\dot{Q}$ were obtained before each zero-flow pressure measurement. Double occlusion venous plateau pressures before and after each series of measurements were averaged to obtain P_{el}.

In general, the relation between flow and P_{per} during a ramp to zero flow was linear. In a few experimental runs, a curvilinear phase convex to the pressure axis occurred at high flows. This was most likely due to passive stretching of the arterial walls, and has been noted by other authors (5,17). Occasionally, a curvilinear phase convex to the pressure axis occurred at low flows. Two possibilities may account for this. First, it is possible that reactive vasodilation occurred in response to the decreased flow or pressure, even though the time to zero-flow was less than ten seconds. Second, the rate of decrease in pump speed may have slowed as flow approached zero (due to human or mechanical factors). To avoid the influence of these factors and to be consistent with runs not exhibiting a curvilinear phase, we plotted the regression line for the linear phase, and used the calculated x-intercept as the zero-flow pressure intercept (17).

We have previously shown that if the ramp time to zero-flow is between 5-10 seconds, the zero-flow pressure intercept approximates P_{crit} under both control (17,27) and maximally vasodilated conditions (28). The two P_{crit} values obtained at each P_{per} were averaged. R_a was then calculated as $(P_{per}-P_{crit})/\dot{Q}$. The upstream pressure for venous return is the pressure in the most compliant region of the bed (P_{el}), and therefore R_v was calculated as $(P_{el}-P_v)/\dot{Q}$ (18).

Statistics

Changes in P_{crit}, R_a, R_v, and P_{el} over the range of perfusion pressures were analyzed with ANOVA for repeated measures. Comparisons between control and nifedipine conditions were analyzed using a paired t-test at P_{per} of 75 mmHg. In order to quantify the change in P_{crit} with changing P_{per}, we plotted all the data from all animals and calculated the least squares linear regression for the control data, and for the nifedipine data. The two regression lines were then compared to see if the slopes were different. A similar analysis was done for arterial resistance. Results were considered significant if $p<0.05$.

6.4. RESULTS

The PCO_2 was 37.3±5.0 mmHg (mean±S.D.) and PO_2 was 169±26 mmHg. Rectal temperature was 38.2±1.4 °C and hemoglobin was 13.7±2.3 $g \cdot dl^{-1}$. The $[H^+]$ was $4.47x10^{-8}\pm0.51x10^{-8}$ M (pH=7.35).

Figure 6.2a shows the steady-state relationship between flow and perfusion pressure before (●), and after (O) 10^{-7} M nifedipine infusion (n=6). In figure 6.2b, we plotted all the data from the three animals in which we infused both 10^{-7} M and 10^{-6} M nifedipine (n=3). There was no difference in the results with the two concentrations. This was also true when we compared the results for P_{crit}, R_a, and R_v (data not shown). Infusion of the vehicle (0.5% acetone for 10^{-7} M nifedipine and 5%

acetone for 10^{-6} M nifedipine) at 1/100 the flow rate did not affect P_{per} during constant flow conditions.

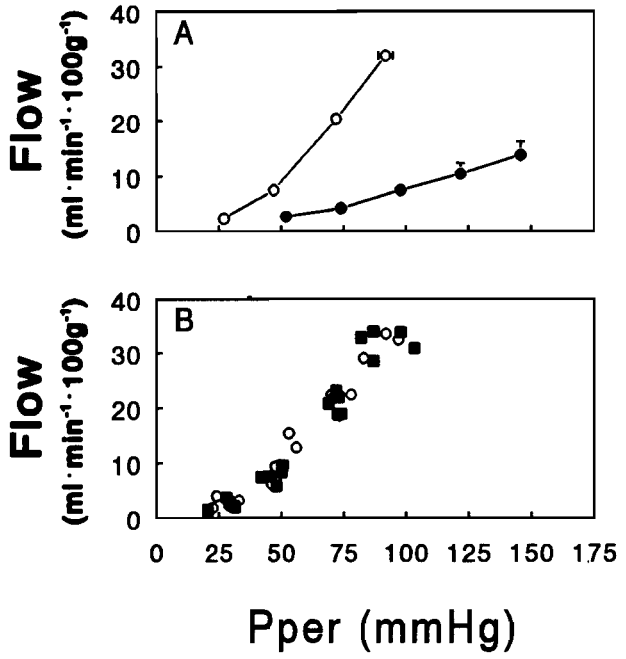

Figure 6.2: In A, flow is plotted against perfusion pressure (P_{per}) before (●) and after (O) nifedipine infusion. Results are mean±S.E.M. in both axes. In most cases, the error bars are two small to be seen. In B, we plotted the results from the three animals in which both 10^{-7} M (O) and 10^{-6} M (■) nifedipine were used. The results were identical under the two conditions.

In figure 6.3a, the changes in critical pressure (P_{crit}) and arterial resistance (R_a) are shown with increasing perfusion pressure, before (●) and after (O) nifedipine-induced vasodilation. Vasodilation significantly decreased P_{crit} at P_{per} of 75 mmHg ($p<0.01$). Before nifedipine infusion, P_{crit} increased from 24.2±1.5 to 42.5±2.2 mmHg when P_{per} was increased from 52±1 to 146±2 mmHg ($p<0.001$). After

nifedipine infusion, P_{crit} also increased with increasing P_{per} ($p<0.001$) but the rate of increase was less ($p<0.001$) as P_{crit} increased from 14.5 ± 1.5 mmHg at a perfusion pressure of 27 ± 2 mmHg, to only 20.2 ± 1.9 at P_{per} of 92 ± 3 mmHg.

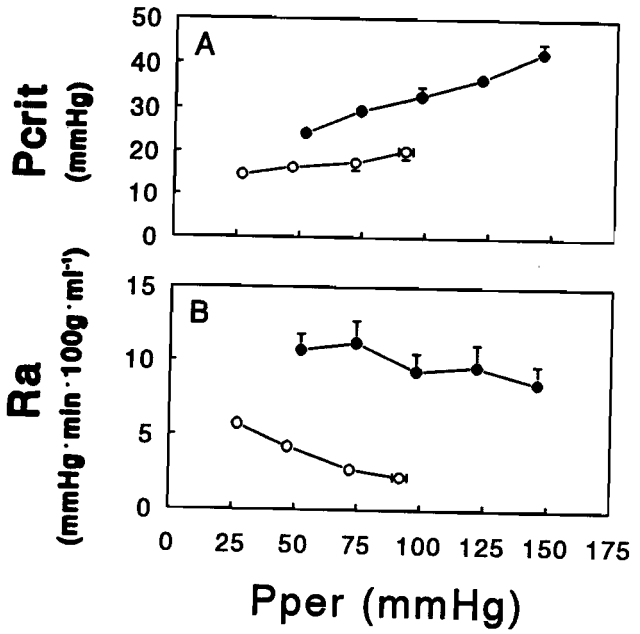

Figure 6.3: In A, the critical pressure (P_{crit}) is plotted against P_{per} for control (●) and 10^{-7} M nifedipine conditions (O). P_{crit} increased with increasing P_{per} under both conditions ($p<0.001$), but the rate of increase was less with nifedipine ($p<0.01$). In addition, the position of the curve was shifted downwards ($p<0.01$). In B, arterial resistance (R_a) is plotted against P_{per}. Under control conditions, there was a slight decrease in R_a at the highest P_{per} ($p<0.05$). During nifedipine infusion, the position of the curve was shifted downwards ($p<0.01$), and the rate of decrease in R_a was increased. Results are mean$\pm$S.E.M. in both axes. In most cases, the error bars are two small to be seen.

Figure 6.3b shows that R_a was also decreased at 75 mmHg perfusion pressure during nifedipine infusion ($p<0.01$). However, increasing P_{per} under control conditions caused a decrease in R_a from 10.7 ± 1.1 to 8.1 ± 1.2 mmHg·min·100g·ml^{-1} over the pressure range 52 to 146 mmHg ($p<0.01$). During nifedipine infusion, the decrease in R_a with increasing P_{per} was accentuated ($p<0.01$), and R_a decreased from 5.7 ± 0.4 to 2.2 ± 0.1 mmHg·min·100g·ml^{-1} over the pressure range of 27 to 92 mmHg ($p<0.001$).

In figure 6.4a, R_v is plotted against increasing P_{per}. Similar to R_a, R_v decreased with increasing P_{per}. However, the venous system is not exposed to the high pressures of the arterial system. In figure 6.4b, R_v is therefore plotted against the pressure in the venous compliant region (P_{el}) obtained by the double occlusion method (18).

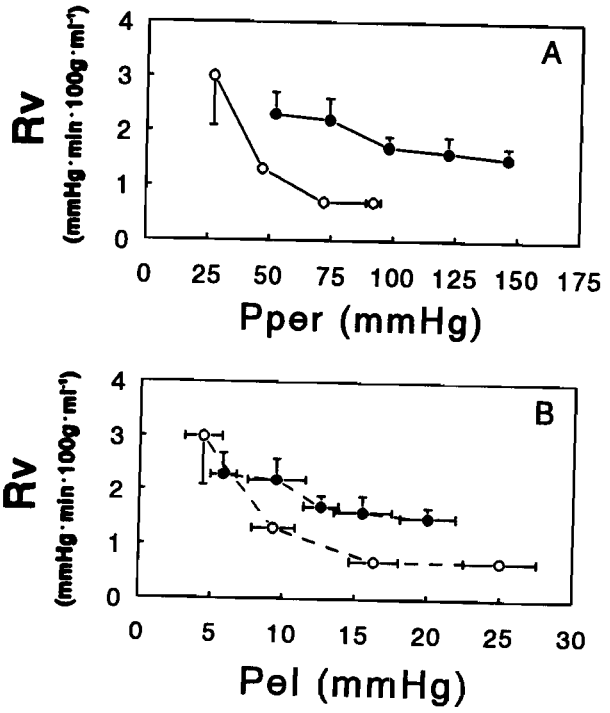

Figure 6.4: In A, venous resistance (R_v) is plotted against P_{per} for control (●) and 10^{-7} M nifedipine conditions (O). R_v was decreased after nifedipine infusion. R_v was constant at high P_{per}, but increased at low P_{per} both before and after nifedipine. In B, R_v is plotted against P_{el} for both

control (●) and 10^{-7} M nifedipine conditions (O). The curve is again shifted downward after nifedipine, and there is an increase in R_v at the lowest P_{el} ($p<0.05$). Results are mean±S.E.M.

Nifedipine decreased R_v at each P_{el} ranging from 7 to 25 mmHg. It should be noted that venous resistance decreases under both control and vasodilated conditions when P_{el} was increased from very low values.

Nifedipine decreased P_{crit}, R_a, and R_v. The overall effect on P_{el}, and presumably capillary pressure, is dependent on the interaction of these variables as is shown in figure 6.5. Nifedipine increased P_{el} at each P_{per}. P_{el} at P_{per}=75 mmHg during nifedipine infusion was still greater than P_{el} at P_{per}=100 mmHg during control conditions (16.3±1.7 mmHg versus 12.6±1.2 mmHg, $p<0.05$).

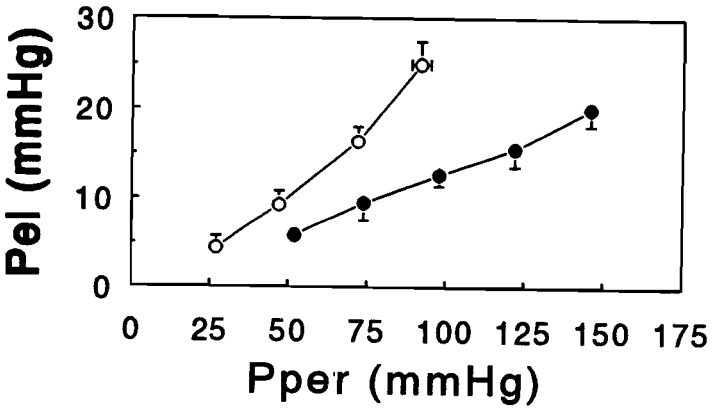

Figure 6.5: P_{el} (elastic recoil pressure) is plotted against increasing P_{per} for control (●) and 10^{-7} M nifedipine conditions (O). The P_{el} curve is shifted upward during nifedipine conditions ($p<0.05$). Results are mean±S.E.M.

6.5. DISCUSSION

We found that nifedipine decreases P_{crit} as well as arterial and venous resistance. In addition, the pressure in the compliant region of the vascular bed increased during nifedipine infusion. Nifedipine decreased the rise in P_{crit}, and increased the fall in R_a, with increases in P_{per}. R_v also declined as P_{per} was increased from low levels. Before discussing these results, some technical considerations must be considered.

Technical Considerations

Complete hindlimb isolation is necessary to obtain accurate values of P_{crit} (9). This is because any collateral circulation that allows inflow to the hindlimb when the pump flow is zero, will maintain microcirculatory flow even though flow through the flow probe has stopped. The P_{per} measured under these conditions will not represent a true "zero-flow pressure intercept", but will reflect the pressure drop across the collateral vessels, i.e. the pressure where the collateral vessels join with the femoral artery circulation. We confirmed hindlimb isolation from the systemic circulation by simultaneously occluding inflow and outflow to the limb (18), and did not continue the experiment unless isolation was confirmed.

Changes in resistance and critical pressure are usually studied with steady-state pressure-flow relations (1,4). However, steady-state measurements are of limited value since they include adjustments from autoregulatory mechanisms (22,30). When flow is decreased in steps, metabolic vasodilation may decrease the tone of the arterial vessels (3). In addition, the decrease in P_{per} could result in further vasodilation due to the myogenic response (12). These two effects might result in a decrease of P_{crit}. Therefore, the values from steady-state measurements might not reflect the instantaneous P_{crit} that exists at higher flows or higher pressures. If P_{crit} is unreliable, then resistance calculations [$R_a = (P_{per}-P_{crit})/\dot{Q}$] are also unreliable. In order to estimate P_{crit} at each P_{per}, we used the dynamic pressure-flow relation. Dynamic pressure-flow

relations, however, can be affected by vessel compliance (2,6,17). If inflow is instantaneously decreased to the value in the compliant region, the inflow pressure gradient decreases to zero. Therefore, flow measured proximally in the vessel ceases even though flow downstream from the compliant region continues, and an artificially high P_{crit} is recorded. This effect is minimized if the ramp time to zero-flow is long enough to allow the compliant region to empty. Compliance effects are negligible for ramp times greater than 5 seconds under both control and vasodilated conditions (17,27,28), and therefore the zero-flow pressure intercepts we measured (ramp times between 5-10 seconds) give good estimates of P_{crit} (17,27).

Finally, we used a dose of 10^{-7} M nifedipine to dilate the hindlimb. Since we did not observe any further vasodilation when the dose was increased to 10^{-6} M (figure 6.2b), this most likely represents the maximal dilating effect of nifedipine. It should be noted that this dose did not abolish reactive hyperemia, and therefore the hindlimb was not maximally vasodilated.

Nifedipine and Critical Pressures

The finding that nifedipine decreases the critical pressure at each P_{per} confirms that P_{crit} is dependent on smooth muscle tone (5,27). Furthermore, P_{crit} increased with increasing P_{per} both pre and post nifedipine.

When P_{per} was increased under control conditions, several factors which influence smooth muscle tone (and hence P_{crit}) were affected. First, the increase in P_{per} was accompanied by an increase in flow. This effect would tend to decrease tone through the release of endothelium-derived relaxing factor (EDRF) (23,25). On the other hand, the higher perfusion pressure should have increased tone through a myogenic stimulus to the vessels (13). A third factor might have been an increase in tone because the increased flow may have removed vasodilator metabolites, but this is not likely to be important in the resting hindlimb (8). Since P_{crit} increased when P_{per} is increased, one must conclude that the vessels responsible for P_{crit} were more sensitive

to the myogenic stimulus than to EDRF. This does not mean that EDRF had no effect on P_{crit} because the increase in P_{crit} might have been greater if EDRF were not present.

During nifedipine infusion, the response of P_{crit} to increasing P_{per} was blunted but not eliminated. It is unlikely that higher doses would have been more effective since there was no further decrease in P_{crit} when the dose of nifedipine was increased 10-fold. Others have also found that L-type voltage-gated calcium channels such as nifedipine do not abolish the myogenic response (10), even though the myogenic response is dependent on extracellular calcium (31,34). This suggests that L-type voltage-gated calcium channels modulate the myogenic response, but are not responsible for it. It should be noted that infusion of adenosine and nitroprusside also decreases the myogenic response of P_{crit}, but does not eliminate it (28). The mechanism by which P_{crit} increases in response to increasing P_{per} remains unknown.

Nifedipine and Arterial Resistance

Nifedipine decreased R_a at P_{per}=75 mmHg, in addition to its effect on P_{crit}. Therefore, the drug affects both small and large vessel tone. However, unlike the increase in P_{crit} observed with increasing P_{per}, R_a decreased with increasing P_{per}, and the decrease was accentuated after nifedipine infusion. This confirms our previous findings (33) and extends the observation to include nifedipine-induced vasodilation. Under control conditions, the decrease in R_a suggests that the effects of the increased vasodilating forces during increasing P_{per} (passive and endothelial-derived relaxing factor) is stronger than the effects of the increased vasoconstricting forces (metabolic and myogenic).

The exaggerated response of R_a during nifedipine infusion can be explained through a decrease in the myogenic response of the vessels responsible for R_a, similar to the decreased myogenic response observed for P_{crit} during nifedipine infusion. This would mean that the increased production of EDRF stimulated by the increased flow, would not be attenuated as much by the myogenic response, and the decrease in R_a

would be greater for each change in P_{per}. This type of reciprocal inhibition between EDRF and the myogenic response has previously been shown *in vitro* (16,25), and *in vivo* during direct recordings of microvascular diameters (15) and by pressure-flow relations (26).

Nifedipine and Venous Resistance

Nifedipine infusion lowered venous resistance at a P_{per} of 75 mmHg, supporting previous results that calcium channel blockers have an effect on the venous system (32). In addition, although R_v was constant at high P_{per}, it increased when P_{per} was lowered both before and after nifedipine infusion. These findings are consistent with studies by Johnson and Hanson (14), and Mellander et. al. (22). The mechanism by which R_v is increased at low P_{per} cannot be myogenic, since a myogenic reflex would have had the opposite effect. We have also previously found that R_v increases during inhibition of EDRF synthesis with L-nitro-arginine (see chapter 4) and is therefore not due to flow-mediated decreases in EDRF. The increased venous resistance may be due to passive collapse of the vessels or an increased apparent blood viscosity at low flows (11). This may be important in maintaining a relatively constant capillary pressure (11,21,22,35).

Clinical Relevance

A major side effect of nifedipine is peripheral edema. This could be due to a change in capillary permeability, but most likely represents an alteration in the capillary hydrostatic pressure. Our results show that nifedipine causes both arterial and venous vasodilation, and a reduction in P_{crit}. The overall effect on capillary pressure depends on whether inflow to the region, determined by $(P_{per}-P_{crit})/R_a$, increases more than outflow from the region, determined by $(P_{el}-P_v)/R_v$. Figure 6.4b shows that P_{el} was increased at each P_{per} during nifedipine infusion, indicating that the effect on inflow was greater than the effect on outflow, and therefore nifedipine increases the Starling

forces across the capillary wall. This will lead to an increase in transudation, and may explain the peripheral edema observed in patients.

In conclusion, nifedipine decreases arterial pressure through a decrease in both the vascular waterfall pressure and arterial resistance. Capillary pressure rises during nifedipine infusion because the effects on inflow due to a decreased P_{crit} and R_a are greater than the effects on outflow due to a decreased R_v.

6.6. REFERENCES

1. Ashton, H. Critical closing pressure in human peripheral vascular beds. *Clin. Sci.* 22: 79-87, 1962.

2. Aversano, T., F.J. Klocke, R.E. Mates, and J.M. Canty,Jr.. Preload-induced alterations in capacitance-free diastolic pressure-flow relationships. *Am. J. Physiol.* 246: H410-H417, 1984.

3. Björnberg, J., U. Albert, and S. Mellander. Resistance responses in proximal arterial vessels, arterioles and veins during reactive hyperaemia in skeletal muscle and their underlying regulatory mechanisms. *Acta Physiol. Scand.* 139: 535-550, 1990.

4. Braakman, R., P. Sipkema, and N. Westerhof. Pressure-flow relationships of the canine iliac periphery and systemic hemodynamics: Effects of sodium nitroprusside and adenosine. *Pflügers Arch.* 407: 432-439, 1986.

5. Braakman, R., P. Sipkema, and N. Westerhof. Two zero-flow pressure intercepts exist in autoregulating isolated skeletal muscle. *Am. J. Physiol.* 258: H1806-H1814, 1990.

6. Eng, C., J.H. Jentzer, and E.S. Kirk. The effects of the coronary capacitance on the interpretation of diastolic pressure-flow relationships. *Circ. Res.* 50: 334-341, 1982.

7. Farhi, E.R., F.J. Klocke, R.E. Mates, K. Kumar, R.M. Judd, J.M. Canty,Jr., S. Satoh, and B. Sekovski. Tone-dependent waterfall behaviour during venous pressure elevation in isolated canine hearts. *Circ. Res.* 68: 392-401, 1991.

8. Folkow, B. Intravascular pressure as a factor regulating the tone of the small vessels. *Acta Physiol. Scand.* 17: 289-310, 1949.

9. Green, H.D., C.E. Rapela and M.C. Conrad. Resistance (conductance) and capacitance phenomena in terminal vascular beds. In: *Handbook of Physiology. Circulation. Section 2, Volume II*, Washington, D.C.: American Physiological Society, 1963, p. 935-960.

10. Hayashi, K., M. Epstein, and R. Loutzenhiser. Enhanced myogenic responsiveness of renal interlobular arteries in spontaneously hypertensive rats. *Hypertension* 19: 153-160, 1992.

11. House, S.D. and P.C. Johnson. Microvascular pressure in venules of skeletal muscle during arterial pressure reduction. *Am. J. Physiol.* 250: H838-H845, 1986.

12. Johnson, P.C. Autoregulatory responses of cat mesenteric arterioles measured *in vivo*. *Circ. Res.* 22: 199-212, 1968.

13. Johnson, P.C. The myogenic response. In: *Handbook of Physiology. Section 2: The Cardiovascular System. Volume II. Vascular Smooth Muscle*, edited by D.F. Bohr, A.P. Somlyo and H.V. Sparks,Jr.. Bethesda, Maryland: American Physiological Society, 1980, p. 409-442.

14. Johnson, P.C. and K.M. Hanson. Effect of arterial pressure on arterial and venous resistance of intestine. *J. Appl. Physiol.* 17(3): 503-508, 1962.

15. Koller, A. and G. Kaley. Role of endothelium in reactive dilation of skeletal muscle arterioles. *Am. J. Physiol.* 259: H1313-H1316, 1990.

16. Kuo, L., W.M. Chilian, and M.J. Davis. Interaction of pressure- and flow-induced responses in porcine coronary resistance vessels. *Am. J. Physiol.* 261: H1706-H1715, 1991.

17. Magder, S. Starling resistor versus compliance. Which explains the zero-flow pressure of a dynamic arterial pressure-flow relation? *Circ. Res.* 67: 209-220, 1990.

18. Magder, S. Vascular mechanics of venous drainage in dog hindlimbs. *Am. J. Physiol.* 259: H1789-H1795, 1990.

19. Mayers, I. and D.H. Johnson. Vasodilators do not abolish pulmonary vascular critical closing pressure. *Respir. Physiol.* 81: 63-74, 1990.

20. Meininger, G.A. and J.E. Faber. Adrenergic facilitation of myogenic response in skeletal muscle arterioles. *Am. J. Physiol.* 260: H1424-H1432, 1991.

21. Mellander, S. and J. Björnberg. Regulation of vascular smooth muscle tone and capillary pressure. *N. I. P. S.* 7: 113-119, 1992.

22. Mellander, S., M. Maspers, J. Björnberg, and L.-O. Andersson. Autoregulation of capillary pressure and filtration in cat skeletal muscle in states of normal and reduced vascular tone. *Acta Physiol. Scand.* 129: 337-351, 1987.

23. Müggе, A., J.A.G. Lopez, D.J. Piegors, K.R. Breese, and D.D. Heistad. Acetylcholine-induced vasodilatation in rabbit hindlimb *in vivo* is not inhibited by analogues of L-arginine. *Am. J. Physiol.* 260: H242-H247, 1991.

24. Permutt, S. and R.L. Riley. Hemodynamics of collapsible vessels with tone: the vascular waterfall. *J. Appl. Physiol.* 18(5): 924-932, 1963.

25. Pohl, U., K. Herlan, A. Huang, and E. Bassenge. EDRF-mediated shear-induced dilation opposes myogenic vasoconstriction in small rabbit arteries. *Am. J. Physiol.* 261: H2016-H2023, 1991.

26. Randall, M.D. and C.R. Hiley. Detergent and methylene blue affect endothelium-dependent vasorelaxation and pressure/flow relations in rat blood perfused mesenteric arterial bed. *Br. J. Pharmacol.* 95: 1081-1088, 1988.

27. Shrier, I., S.N.A. Hussain, and S. Magder. Effect of carotid sinus stimulation on resistance and critical closing pressure of the canine hindlimb. *Am. J. Physiol.* 1992.(In Press)

28. Shrier, I. and S. Magder. A zero-flow pressure intercept still exists in the canine hindlimb during maximal vasodilation. *Clin. Invest. Med.* 15 (Suppl): A13, 1992.(Abstract)

29. Spaan, J.A.E. Coronary diastolic pressure-flow relation and zero flow pressure explained on the basis of intramyocardial compliance. *Circ. Res.* 56: 293-309, 1985.

30. Stainsby, W.N. and E.M. Renkin. Autoregulation of blood flow in resting skeletal muscle. *Am. J. Physiol.* 201(1): 117-122, 1961.

31. Urchida, E. and D.F. Bohr. Myogenic tone in isolated perfused resistance vessels from rats. *Am. J. Physiol.* 216: 1343-1350, 1969.

32. Van Nueten, J.M. and P.M. Vanhoutte. Calcium entry blockers and vascular smooth muscle heterogeneity. *Fed. Proc.* 40: 2862-2865, 1981.

33. Vanelli, G., I. Shrier, and S. Magder. Critical closing pressure and arterial resistance have opposing responses to increases in perfusion pressure. *FASEB J.* 6(4): A1472, 1992.(Abstract)

34. Winquist, R.J. and J. A. Bevan. *In vitro* model of maintained myogenic vascular tone. *Blood Vessels* 18: 134-138, 1981.

35. Zweifach, B.W. Local regulation of capillary pressure. *Circ. Res.* 28-29 (Suppl. I): I-129-I-134, 1971.

CHAPTER 7

GENERAL CONCLUSIONS

7.1. CONCLUSIONS

The purpose of this thesis was to determine the mechanisms controlling the critical closing pressure and arterial resistance in the canine hindlimb. The studies discussed in the thesis cover the influence of neural, mechanical, and flow-mediated control systems on P_{crit} and R_a. I also tested the hypothesis that P_{crit} is eliminated under conditions of maximal vasodilation, and that the myogenic response of P_{crit} is eliminated when calcium channels are blocked.

In the first project, I tested the hypothesis that the carotid sinus baroreflex affects P_{crit} in addition to its effects on R_a. When the carotid sinus pressure was lowered, both P_{crit} and R_a increased. In addition, since arterial compliance decreased, the time constant of the arterial system (compliance*resistance) did not change. The opposite changes were observed when carotid sinus pressure was raised. These results confirmed that P_{crit} is tone-dependent and is affected by *in vivo* control systems.

In project 1, a change in carotid sinus pressure caused a change in arterial pressure. In those experiments we measured P_{crit} and R_a at the new perfusion pressure. However, arterial vessels *in vitro* exhibit a myogenic response and constrict when transmural pressure is increased. Therefore, in project 2, we measured the changes in P_{crit} and R_a with changes in P_{per} before and after lowering carotid sinus pressure. We found that increasing P_{per} caused an increase in P_{crit} but a decrease in R_a. Since flow also increased when P_{per} was increased, the changes in P_{crit} and R_a represent the interaction of myogenic and flow-mediated control systems. For instance, the increase in P_{crit} with increases in P_{per} is predominantly due to the myogenic response, but the effect may be attenuated by flow-mediated responses. Similarly, the decrease in R_a with increases in P_{per} is predominantly due to flow-mediated responses, but may be attenuated by a myogenic response. Metabolic effects can be considered negligible in the resting hindlimb (1). When carotid sinus pressure was lowered, P_{crit} and R_a

increased at every P_{per}. These results indicate that the effects observed in the first project were due to a combination of myogenic, flow-mediated, and neural responses. The results also suggest that steady-state pressure-flow relations should be reinterpreted to include a changing P_{crit} (figure 7.1)

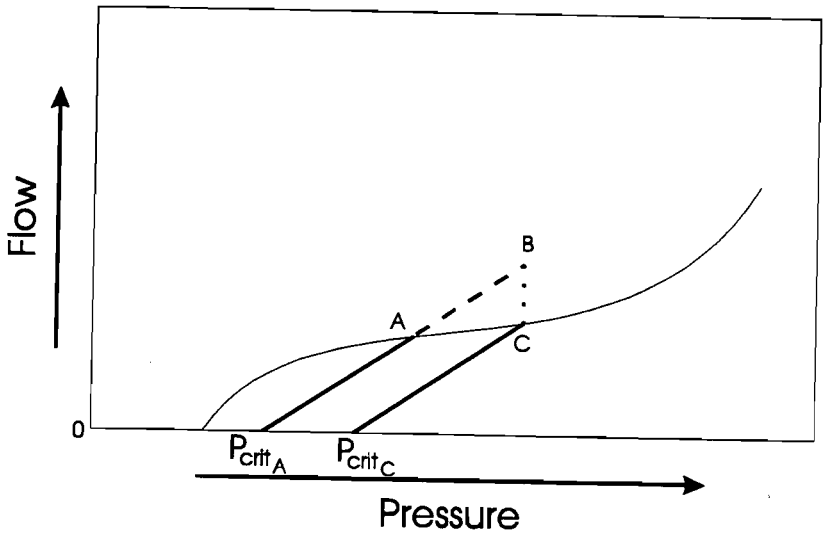

Figure 7.1: The curved solid line represents the steady-state pressure-flow relationship. The critical closing pressure at A is P_{crit_A}. If the perfusion pressure is increased from point A, the flow increases from A to B. The vasculature reacts to the increased pressure and/or flow by increasing the critical closing pressure, which decreases flow to C. At C, the critical closing pressure is increased compared to the original condition (P_{crit_C}), but the resistance is unchanged or decreases slightly (inverse of the slope of the dark solid line). Autoregulation has occurred and refers to the change in both critical closing pressure and resistance.

Since flow increased when we increased P_{per} in projects 2, we hypothesized that after blocking EDRF synthesis with L-NNA, an increase in P_{per} would cause 1) a greater rate of rise of P_{crit}, and 2) the fall in R_a would be eliminated (project 3). The results were consistent with our hypothesis, but we also observed the same effects when

vascular tone was increased with phenylephrine, an α_1-agonist. These results suggest the effects of L-NNA are not specific for EDRF blockade, and the myogenic response may be increased because of a non-specific increase in vascular tone. The absence of such an interaction in project 1 was most likely a ß-error as discussed in that chapter.

In project 4, we tested the hypothesis that an arteriolar P_{crit} would be eliminated during maximal vasodilation. First, we compared the results of the relationship P_{zf} versus ramp time with the predicted values based on two models of the circulation. These results indicated that a critical closing pressure was still present during maximal vasodilation, although it had decreased from 56.4±5.1 to 11.0±0.6 mmHg. This P_{crit} was still at the arteriolar level because it was greater than the simultaneously measured small venular pressure. However, P_{crit} was less than small venular pressure during normal flow, suggesting that waterfall behaviour might not occur. We tested this hypothesis by raising venous pressure during constant flow conditions, and observed an immediate rise in P_{per}. Therefore, maximal vasodilation decreased P_{crit} below the level of the waterfall, but did not eliminate smooth muscle tone. Finally, we showed that the smooth muscle tone which persists during maximal vasodilation is still capable of increasing when P_{per} increases, albeit at a slower rate than during control conditions. Therefore, maximal vasodilation does not abolish the myogenic response. These results also suggest an interaction between the myogenic response and the effects of an adenosine/nitroprusside solution. Although indomethacin was also used in these experiments, results from a separate group of animals showed indomethacin had no significant effect on P_{crit} or R_a in the canine hindlimb.

The mechanism of the myogenic response we observed in projects 2,3, and 4 is still unknown. *In vitro*, it is dependent on extracellular calcium (4,5). Whereas some studies suggest it can be abolished with calcium channel blockers (3), others have opposite conclusions (2). Therefore, in project 5, we tested the hypothesis that nifedipine would 1) decrease both P_{crit} and R_a, and 2) eliminate the myogenic response

of P_{crit}. The results confirmed the first hypothesis, but the myogenic response was only decreased with 10^{-7} M nifedipine and not eliminated. It is unlikely that higher doses would have achieved a greater effect because no further change in P_{crit} or R_a were observed with 10^{-6} M infusion. Two possibilities can account for these results. First, calcium channels may be only one mechanism by which the myogenic response occurs. Second, calcium channel blockers may affect some intermediate step in the myogenic response and affect its gain, but not its presence. With respect to R_a, we found that the decrease observed with increases in P_{per} was accentuated. These results support the hypothesis that the decrease in R_a under control conditions is attenuated by a myogenic response. When the myogenic response is decreased with nifedipine, a larger decrease in R_a is observed. In this project, we also found that nifedipine decreased venous resistance. However, the pressure in the small venules still increased because inflow increased (due to the decrease in P_{crit} and R_a) more than outflow increased (due to the decrease in R_v). This may explain the side effect of peripheral edema in patients taking nifedipine for hypertension.

P_{crit} is therefore affected by neural, mechanical, and flow-mediated control systems. Although R_a is also affected by these systems, it is not always in the same direction as P_{crit}. This may be because 1) different parts of the arterial tree may have different sensitivities to the different stimuli or 2) P_{crit} is dependent on tone whereas R_a is dependent on diameter. For instance, the vessels responsible for P_{crit} may be at their largest diameter during maximal vasodilation, but they may still have tone that only becomes evident when the intraluminal pressure decreases. This tone could change with increases in P_{per} even though the diameter remains constant. R_a, which is dependent on diameter, would remain constant with changes in P_{per}. Finally, this thesis supports the notion that different control systems interact, and the presence of one may potentiate or inhibit the gain of another.

7.2. REFERENCES

1. Folkow, B. Intravascular pressure as a factor regulating the tone of the small vessels. *Acta Physiol. Scand.* 17: 289-310, 1949.

2. Hayashi, K., M. Epstein, and R. Loutzenhiser. Enhanced myogenic responsiveness of renal interlobular arteries in spontaneously hypertensive rats. *Hypertension* 19: 153-160, 1992.

3. Kulik, T.J., J.N. Evans, and W.J. Gamble. Stetch-induced contraction in pulmonary arteries. *Am. J. Physiol.* 255: H1391-H1398, 1988.

4. Urchida, E. and D.F. Bohr. Myogenic tone in isolated perfused resistance vessels from rats. *Am. J. Physiol.* 216: 1343-1350, 1969.

5. Winquist, R.J. and J.A. Bevan. *In vitro* model of maintained myogenic vascular tone. *Blood Vessels* 18: 134-138, 1981.

CLAIMS TO ORIGINALITY

The following observations are original contributions towards understanding the mechanisms controlling the critical closing pressure and arterial resistance.

1) The carotid sinus baroreflex controls P_{crit} in addition to controlling arterial resistance, suggesting P_{crit} is affected by changes in sympathetic activity *in vivo*.

2) Although the percent changes in P_{crit} and R_a in response to changes in carotid sinus pressure were different, the effect of the changes on flow was the same.

3) A local increase in perfusion pressure (P_{per}) causes an increase in P_{crit} (i.e. myogenic effect predominates), but a decrease in R_a (passive or flow-mediated effects predominate). These results support *in vivo* microscopic experiments showing that different segments of the arterial tree respond differently to changes in P_{per}.

4) The rate of increase in P_{crit} with increases in P_{per} is increased by blocking endothelial-derived relaxing factor (EDRF) synthesis with L-nitro-arginine (L-NNA). The same effect occurs if baseline tone is increased with phenylephrine. These results indicate that the myogenic response of P_{crit} is increased during increases in baseline tone.

5) The decrease in R_a with increases in P_{per} is abolished with both L-NNA and phenylephrine. The decrease in R_a with increases in P_{per} is accentuated with nifedipine. These results support *in vitro* data which shows a myogenic response in large vessels. Under control conditions, the myogenic response is overshadowed by EDRF and passive effects. Under conditions of increased tone, the myogenic response is enhanced and prevents the decrease in R_a normally observed. When the myogenic response is decreased with nifedipine, the decrease in R_a is accentuated.

6) Indomethacin has no effect on P_{crit} or R_a under normal conditions in the canine hindlimb.

7) Abolishing reactive hyperemia by infusing a solution of adenosine and nitroprusside decreases P_{crit} below the level of the downstream pressure.

8) In contrast to the response in vessels with normal tone, increases in venous pressure after reactive hyperemia has been abolished results in immediate effects on P_{per}. This supports the notion that P_{crit} is decreased to a level below the downstream pressure.

9) Even after reactive hyperemia has been abolished, P_{crit} still increases with increases in P_{per}. These results suggest that myogenic tone remains at the arteriolar level even during "maximal vasodilation".

10) The rate of increase in P_{crit} with increases in P_{per} is reduced by the calcium channel blocker nifedipine, but could not be eliminated. These results imply the myogenic response of P_{crit} is affected by calcium channels but calcium entry is either 1) only one mechanism for increased tone, or 2) affects the myogenic response through indirect means.

11) Taken together, these results suggest that changes in P_{crit} and R_a with changes in P_{per} reflect the interaction of changes in metabolic, myogenic, and flow-mediated stimuli.

APPENDIX 1

SI unit Equivalents

1 Pascal (Pa) = 0.075 mmHg
= 0.01 cmH_2O

APPENDIX 2

Abbreviations

°C	degrees Celsius
α	alpha
β	rate of change of flow
β-error	beta error
Δ	delta
μ	viscosity
μg	micrograms
μl	microliters
um	micrometers
π	pi
ρ	density
τ	time constant
A-D	analog to digital
ANOVA	analysis of variance
A-V diff	arterial-venous difference
C_a	arterial compliance
D_5W	5% dextrose solution
d	diameter
dl	deciliter
$EC_{\#}$	equilibrium curve calculated at a transmural pressure equal to # mmHg
EDRF	endothelial-derived relaxing factor
EDNO	endothelial-derived nitric oxide
EDHF	endothelial-derived hyperpolarizing factor
g	grams
$[H^+]$	hydrogen ion concentration
HC	high carotid sinus pressure condition
HCl	hydrochloric acid
kg	kilograms
kPa	kilopascals

L	length
LC	low carotid sinus pressure condition
L-NNA	L-nitro-arginine
M	molar
mg	milligrams
min	minutes
ml	milliliters
mmole	millimoles
ms	milliseconds
n	number
N	Normal
ΔP	driving pressure
P_a	arterial pressure
P_{car}	carotid sinus pressure
P_{crit}	critical closing pressure
P_{el}	elastic recoil pressure
P_e	external pressure
P_i	internal pressure
P_{in}	inflow pressure
P_{out}	outflow pressure
P_{per}	perfusion pressure
P_{sur}	surrounding pressure
P_{tm}	transmural pressure
P_v	venous pressure
P_{zf}	zero-flow pressure intercept
PCO_2	partial pressure of carbon dioxide
PE240	size 240 polyethylene tubing
pH	-log of hydrogen ion concentration
PO_2	partial pressure of oxygen
$\dot{Q}$	flow
$Q_{i(0)}$	initial flow
r	radius
r_i	internal radius
r_e	external radius
R	resistance
R_a	arterial resistance
Re	Reynolds number
R_{tot}	total resistance
R_v	venous resistance

s	seconds
SD	standard deviation
S.E.M.	standard error of the mean
T_A	active wall tension
T_E	elastic wall tension
T_W	total wall tension
t_{zf}	ramp time to zero-flow
U	mean fluid velocity
X	entrance length before Poiseuille Flow resumes